Supporting Information

Charge-Gating Dibenzothiophene-*S,S*-dioxide Bridges in Electron Donor–Bridge–Acceptor Conjugates

Gilles Yzambart,[a,II] Anna Zieleniewska,[b,II] Stefan Bauroth,[b] Timothy Clark,[c] Martin R. Bryce,[,a] Dirk M. Guldi*[,b]*

[a] Department of Chemistry, Durham University, Durham DH1 3LE, United Kingdom.

[b] Department of Chemistry and Pharmacy & Interdisciplinary Center for Molecular Materials, Friedrich-Alexander-Universität Erlangen-Nürnberg, Egerlandstr. 3, 91058 Erlangen, Germany.

[c] Computer-Chemie-Centrum & Interdisciplinary Center for Molecular Materials, Department of Chemistry and Pharmacy, Friedrich-Alexander-Universität Erlangen-Nürnberg, Nägelsbachstr. 25, 91052 Erlangen, Germany.

Table of Contents: **Page**

I. General Information.

^{1}H (600 or 700 MHz) and ^{13}C NMR (101, 151 or 176 MHz) spectra were recorded on Varian VNMRS-700 MHz spectrometers. 400 MHz NMR spectra were recorded on a Bruker Avance-400 MHz instrument. Chemical shifts are reported in ppm and referenced to residual solvent. Melting points were measured using a Stuart SMP40 melting point apparatus. The temperatures at the melting point were ramped at 1 ^{o}C/min and are uncorrected. Elemental analysis was performed at the Elemental Microanalysis Service of the University of Durham (United Kingdom) using an Exeter CE-400 Elemental Analyser. MALDI TOF MS Mass spectrometry and high resolution mass spectra were obtained using an Autoflex II ToF/ToF (Bruker) and a LCT Premier XE (Waters) respectively.

UV/Vis spectra were collected at room temperature using a Perkin Elmer Lambda 2 spectrometer. The data was recorded with the software UV WinLab using a slit width of 2 nm and a scan rate of 480 nm/min. Steady-state fluorescence studies were carried out with a Flouromax3 spectrometer (Horiba Scientific). The quantum yields (QYs) were determined using the comparative method, which involved the use of well characterised standard references. Femtosecond transient absorption studies were performed using 387 nm and 430 nm laser pulses (1 kHz, 150 fs pulse width, energy between 200 and 300 nJ) from an amplified Ti:Sapphire fs laser system (Model CPA 2101 and 2110 Clark MXR), using transient absorption pump/probe detection systems (Helios and EOS, Ultrafast Systems). The excitation wavelength at 430 nm was generated with a non-collinear optical parameter (NOPA, Clark MXR). All measurements were conducted in a 2 mm quartz cuvettes under argon atmosphere. Obtained data were treated by means of multi-wavelength analyses. Kinetic analyses were performed using Origin 2016 software. A minimum of five spectral regions of significant absorption changes were taken from the transient absorption and fitted either mono- or multi-exponentially. The specific type of fit is indicated in the main text. Transient kinetics were evaluated using the entire time range. The obtained values of corresponding components were averaged. The data points in the 725 – 770 nm regime were removed as they stem from the

fundamental excitation wavelength. Temperature-dependent measurements were performed using a copper cuvette holder with an integrated Peltier element to vary the temperature between 280 and 350 K. Cyclic voltammetry and differential pulse voltammetry were performed at room temperature, and the applied potential was controlled with µAutolab III/FRA2 potentiostat from METROHM. Current vs the applied potential was recorded by means of the software NOVA 1.10. Measurements were carried out in a homemade cell containing a 0.1 M tetrabutylammonium hexafluorophosphate ($TBAPF_6$) as the supporting electrolyte. A three-electrode configuration was used with a glassy carbon working electrode (3 mm diameter), Pt wire acting as the counter electrode, and a Ag-wire as the quasi-reference electrode. The Fc/Fc+ redox couple was used as an internal standard. All chemicals were purchased from Acros Organics, Sigma Aldrich, Alfa Aesar and used without further treatment. Dry solvents were obtained from a solvent purification system. All air-sensitive reactions were conducted under a blanket of argon which was dried by passage through a column of phosphorus pentoxide. Column chromatography was performed using silica gel from Sigma Aldrich.

II. Synthesis

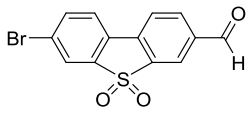

7-bromodibenzothiophene-*S*,*S*-dioxide-3-carbaldehyde (Br-S-CHO) (2). Lithium tri-*n*-butylmagnesiate was prepared as follows: *n*-BuLi in hexane (0.47 mL, 1.19 mmol) was added to a solution of *n*-BuMgCl (0.3 mL, 0.59 mmol) in dry THF (3 mL) and was stirred for 30 minutes to room temperature. 3,7-Dibromodibenzothiophene-*S,S*-dioxide **1** (0.5 g, 1.49 mmol) was dissolved in dry THF (45 mL) and cooled to 0 ^{O}C. After complete dissolution of the solid, the lithium tri-*n*-butylmagnesiate solution was added dropwise and the solution was stirred for 1 hour to 0 ^{O}C. Then, dry DMF (0.12 mL, 1.63 mmol) was added and the mixture was stirred overnight at room

temperature. The brown mixture was cooled in an ice/ acetone bath to -2 ^{O}C, aqueous periodic acid (10 wt %, 0.93 mL, 0.41 mmol) was added and after 20 minutes, aqueous 3 M HCl (0.93 mL, 2.81 mmol, 190 mol %) was added and the mixture was stirred for 1 hour. The aqueous layer was removed and solvent was evaporated from the organic layer. Then DCM was added and the mixture was successively washed with aqueous sodium thiosulfate (2 wt %, 14 mL), water, dried with magnesium sulfate, filtered and the solvent was evaporated. Purification using DCM as eluent on silica gel followed by crystallization in $CHCl_3$ led to white crystals of **2** (311 mg, 72%). mp: > 320 ^{o}C. ^{1}H NMR (500 MHz, $CDCl_3$): δ 10.09 (1 H, s), 8.32 (1H, d), 8.19 (1H, dd, *J* = 8.0, 1.5 Hz), 8.01 (1H, d, *J* = 1.8 Hz), 7.96 (1H, d, *J* = 8.0 Hz), 7.84 (1H, dd, *J* = 8.2, 1.8 Hz), 7.76 (1H, d, *J* = 8.2 Hz). ^{13}C NMR (151 MHz, $CDCl_3$): δ 189.39, 140.36, 138.68, 138.05, 137.44, 135.84, 135.10, 129.31, 126.19, 126.04, 123.96, 123.75, 122.37. HRMS-ASAP^{+} calcd for $C_{13}H_7BrO_3S$ 321.9299; found $[M]^{+}$ 321.9301. Anal Calcd for $C_{13}H_7BrO_3S$: C, 48.32, H, 2.18. Found: C, 47.82, H 2.18.

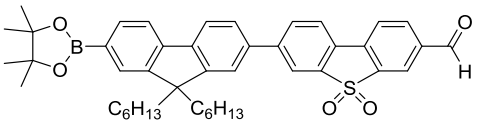

7-[7-(4,4,5,5-tetramethyl-1,2,3-dioxaborolan-2-yl)-9,9-dihexylfluorene-2-yl]-dibenzothiophene-*S*,*S*-dioxide-3-carbaldehyde (BE-Fl-S-CHO) (4). 2,7-Bis(4,4,5,5-tetramethyl-1,2,3-dioxaborolan-2-yl)-9,9-dihexylfluorene **3** (364 mg, 0.62 mmol), Br-S-CHO **2** (200 mg, 0.62 mmol), $Pd(PPh_3)_2Cl_2$ (20 mg) and K_2CO_3 (685 mg, 4.96 mmol) were dried under vacuum. After 1 hour, the compounds were solubilized in a mixture of DMF/toluene (60 mL / 25 mL). The reaction was stirred overnight at 90 ^{o}C, then filtered on celite and the solvents were removed under reduced pressure. The purification of the mixture using silica gel and DCM as eluent gave **4** as a yellow powder (150 mg, 34 %). mp: 166 ^{o}C. ^{1}H NMR (600 MHz, $CDCl_3$): δ 10.10 (1H, s), 8.35 (1H, d, *J* = 1.3 Hz), 8.18 (1H, dd, *J* = 1.3, 7.9 Hz), 8.17 (1H, d, *J* = 1.3 Hz), 8.01-7.95 (3H, m), 7.85-7.74 (4H,m), 7.63 (1H, dd, *J* = 1.7, 7.9 Hz), 7.60 (1H,d, *J* = 1.7Hz), 2.05 (4H,m), 1.4 (12H,s), 1.06 (12H,m), 0.75 (6H, t, *J* = 6.9 Hz), 0.63 (4H, m). ^{13}C NMR (151 MHz,

$CDCl_3$) δ 189.56, 152.74, 150.44, 145.97, 143.21, 142.22, 139.69, 139.09, 137.61, 137.59, 136.81, 135.03, 134.05, 132.93, 129.09, 128.75, 126.16, 123.72, 123.09, 122.30, 121.53, 121.05, 120.99, 119.54, 83.96, 55.62, 40.42, 31.62, 29.78, 25.10, 23.88, 22.72, 14.14. HRMS-ASAP$^+$ calcd for $C_{44}H_{51}BO_5S$ 702.3550; found $[M–H]^+$ 701.3601.

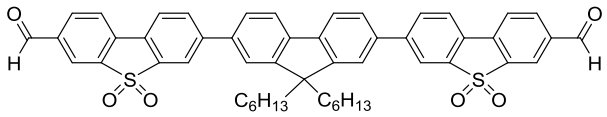

OHC-S-Fl-S-CHO (5). The purification of the mixture of the reaction which gave **4** using silica gel and DCM as eluent gave **5** as a light yellow powder (30 mg, 6%). ^{1}H NMR (400 MHz, $CDCl_3$): δ 10.11 (2H, s), 8.36 (2H, d, *J* = 1.0 Hz), 8.22-8.18 (4H, m), 8.03-7.97 (6H, m), 7.87 (2H, d, *J* = 7.9 Hz), 7.67 (2H, dd, *J* = 7.9, 1.7 Hz), 7.64 (2H, d, *J* = 1.3 Hz), 2.13-2.09 (4H, m), 1.15-1.03 (12H, m), 0.76 (6H, t, *J* = 7.0 Hz), 0.68 (4H,m). ^{13}C NMR (101 MHz, $CDCl_3$) δ 189.79, 152.75, 145.94, 141.57, 139.92, 139.27, 138.06, 137.85, 136.97, 135.27, 133.15, 129.10, 126.65, 123.96, 123.35, 122.55, 121.78, 121.30, 121.23, 56.11, 40.83, 31.86, 30.01, 24.23, 22.94, 14.35. HRMS-ASAP$^+$ calcd for $C_{51}H_{46}O_6S_2$ 818.2736; found $[M]^+$ 818.2726.

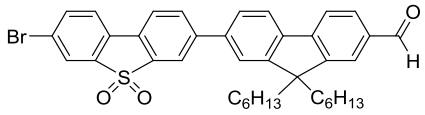

7-(7-bromo-dibenzothiophene-*S,S*-dioxide-3-yl)-9,9-dihexylfluorene-2-carbaldehyde (Br-S-Fl-CHO) (7). 2,7-Dibromo-dibenzothiophene-*S,S*-dioxide **1** (1.313 g, 3.53 mmol), 7-(4,4,5,5-tetramethyl-1,3,2-dioxaborolan-2-yl)-9,9-dihexylfluorene-2-carbaldehyde **6** (576 mg, 1.18 mmol), K_2CO_3 (1.304 mg, 9.44 mmol) and $Pd(PPh_3)_2Cl_2$ (35 mg) were dried together under vacuum for 2 hours. Then dry DMF (40 mL) and dry toluene (20 mL) were added and the mixture was stirred overnight at 90 ^{O}C under argon. A precipitate was removed by filtration, solvents were evaporated and a purification by column chromatography on SiO_2 using a mixture of DCM/hexane (7/3 v/v) then DCM as eluents gave

the compound **7** (620 g, 81 %) as a white solid. mp: 165 °C. ^{1}H NMR (600 MHz, $CDCl_3$): δ 10.09 (1H, s), 8.11 (1H, d, *J* = 1.7 Hz), 7.98 (1H, d, *J* = 1.7 Hz), 7.94 (1H, dd, *J* = 8.0, 1.7 Hz), 7.91-7.86 (5H, m), 7.79 (1H, dd, *J* = 8.1, 1.8 Hz), 7.71 (1H, d, *J* = 8.2 Hz), 7.65 (1H, dd, *J* = 7.9, 1.7 Hz), 7.62 (1H,s), 2.13-2.04 (4H, m), 1.13-1.00 (12H, m), 0.75 (6H, t, *J* = 7.1 Hz), 0.67-0.56 (4H, m). ^{13}C NMR (151 MHz, $CDCl_3$) δ 192.41, 153.50, 152.02, 146.69, 144.36, 140.44, 139.55, 139.17, 138.44, 137.18, 135.84, 132.95, 130.69, 130.48, 129.62, 126.46, 125.73, 124.33, 123.34, 123.10, 122.16, 121.81, 121.64, 120.99, 120.53, 55.78, 40.41, 31.62, 29.73, 23.97, 22.69, 14.11. HRMS-ASAP$^+$ calcd for $C_{38}H_{39}BrO_3S$ 654.1803; found $[M]^+$ 654.1818.

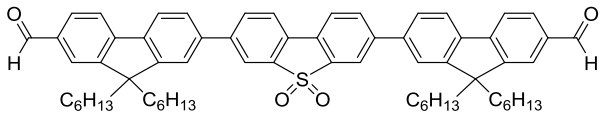

OHC-Fl-S-Fl-CHO (8). Br-Fl-CHO **6**[1] (250 mg, 0.58 mmol), BE-S-BE[2] (90 mg, 0.19 mmol), K_2CO_3 (240 mg, 1.74 mmol) and $Pd(PPh_3)_2Cl_2$ (16 mg) were reacted together following the process used for the synthesis of BE-Fl-S-CHO **4**. Purification on silica gel using DCM as eluent led to **8** as a yellow powder (150 mg, 83%). mp: 210 °C. ^{1}H NMR (400 MHz, $CDCl_3$): δ 10.10 (2H,s), 8.17 (2H, d, *J* = 1.5 Hz), 7.98-7.87 (12H, m), 7.68-7.66 (4H, m), 2.16-2.04 (8H, m), 1.16-0.98 (24H, m), 0.76 (12H, t, *J* = 7.1 Hz), 0.69-0.57 (8H, m). ^{13}C NMR (101 MHz, $CDCl_3$) δ 192.40, 153.47, 152.00, 146.73, 143.93, 140.31, 139.31, 138.87, 135.79, 132.86, 130.68, 130.36, 126.43, 123.32, 122.22, 121.78, 121.62, 120.96, 120.48, 55.75, 40.41, 31.61, 29.72, 23.96, 22.68, 14.10. HRMS-ASAP$^+$ calcd for $C_{64}H_{72}O_4S$ 936.5151; found $[M]^+$ 936.5161.

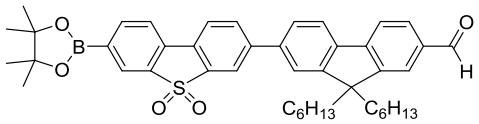

7-[7-(4,4,5,5-tetramethyl-1,2,3-dioxaborolan-2-yl)-dibenzothiophene-*S*,*S*-dioxide-3-yl]-9,9-dihexylfluorene-2-carbaldehyde (BE-S-Fl-CHO) (9). Br-S-Fl-CHO **7** (80 mg, 0.12 mmol),

bis(pinacolato)diboron (74.2 mg, 0.30 mmol), KOAc (87.49 mg, 0.90 mmol) and $Pd(OAc)_2$ (4 mg) were dried together under vacuum for 2 hours. Then dry DMF (10 mL) was added and the mixture was stirred overnight at 90 ^{0}C under argon. After evaporation of the DMF, the crude mixture was solubilized with DCM (30 mL) and filtrated through celite. Evaporation of the solvent led to a yellow mixture and the compound **9** could not be purified by chromatography. ^{1}H NMR (600 MHz, $CDCl_3$): δ 10.08 (1H, s), 8.32 (1H, s), 8.12 (1H, d, *J* = 1.0 Hz), 8.08 (1H, dd, *J* = 1.0, 7.6 Hz), 8.01 (1H, s), 7.93-7,87 (5H,m), 7.83 (1H, d, *J* = 7.7 Hz), 7.65 (1H, dd, *J* = 1.2, 7.9 Hz), 7.62 (1H, d, *J* = 1.5 Hz), 2.08 (4H, m), 1.37 (12H, s), 1.06 (12H, m), 0.75 (6H, t, *J* = 6.9 Hz), 0.61 (4H, m). Compound **9** was used in the next step without further purification.

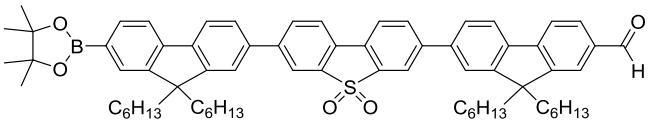

7-[7-[7-(4,4,5,5-tetramethyl-1,2,3-dioxaborolan-2-yl)-9,9-dihexylfluorene-2-yl]-dibenzothiophene-*S*,*S*-dioxide-3-yl]-9,9-di-n-hexylfluorene-2-carbaldehyde (BE-Fl-S-Fl-CHO) (10). Br-S-Fl-CHO **7** (135 mg, 0.21 mmol), 2,7-bis(4,4,5,5-tetramethyl-1,2,3-dioxaborolan-2-yl)-9,9-dihexylfluorene **3** (361 mg, 0.62 mmol), K_2CO_3 (228 mg, 1.65 mmol) and $Pd(PPh_3)_2Cl_2$ (8 mg) were reacted together following the process used for the synthesis of BE-Fl-S-CHO **4**. Purification on silica gel using DCM as eluent led to a **10** as a yellow powder (110 mg, 52%). mp: 123.5-128 ^{o}C. ^{1}H NMR (400 MHz, $CDCl_3$): δ 10.09 (1H, s), 8.16 (2H, s), 7.98-7.89 (8H, m), 7.86-7.74 (4H, m), 7.68 (1H, dd, *J* = 1.67, 7.89 Hz), 7.65-7.61 (3H, m), 2.15-2.00 (8H, m), 1.41 (12H, s), 1.14-1.00 (24H, m), 0.76 (12H, t, *J* = 6.8 Hz), 0.67-0.57 (8H, m). ^{13}C NMR (176 MHz, $CDCl_3$) δ 192.44, 153.48, 152.67, 152.04, 150.42, 146.81, 144.51, 143.80, 143.36, 141.86, 140.29, 139.44, 138.91, 138.82, 138.02, 135.80, 134.04, 132.85, 132.83, 130.70, 130.56, 130.00, 129.08, 126.45, 126.05, 123.35, 122.15, 121.79, 121.66, 121.49, 120.98, 120.92, 120.89, 120.49, 119.47, 83.95, 55.78, 55.60, 40.46, 40.44, 31.64, 29.81, 29.75, 25.11, 23.99, 23.89, 22.74, 22.70, 14.16, 14.12. HRMS-ASAP$^+$ calcd for $C_{69}H_{83}BO_5S$ 1034.6054; found $[M–H]^+$ 1033.6133.

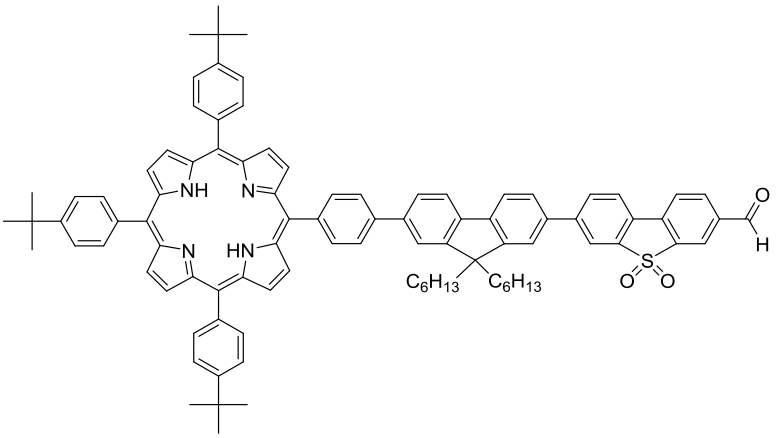

H_2P-Ph-Fl-S-CHO (12). BE-Fl-S-CHO **4** (40 mg, 5.7×10^{-2} mmol), porphyrin **11** [isolated and used as a ca. 1:1 mixture with 5,10,15,20-tetrakis(4-*t*-butylphenyl)porphyrin][3] (148 mg, excess), $Pd(PPh_3)_2Cl_2$ (3 mg) and K_2CO_3 (71 mg, 0.51 mmol) were dried under vacuum for 1 hour. After solubilization in a mixture of dry DMF/toluene (20 mL / 10 mL), the reaction was stirred overnight at 100 ^{o}C. The resulting mixture was filtrated through celite, solvents were evaporated and purification on silica gel using DCM as eluent gave **12** as a purple solid (40 mg, 52%). ^{1}H NMR (400 MHz, $CDCl_3$): δ 10.08 (1H, s), 8.95 (4H, dd, *J* = 4.8, 13.9 Hz), 8.90 (4H, s), 8.36-8.34 (3H, m), 8.22-8.09 (10H, m), 7.98-7.85 (7H, m), 7.78 (6H, d, *J* = 8.4 Hz), 7.68-7.66 (2H, m), 2.27-2.14 (4H, m), 1.62 (27H, s), 1.21-1.12 (12H, m), 0.89-0.76 (10H, m), -2.69 (2H, s). ^{13}C NMR (176 MHz, $CDCl_3$) δ 189.56, 152.52, 152.28, 150.68, 145.95, 142.12, 141.59, 140.61, 140.52, 139.94, 139.70, 139.33, 139.06, 137.57, 136.78, 135.40, 135.00, 134.67, 134.64, 132.86, 128.69, 126.66, 126.34, 125.55, 123.77, 123.75, 123.68, 123.06, 122.23, 121.80, 121.55, 121.01, 120.82, 120.74, 120.56, 120.46, 119.54, 55.84, 40.74, 35.07, 31.86, 31.72, 29.92, 24.11, 22.80, 14.20. MALDI-TOF MS, calcd for $C_{94}H_{92}N_4O_3S$: 1356.7 found (m/z): 1356.7 (M^+, 100%).

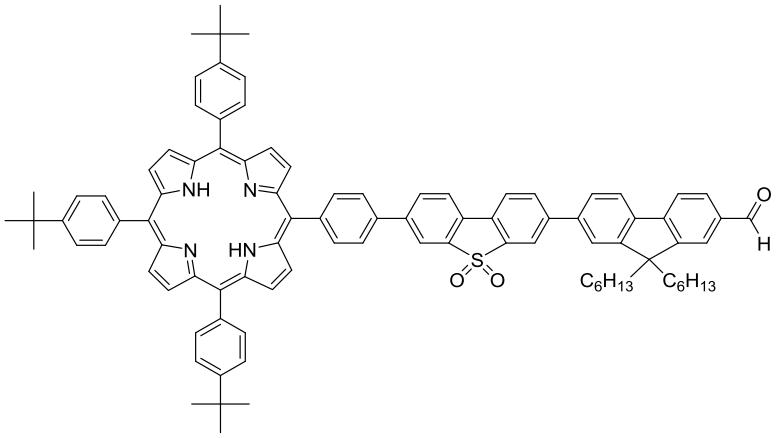

H_2P-Ph-S-Fl-CHO (13). A mixture of BE-S-Fl-CHO **9** (192 mg), porphyrin **11**[3] (352 mg, excess), $Pd(PPh_3)_2Cl_2$ (13 mg) and K_2CO_3 (170 mg, 1.23 mmol) were reacted together following the process used for the synthesis of H_2P-Ph-Fl-S-CHO **12**. Purification was realised on silica using DCM as eluent to afford **13** as a purple powder (40 mg, 10%). ^{1}H NMR (400 MHz, $CDCl_3$): δ 10.10 (1H, s), 8.95-8.88 (8H, m), 8.39 (1H, m), 8.35-8.32 (2H, m), 8.19- 7.75 (23H, m), 7.68-7.63 (2H, m), 2.18-2.06 (4H, m), 1.62 (27H, s), 1.17-1.02 (12H, m), 0.79 (6H, t, *J* = 7.1 Hz), 0.71-0.59 (4H, m), -2.67 (2H, s). ^{13}C NMR (176 MHz, $CDCl_3$) δ 192.44, 153.48, 152.03, 150.71, 146.78, 143.84, 143.55, 143.01, 140.28, 139.39, 139.29, 139.24, 139.01, 138.97, 137.99, 135.79, 135.55, 134.66, 134.63, 132.84, 132.77, 130.70, 130.41, 130.39, 126.44, 125.35, 123.78, 123.34, 122.27, 122.16, 121.77, 121.64, 121.05, 120.92, 120.76, 120.59, 120.48, 118.78, 55.78, 40.44, 35.05, 31.84, 31.65, 29.77, 24.00, 22.72, 14.15. MALDI-TOF MS, calcd for $C_{94}H_{92}N_4O_3S$: 1357.6 found (m/z): 1357.6 (M^+, 100%).

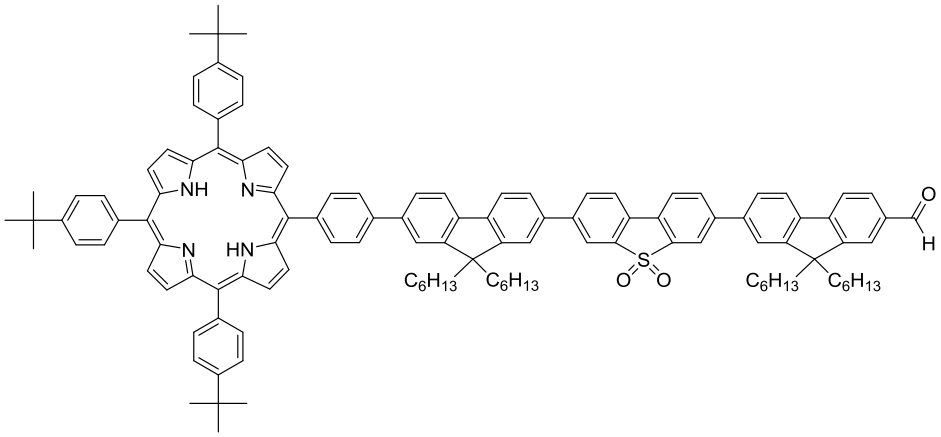

H_2P-Ph-Fl-S-Fl-CHO (14). A mixture of BE-Fl-S-Fl-CHO **10** (63 mg, 6.09×10^{-2} mmol), porphyrin **11**[3] (156 mg, excess), $Pd(PPh_3)_2Cl_2$ (5 mg) and K_2CO_3 (76 mg, 0.55 mmol) were reacted together following the process used for the synthesis of H_2P-Ph-Fl-S-CHO **12**. Purification on silica gel with DCM as eluent gave **14** as a purple powder (62 mg, 61 %). ^{1}H NMR (400 MHz, $CDCl_3$): δ 10.10 (1H, s), 8.95 (4H, dd, *J* = 25.0, 3.9 Hz,), 8.89 (4H, s), 8.35 (2H, d, *J* = 7.8 Hz), 8.21 (1H, d, *J* = 1.7 Hz), 8.18-8.16 (7H, m), 8.11 (2H, d, *J* = 8.0 Hz), 8.02-7.89 (12H, m), 7.78-7.77 (6H, m), 7.71-7.66 (4H, m), 2.25-2.07 (8H, m), 1.62 (27H, s), 1.22-1.02 (24H, m), 0.88-0.77 (16H, m), 0.69-0.60 (4H, m), 2.70 (2H, s). ^{13}C NMR (176 MHz, $CDCl_3$) δ 192.26, 153.31, 152.27, 152.08, 151.86, 150.49, 146.63, 144.35, 143.63, 141.58, 141.38, 140.48, 140.20, 140.12, 139.90, 139.26, 139.16, 138.73, 138.68, 137.51, 135.62, 135.21, 134.49, 134.46, 132.67, 132.62, 130.53, 130.40, 129.81, 126.45, 126.28, 126.05, 125.36, 123.59, 123.57, 123.17, 121.99, 121.97, 121.62, 121.48, 121.34, 120.81, 120.70, 120.56, 120.49, 120.36, 120.32, 120.26, 119.38, 55.64, 55.61, 40.60, 40.28, 34.89, 31.68, 31.56, 31.47, 29.76, 29.58, 23.94, 23.82, 22.63, 22.54, 14.03, 13.95. MALDI-TOF MS, calcd for $C_{119}H_{124}N_4O_3S$: 1688.9 found (m/z): 1689.9 (M^++1, 100%).

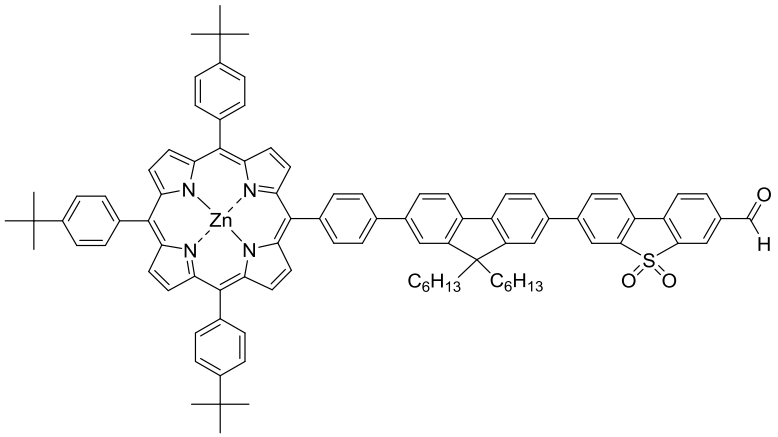

ZnP-Ph-Fl-S-CHO (15). H_2P-Ph-Fl-S-CHO **12** (20 mg, 1.47x10^{-2} mmol) and zinc acetate dihydrate (16 mg, 7.29x10^{-2} mmol) were dried together under vacuum. After 1 hour, dry DMF (10 mL) was added and the reaction was heated at reflux for 3 hours with stirring. Then, solvent was removed by

evaporation and the crude product was purified on silica using DCM as eluent. The compound **15** was isolated as a purple powder (20 mg, 96 %). ^{1}H NMR (400 MHz, $CDCl_3$): δ 10.07 (1H, s), 9.07-8.92 (8H, m), 8.36-7.89 (21H, m), 7.78-7.67 (7H, m), 2.27-2.12 (4H, m), 1.63 (27H, s), 1.23-1.09 (12H, m), 0.91-073 (10H, m). MALDI-TOF MS, calcd for $C_{94}H_{90}N_4O_3SZn$: 1418.6 found (m/z): 1420.5 (M^++2, 100%).

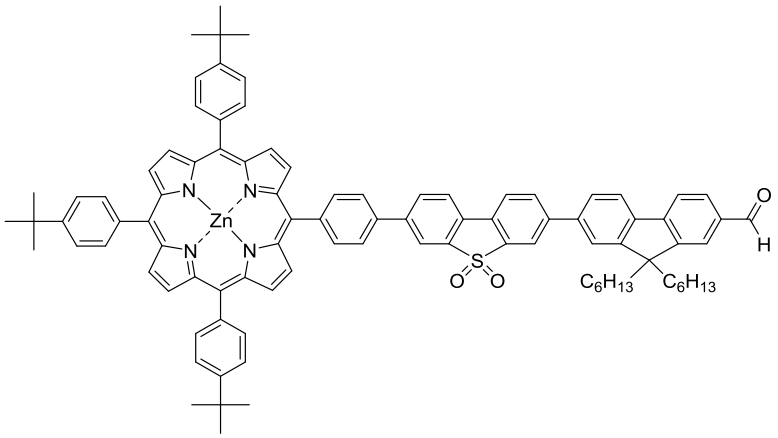

ZnP-Ph-S-Fl-CHO (16). H_2P-Ph-S-Fl-CHO **13** (25 mg, 1.84x10^{-2} mmol) and zinc acetate dihydrate (20 mg, 9.21x10^{-2} mmol) were reacted together following the process used for the synthesis of ZnP-Ph-Fl-S-CHO **15**. Purification on silica with a mixture of DCM/hexane (9/1 v/v) as eluent gave **16** as a purple powder (20 mg, 76%). ^{1}H NMR (400 MHz, $CDCl_3$): δ 10.03 (1H, s), 9.04-8.98 (8H, m), 8.34-8.32 (3H, m), 8.18-8.12 (7H, m), 8.02-7.74 (16H, m), 7.66-7.63 (2H, m), 2.16-2.05 (4H,m), 1.67 (27, s), 1.17-1.03 (12H, m), 0.79 (6H, t, *J* = 7.0 Hz), 0.71-0.59 (4H, m). MALDI-TOF MS, calcd for $C_{94}H_{90}N_4O_3SZn$: 1418.6 found (m/z): 1420.5 (M^++2, 100%).

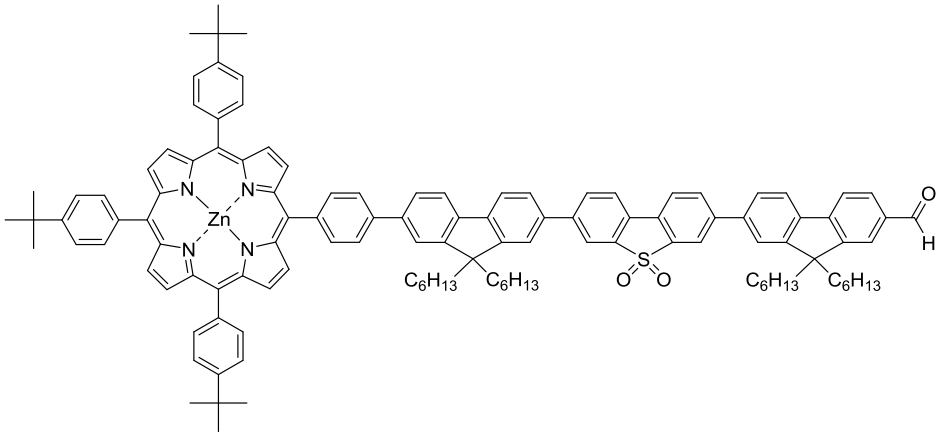

ZnP-Ph-Fl-S-Fl-CHO (17). H_2P-Ph-Fl-S-Fl-CHO **14** (28 mg, 1.16 x 10^{-2} mmol) and zinc acetate dihydrate (20 mg, 9.12 x 10^{-2} mmol) were reacted together following the process used for the synthesis of ZnP-Ph-Fl-S-CHO **15**. Purification on silica with a mixture of DCM/hexane (65:35 v/v) as eluent gave **17** as a purple powder (22 mg, 77%). ^{1}H NMR (700 MHz, $CDCl_3$): δ 10.08 (1H, s), 9.06 (4H, dd, *J* = 26.0, 4.5 Hz), 9.00 (4H, s), 8.36 (2H, d, *J* = 7.4 Hz,), 8.20-8.16 (8H, m), 8.10 (2H, d, *J* = 7.4 Hz), 7.99-7.87 (12H, m), 7.78-7.76 (6H, m), 7.69-7.66 (4H, m), 2.25-2.07 (8H, m), 1.63 (27H, s), 1.22-1.03 (24H, m), 0.90-0.77 (16H, m), 0.69-0.60 (4H, m). MALDI-TOF MS, calcd for $C_{119}H_{122}N_4O_3S$: 1750.9 found (m/z): 1752.9 (M^++2, 100%).

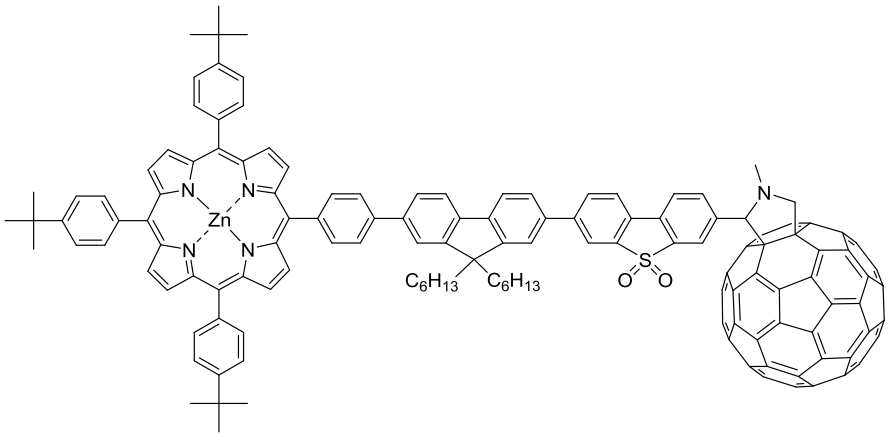

ZnP-Ph-Fl-S-C_{60} (18). Fullerene C_{60} (30.4 mg, 0.04 mmol) was heated to reflux in chlorobenzene (15 mL) for 15 minutes. Then, ZnP-Ph-Fl-S-CHO **15** (10 mg, 7.05 x 10^{-3} mmol) and sarcosine (6.9 mg, 0.77 x 10^{-1} mmol) were added together and the mixture was stirred for 3 hours at reflux. The solvent was

then removed by evaporation and purification using silica gel and DCM/CS_2 (1:1 v/v) as eluent gave **18** as a purple solid (10 mg, 65 %). ^{1}H NMR (400 MHz, $CDCl_3$): δ 9.06-8.93 (8H, m), 8.23-7.94 (16H, m), 7.82-7.52 (12H, m), 4.60 (2H, s, br), 3.84 (1H, s, br), 2.75 (3H, s, br), 2.25-1.99 (4H, m), 1.65 (18H, s), 1.62 (9H, s), 1.14-0.66 (22H, m). MALDI-TOF MS, calcd for $C_{156}H_{95}N_5O_2SZn$: 2165.7 found (m/z): 2168.7 (M^++3, 89.58%), 1446.7 (M^+-C_{60}+2, 5.86 %).

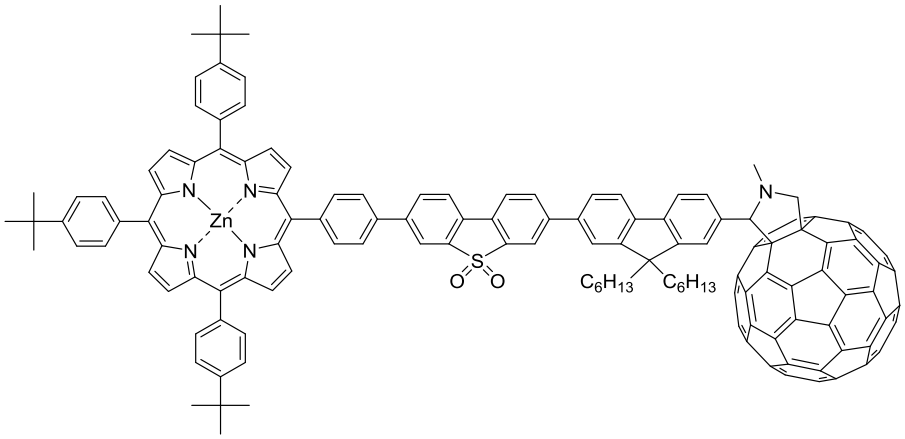

ZnP-Ph-S-Fl-C_{60} (19). ZnP-Ph-S-Fl-CHO **16** (23 mg, 1.62 x 10^{-2} mmol), fullerene C_{60} (70 mg, 0.10 mmol) and sarcosine (15.9 mg, 0.18 mmol) were reacted together following the process used for the synthesis of ZnP-Ph-Fl-S-C_{60} **18**. Purification on silica gel with a mixture of DCM/CS_2 (1:1 v/v) as eluent gave **19** as a purple solid (31 mg, 89%). ^{1}H NMR (400 MHz, $CDCl_3$): δ 9.04-8.95 (8H, m), 8.36 (1H, s, br), 8.20-8.11 (8H, m, br), 7.93-7.64 (17H, m, br), 7.49 (2H, s, br), 4.79 (2H, s, br), 4.09 (1H, s, br), 2.84 (3H, s, br), 2.06 (4H, m, br), 1.64 (18H, s), 1.62 (9H, s), 1.13-0.69 (20H, m, br), 0.46 (1H, s, br), 0.26 (1H, s, br). MALDI-TOF MS, calcd for $C_{156}H_{95}N_5O_2SZn$: 2165.7 found (m/z): 2167.6 (M^++3, 100%), 1447.6 (M^+-C_{60}+3, 18.64 %).

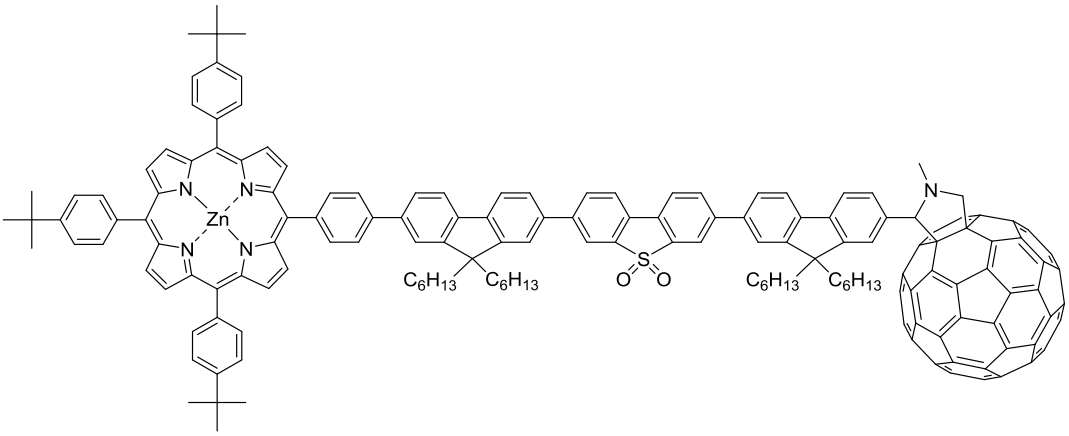

ZnP-Ph-Fl-S-Fl-C_{60} (20). ZnP-Ph-Fl-S-Fl-CHO **17** (14 mg, 7.99 x 10^{-3} mmol), fullerene C_{60} (34.5 mg, 4.79 x 10^{-2} mmol) and sarcosine (7.8 mg, 0.88 x 10^{-1} mmol) were reacted together following the process used for the synthesis of ZnP-Ph-Fl-S-C_{60} **18**. Purification on silica gel with a mixture of DCM/CS_2 (1:2 v/v) as eluent gave **20** as a purple solid (14 mg, 70 %). ^{1}H NMR (400 MHz, $CDCl_3$): δ 9.06-8.98 (8H, m), 8.27-7.50 (34H, m), 4.83 (2H,s, br), 4.10 (1H, s, br), 2.83 (3H, s, br), 2.26-1.95 (8H, m, br), 1.64 (27H, s), 1.21-0.64 (42H, m, br), 0.37 (1H, s,br), 0.18 (1H, s, br). MALDI-TOF MS, calcd for $C_{181}H_{127}N_5O_2SZn$: 2498.5; found (m/z): 2499.6 (M^++1, 100 %), 1779.9 (M^+-C_{60}+2, 23%).

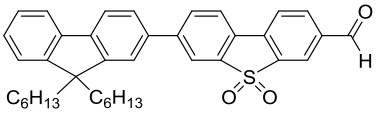

7-(9,9-di-*n*-hexylfluorene-2-yl)dibenzothiophene-*S*,*S*-dioxide-3-carboxaldehyde (Fl-S-CHO) (23). A 2 M Na_2CO_3 aqueous solution (4.2 mL) and toluene (20 mL) were degassed together for 30 minutes prior the addition to a mixture of 2-(boronic acid-2-yl)-9,9'-dihexylfluorene[4] (353 mg, 0.93 mmol), Br-S-CHO **2** (200 mg, 0.62) and $Pd(PPh_3)_4$ (47 mg, 0.04 mmol). The reaction was stirred for 18 hours at 90 ^{o}C then the organic layer was extracted with DCM, dried with $MgSO_4$ and solvent was removed under reduced pressure. A purification using column chromatography on SiO_2 with a mixture of DCM/Hexane (9/1 v/v) as eluent gave **23** as a yellow powder (320 mg, 96%). mp: 171.5 ^{o}C. ^{1}H NMR (700 MHz, $CDCl_3$): δ 10.09 (1H, s), 8.34 (1H, d, *J* = 0.9 Hz), 8.18-8.17 (2H, m), 8.00-7.93 (3H, m), 7.81-

7.74 (2H, m), 7.62-7.60 (2H, m), 7.39-7.34 (3H, m), 2.05-2.03 (4H, m), 1.14-1.02 (12H, m), 0.76 (6H, t, *J* = 7.3 Hz), 0.70-0.61 (4H, m). ^{13}C NMR (176 MHz, $CDCl_3$) δ 189.55, 152.14, 151.25, 145.98, 142.40, 140.25, 139.66, 139.05, 137.58, 137.08, 136.79, 135.05, 132.85, 128.66, 127.86, 127.10, 126.14, 123.64, 123.13, 123.08, 122.28, 121.43, 120.96, 120.51, 120.24, 55.51, 40.55, 31.62, 29.81, 23.92, 22.70, 14.12. HRMS-ASAP$^+$ calcd for $C_{38}H_{40}O_3S$ 576.2698; found $[M]^+$ 576.2695.

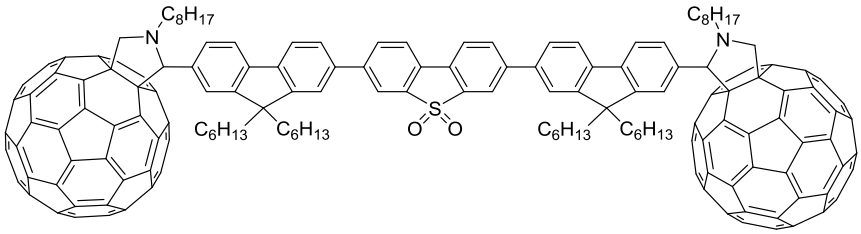

C_{60}-Fl-S-Fl-C_{60} (24): Fullerene (246 mg, 0.34 mmol) was heated to reflux in chlorobenzene (105 mL) for 15 minutes. Then N-octylglycine[5] containing NaCl (104 mg, 0.34 mmol) and **8** (40 mg, 0.04 mmol) was added to the reaction mixture. After 5 h heating at reflux and stirring, the solvent was removed at low pressure and the mixture was purified on silica gel by using CS_2 then a mixture of CS_2/DCM (1:2) as eluent. The compound **24** was isolated as a dark-brown solid (79 mg, 70%). Peak assignments in the ^{1}H NMR spectrum were based on previous reports for similar compounds.[6] ^{1}H NMR (400 MHz, $CDCl_3$+ 3 drops CS_2): 8.12 (2H, s), 8.06 (2H, s, br), 7.79-7.84 (4H, m), 7.75-7.70 (4H, m), 7.57-7.55 (6H, m), 5.17 (2H, s, Ha_1+Ha_2) 5.15 (2H, d, *J* = 9.4 Hz, Hb_1+Hb_2), 4.19 (2H, d, *J* = 9.4 Hz, $Hb_{1'}$+$Hb_{2'}$), 3.27 (2H, s, br, Hc_1+Hc_2), 2.26 (2H, m, $Hc_{1'}$+$Hc_{2'}$), 2.27-1.86 (12H, m), 1.68 (2H, m, br, He_1+He_2), 1.49-1.35 (18H, m, $He_{1'}$+$He_{2'}$+Hf-i), 1.15-0.68 (46H, m), 0.37 (2H,s, br), 0.22 (2H, s, br).

III. ^{1}H, ^{13}C NMR and Mass spectra.

BE-FI-S-CHO (4): ^{1}H (600 MHz, $CDCl_3$)

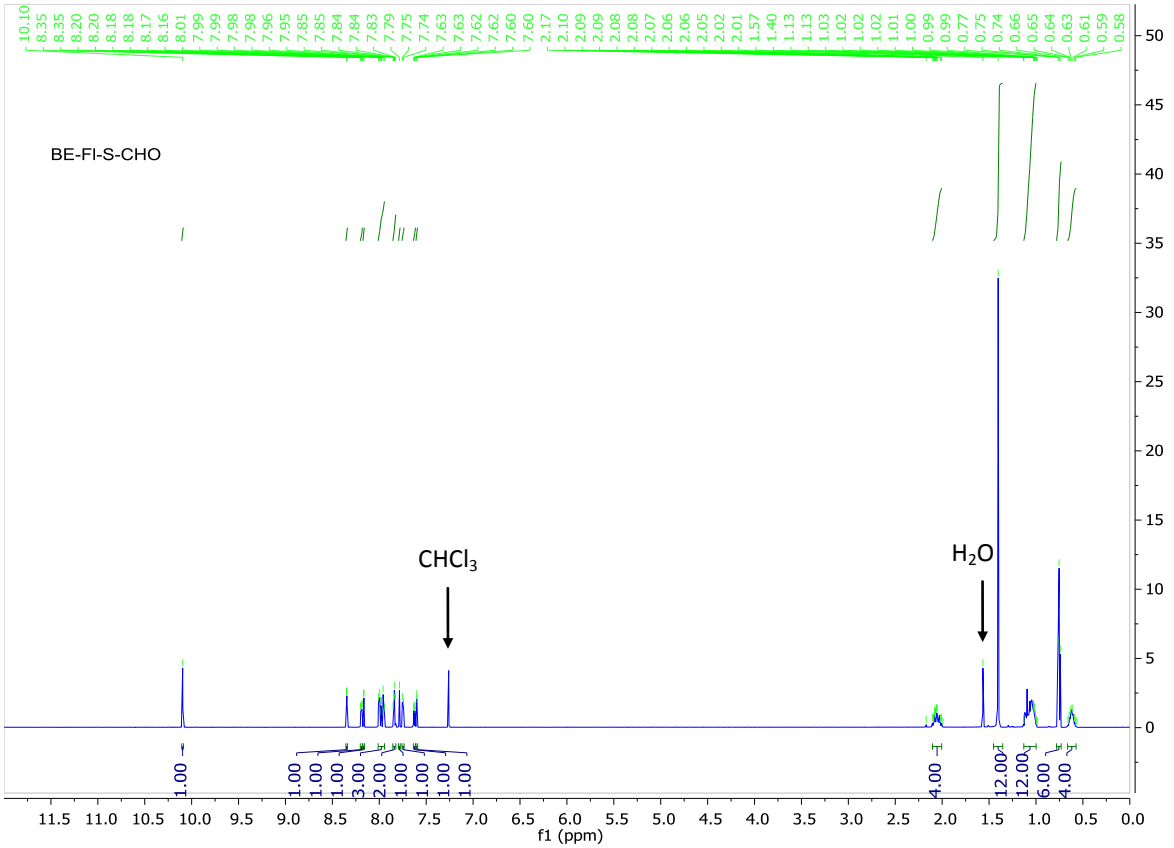

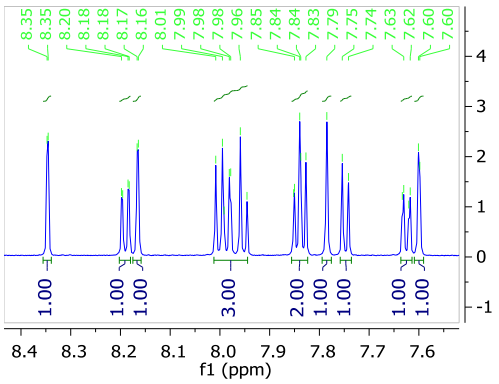

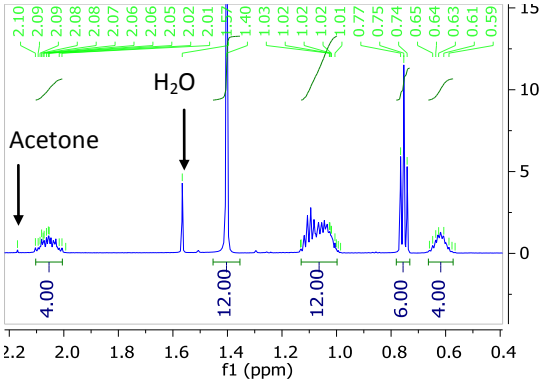

BE-Fl-S-CHO (4): ^{13}C (151 MHz, $CDCl_3$)

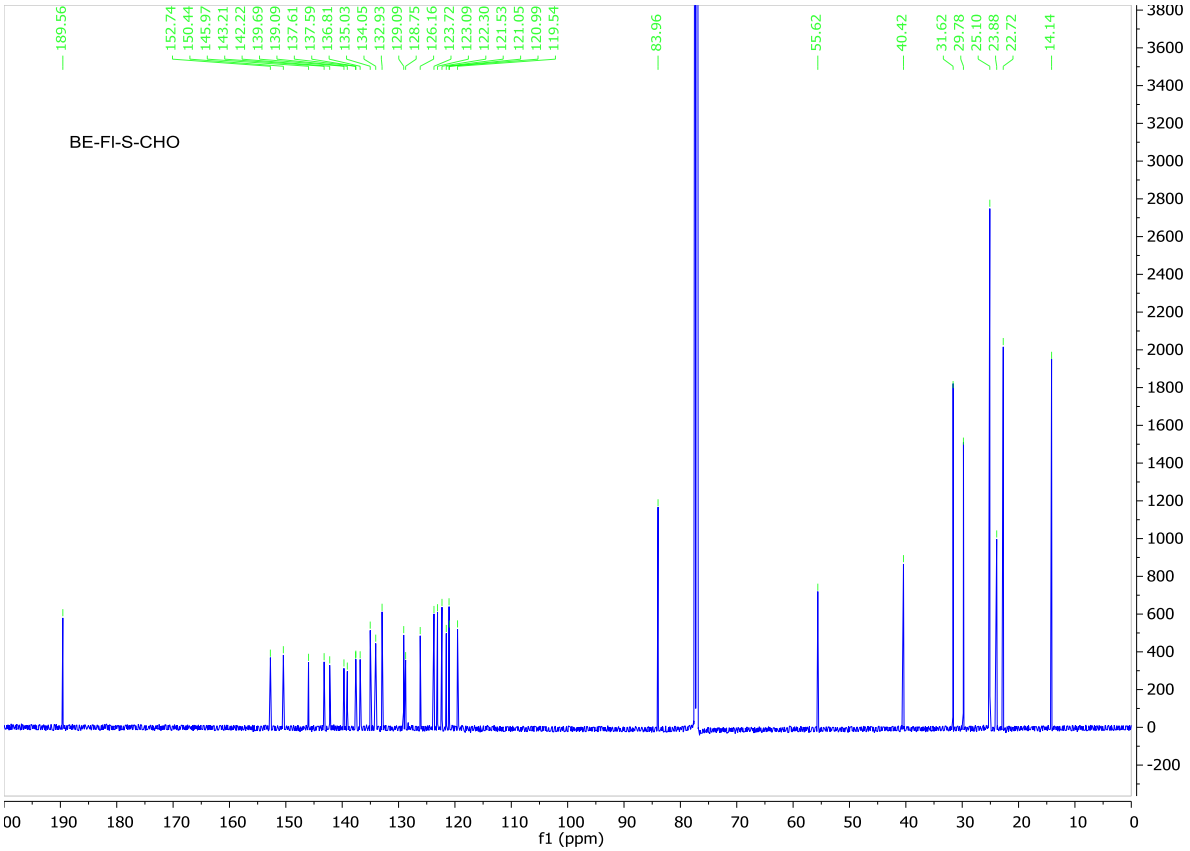

BE-Fl-S-CHO (4): LCT Premier

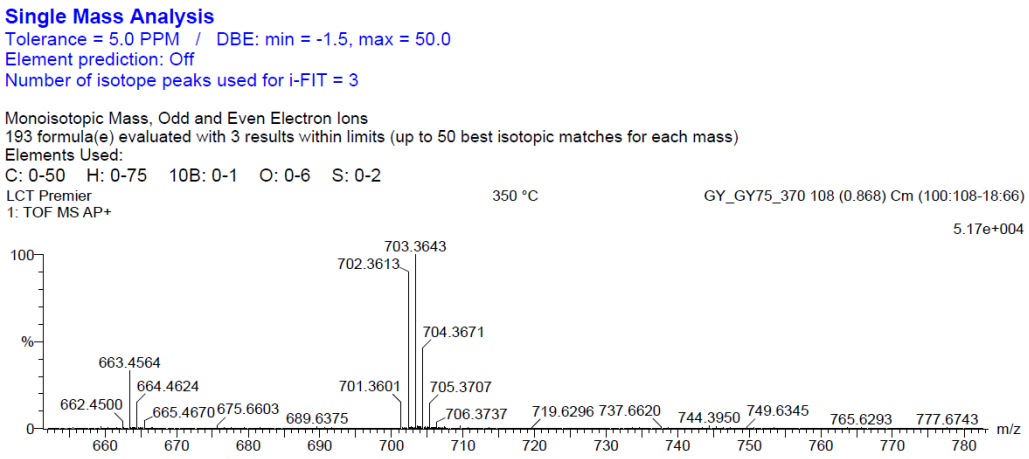

OHC-S-FI-S-CHO (5): ^{1}H (400 MHz, $CDCl_3$)

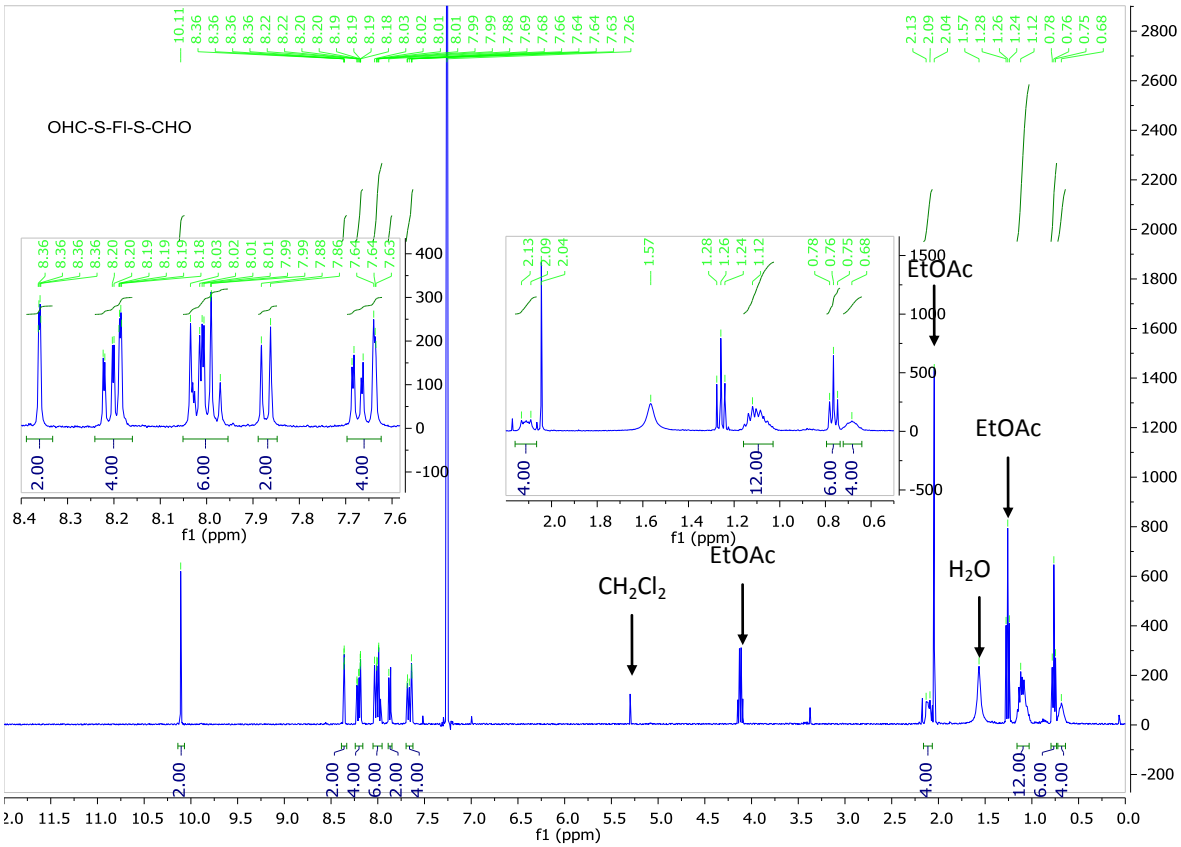

OHC-S-Fl-S-CHO (5): ^{13}C (101 MHz, $CDCl_3$)

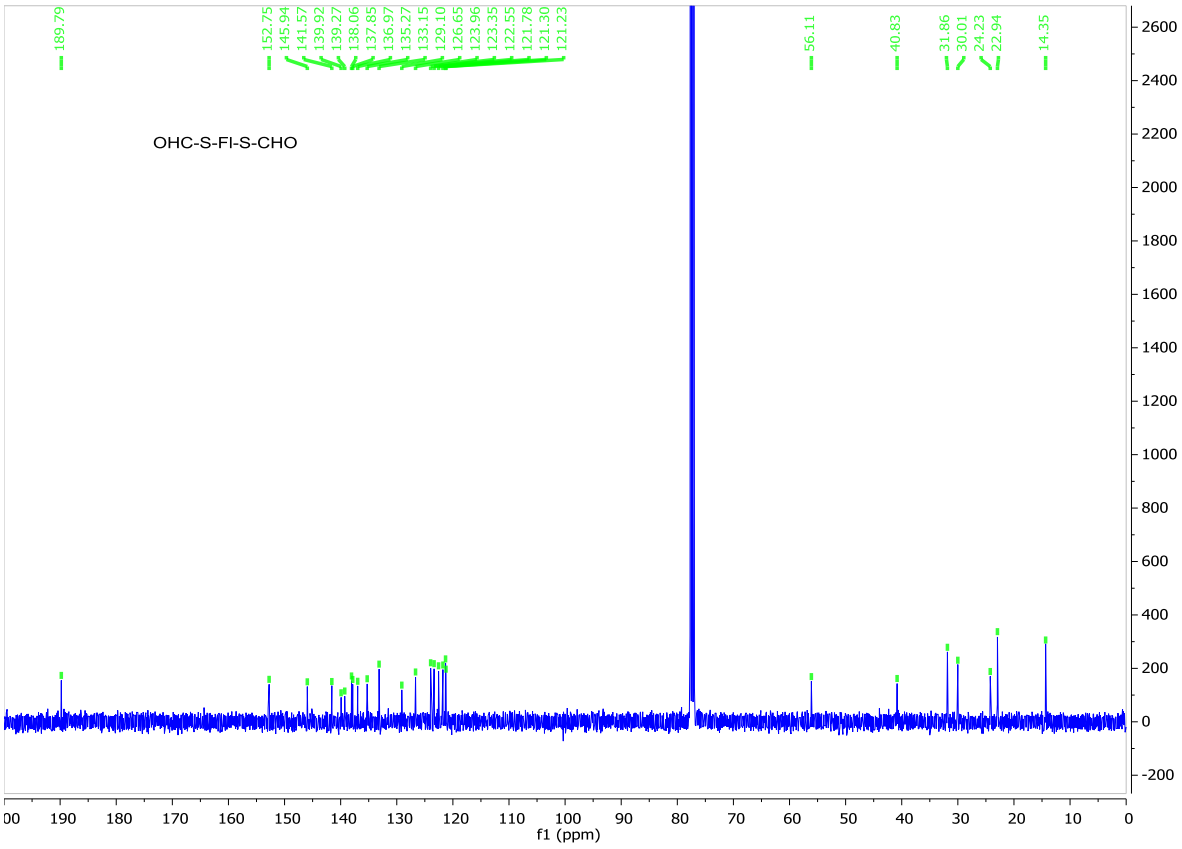

Br-S-Fl-CHO (7): ^{1}H (600 MHz, $CDCl_3$)

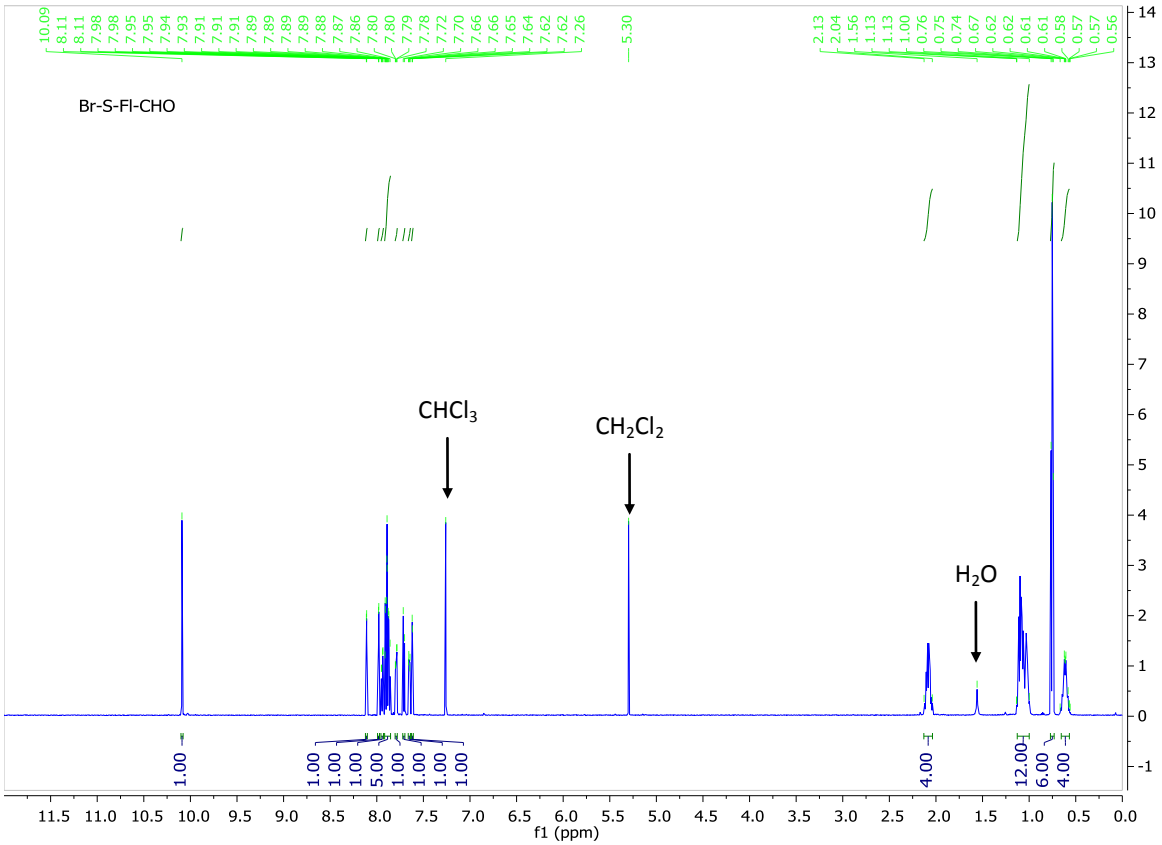

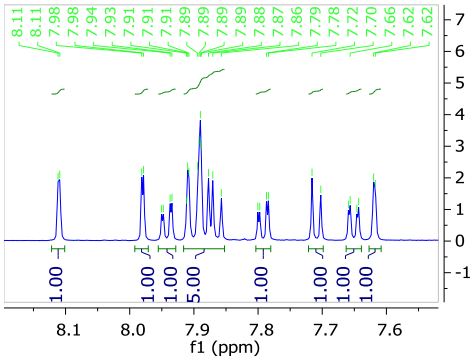

Br-S-Fl-CHO (7): ^{13}C (151 MHz, $CDCl_3$)

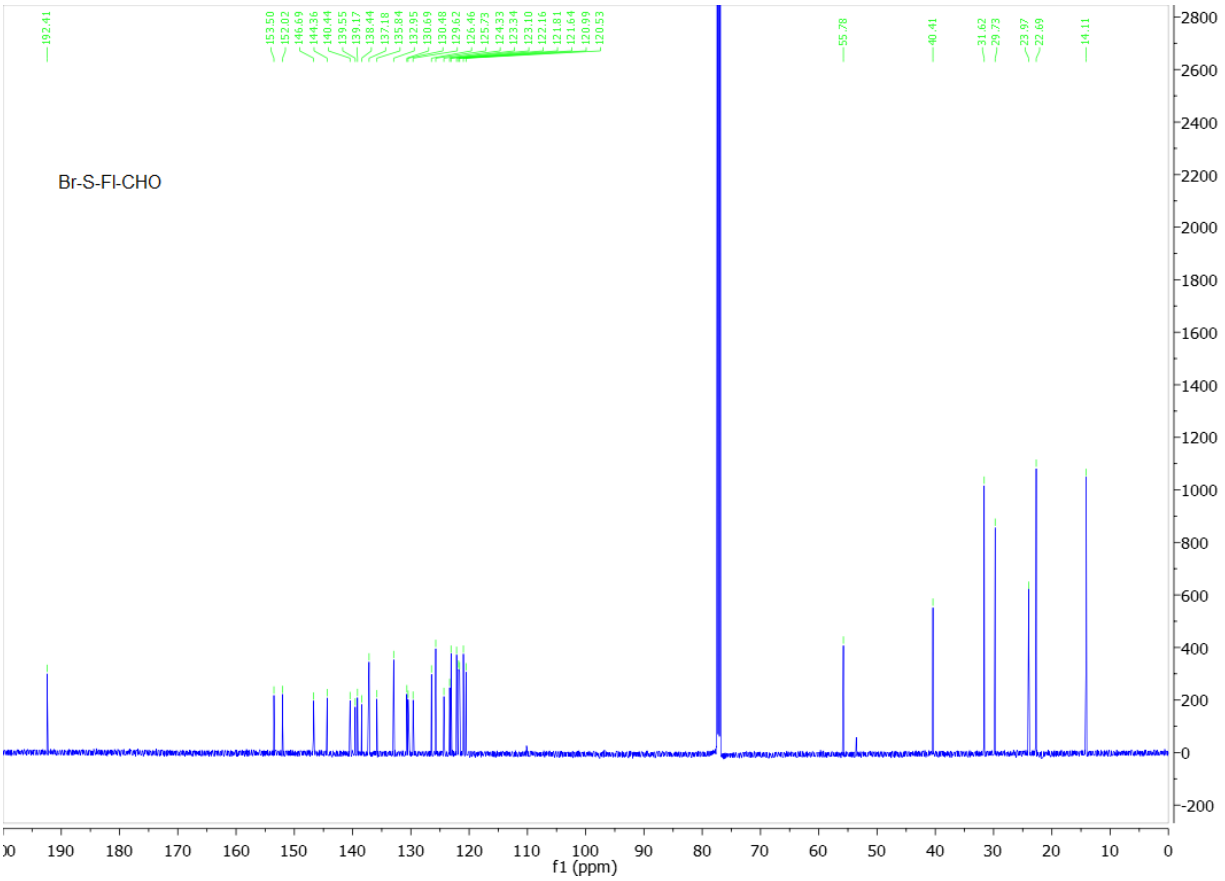

Br-S-Fl-CHO (7): LCT Premier

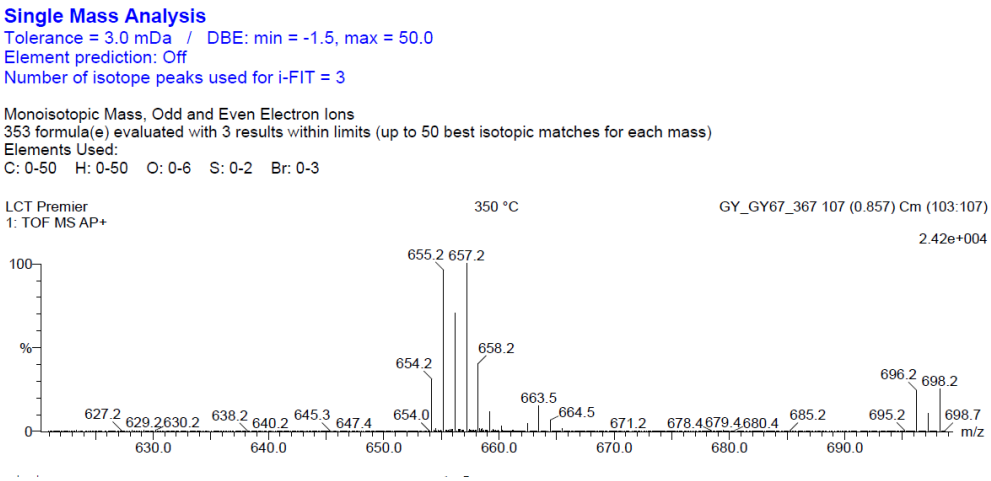

OHC-Fl-S-Fl-CHO (8): ^{1}H (400 MHz, $CDCl_3$)

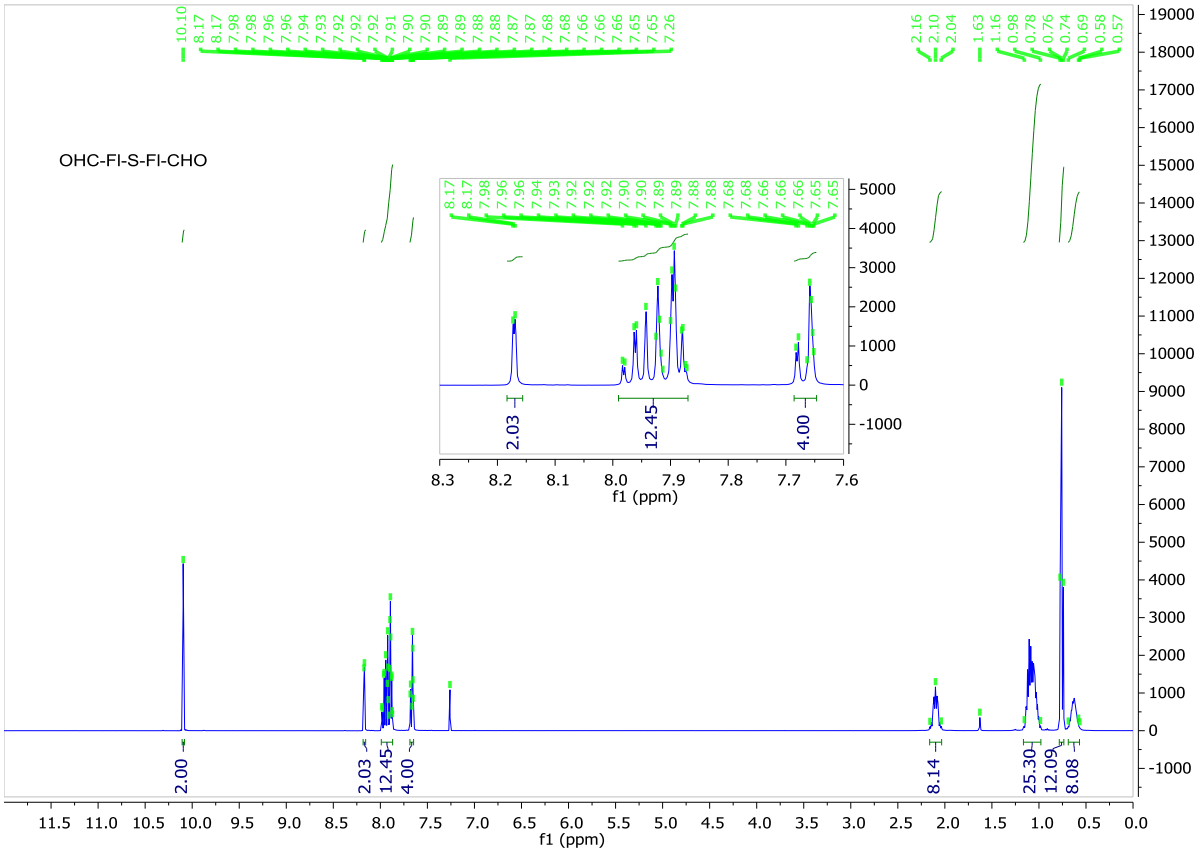

OHC-Fl-S-Fl-CHO (8): ^{13}C (101 MHz, $CDCl_3$)

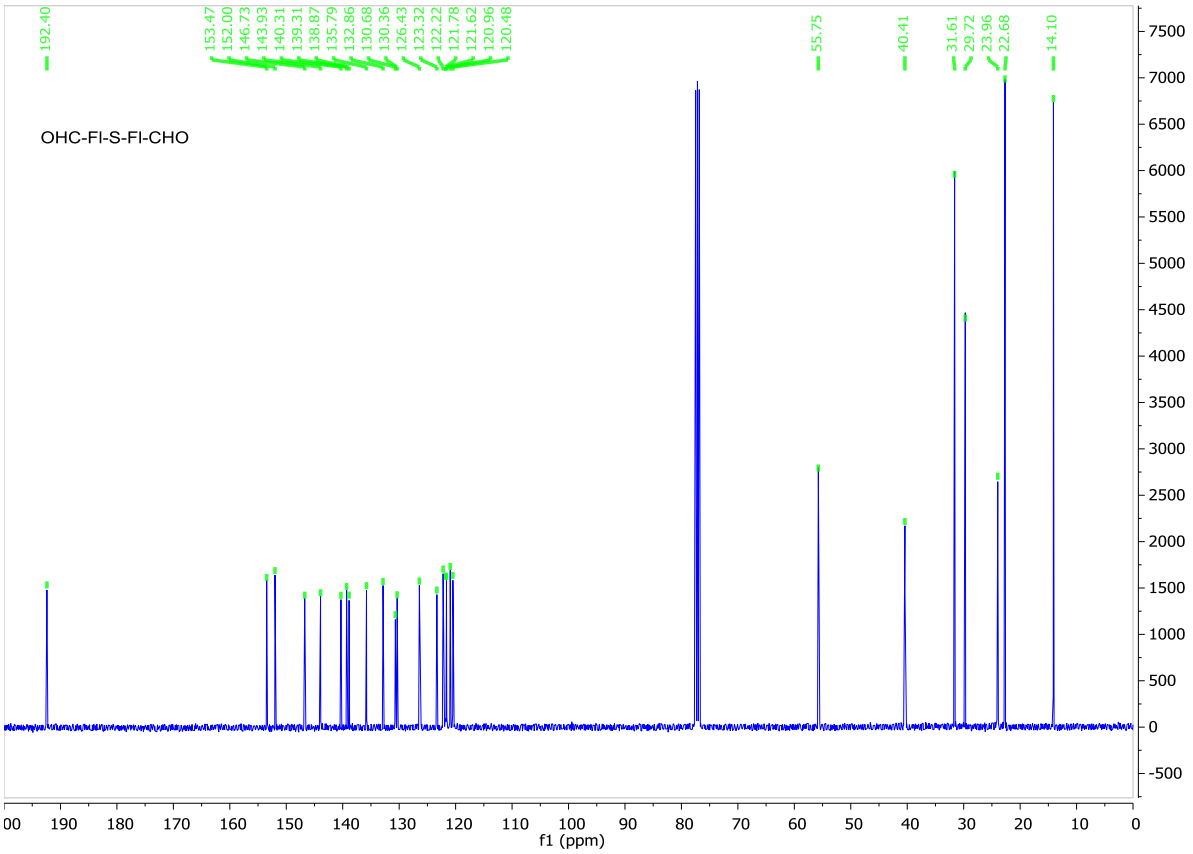

BE-FI-S-FI-CHO (10): ^{1}H (400 MHz, $CDCl_3$)

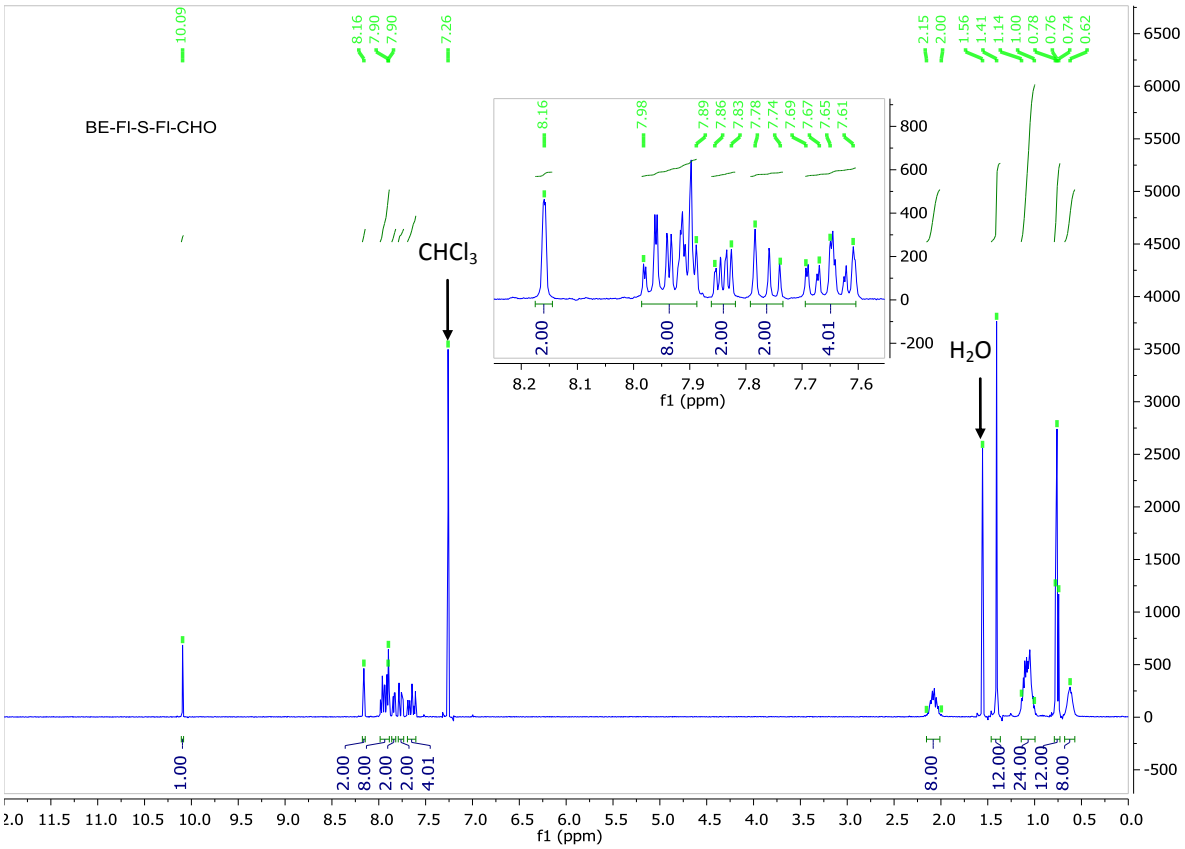

BE-Fl-S-Fl-CHO (10): ^{13}C (176 MHz, $CDCl_3$)

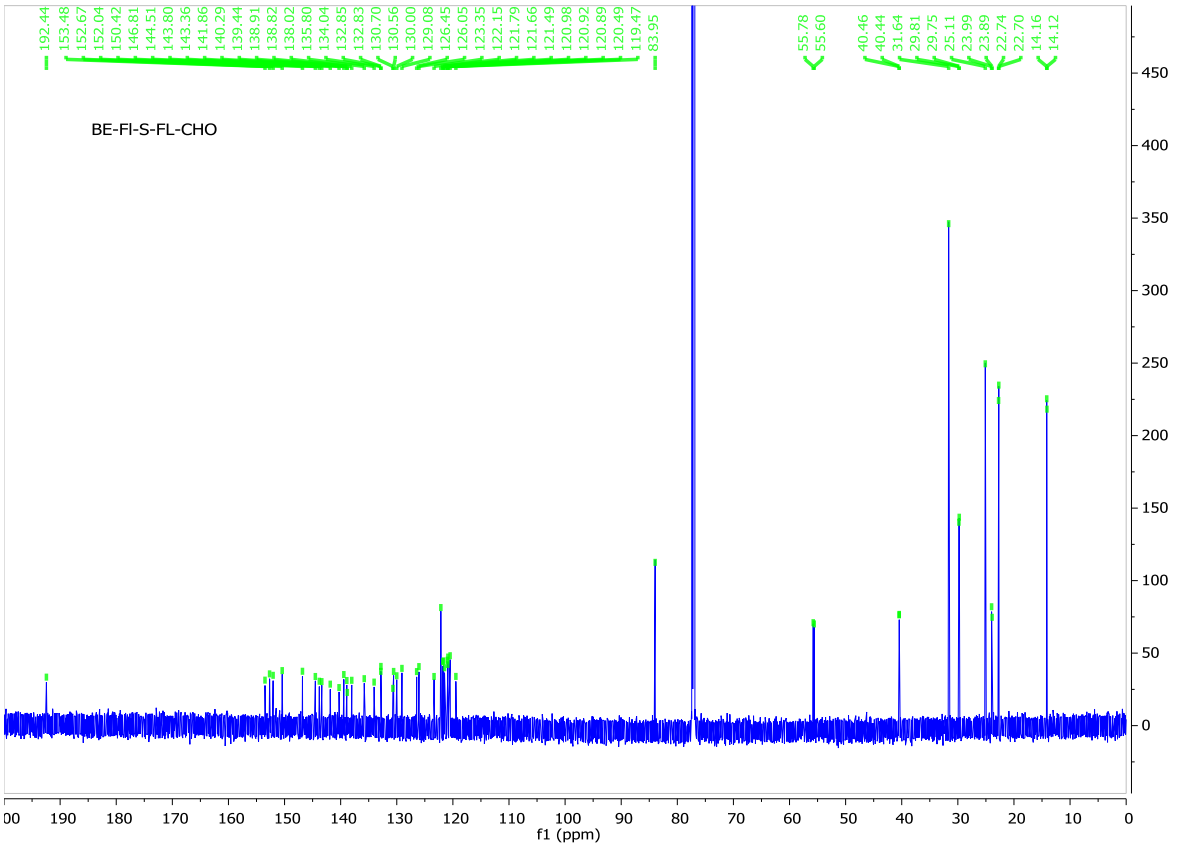

BE-Fl-S-Fl-CHO (10): LCT Premier

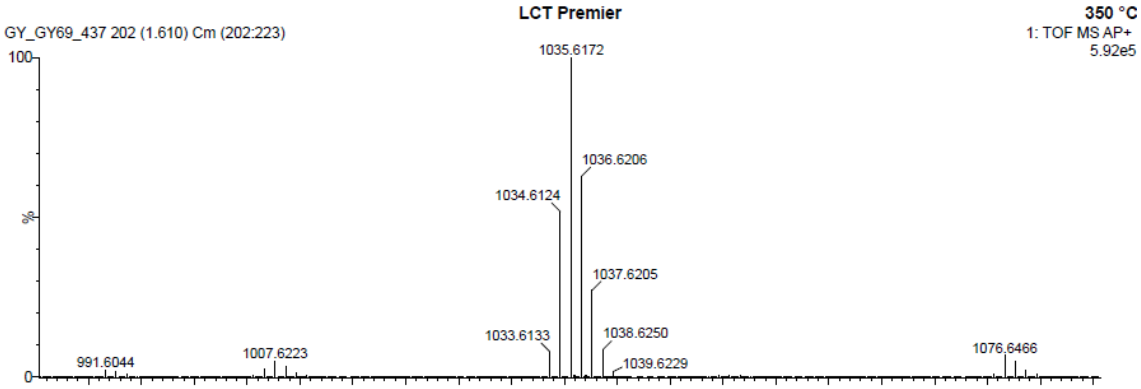

H_2P-Ph-Fl-S-CHO (12): ^{1}H (400 MHz, $CDCl_3$)

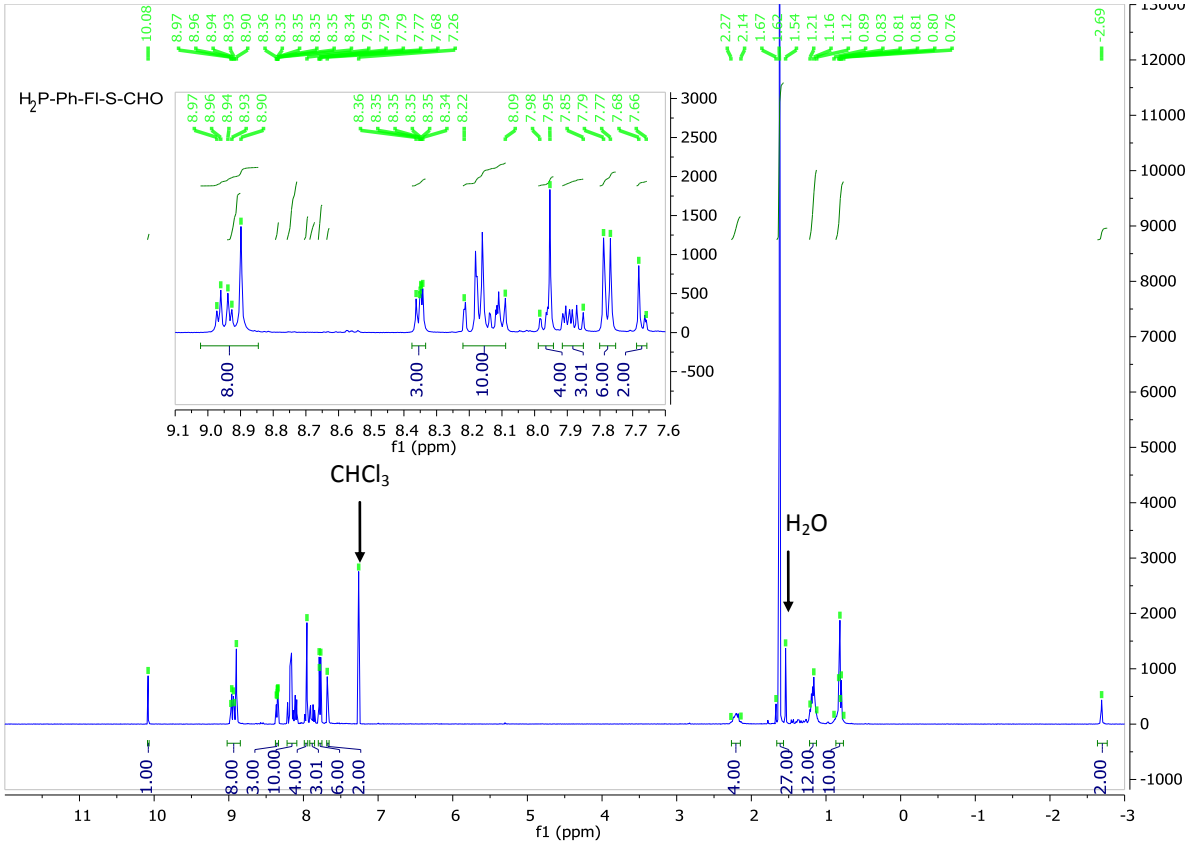

H_2P-Ph-Fl-S-CHO (12): ^{13}C (176 MHz, $CDCl_3$)

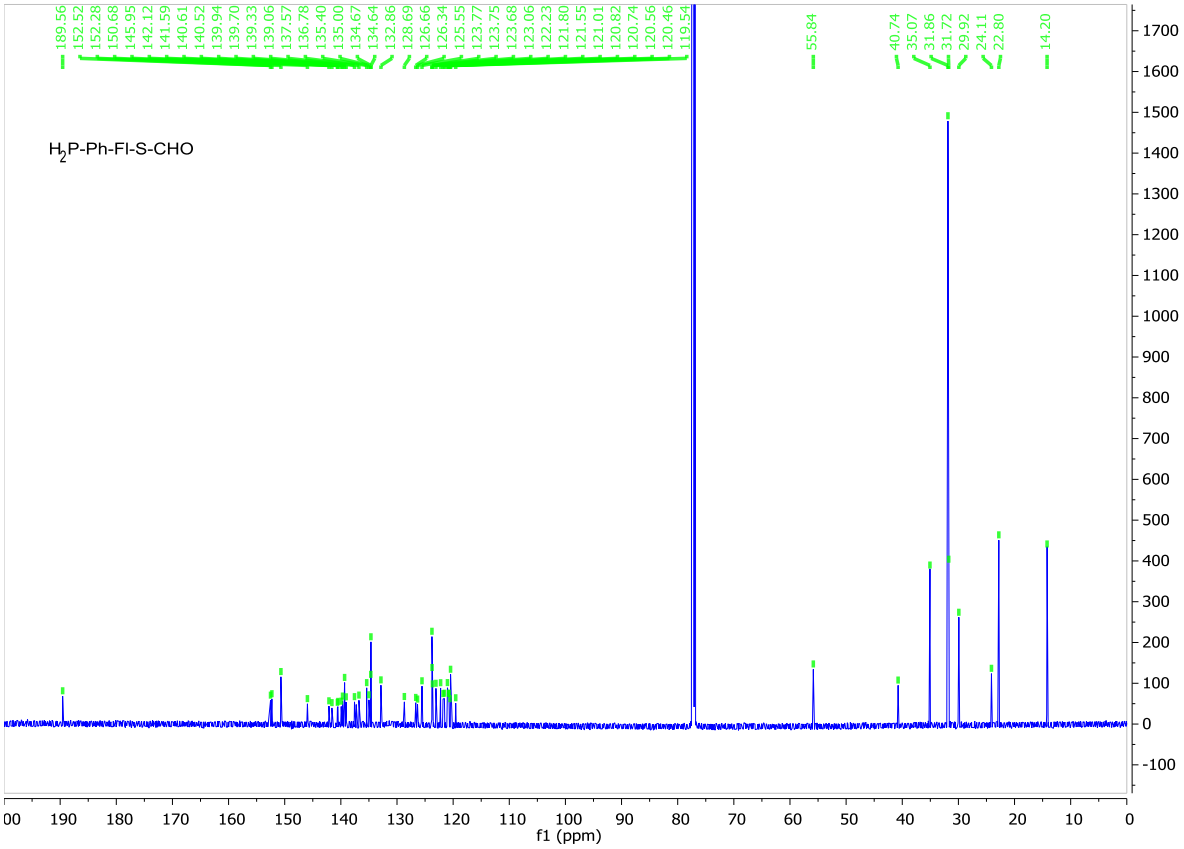

H_2P-Ph-Fl-S-CHO (12): MALDI-TOF MS

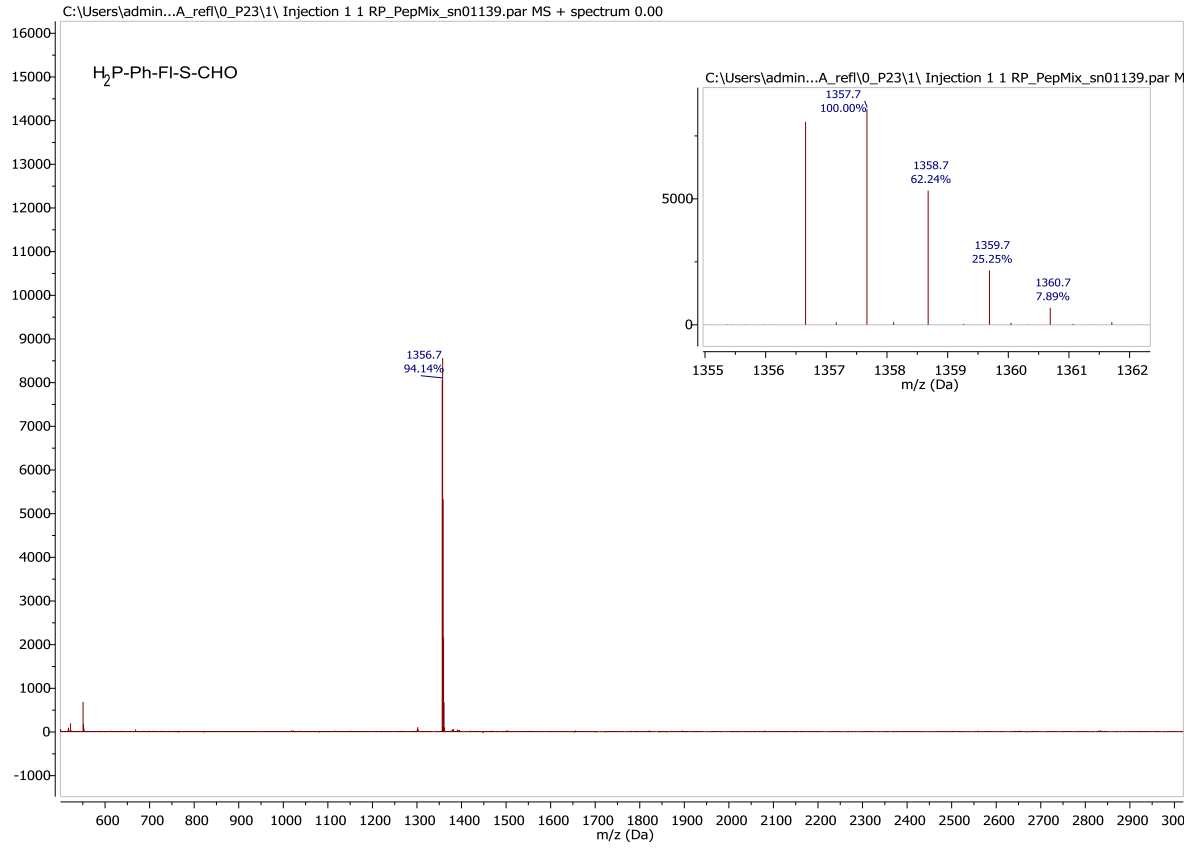

H_2P-Ph-S-Fl-CHO (13): ^{1}H (400 MHz, $CDCl_3$)

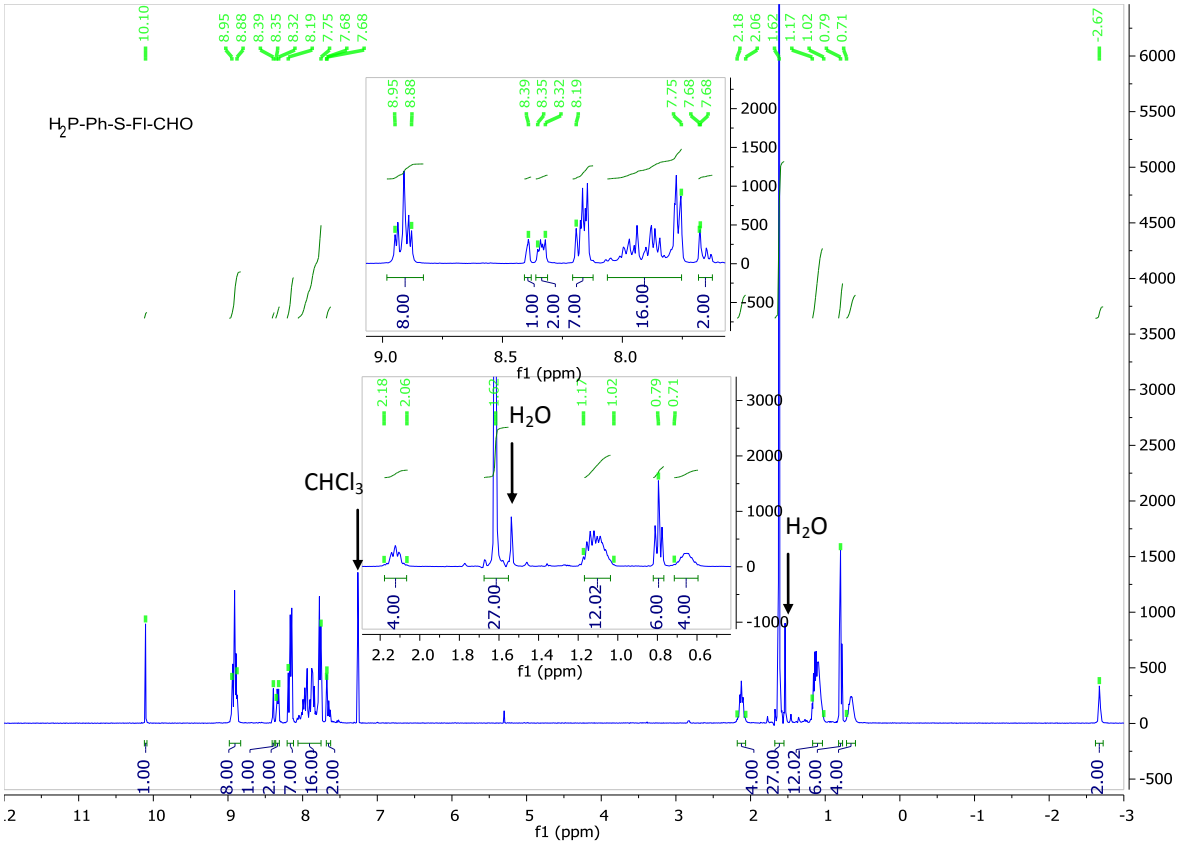

H_2P-Ph-S-Fl-CHO (13): ^{13}C (176 MHz, $CDCl_3$)

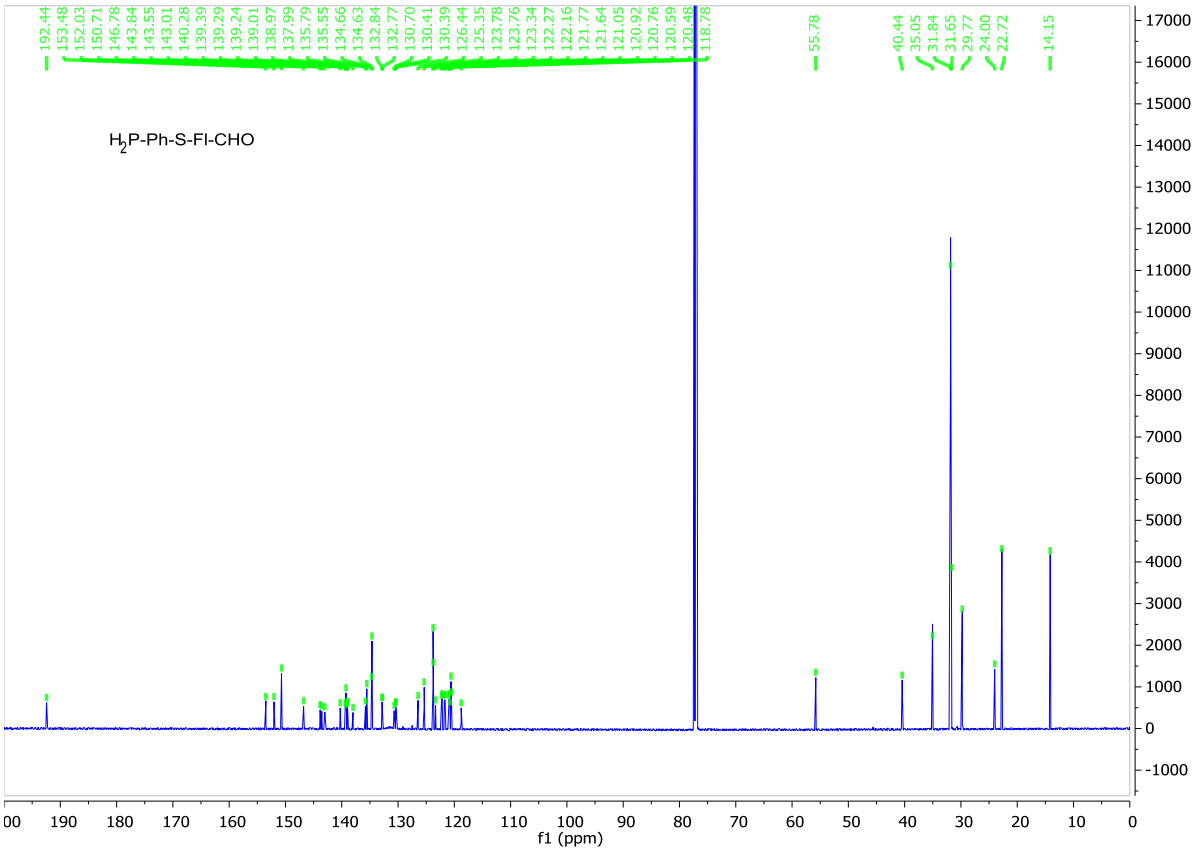

H_2P-Ph-S-Fl-CHO (13): MALDI-TOF MS

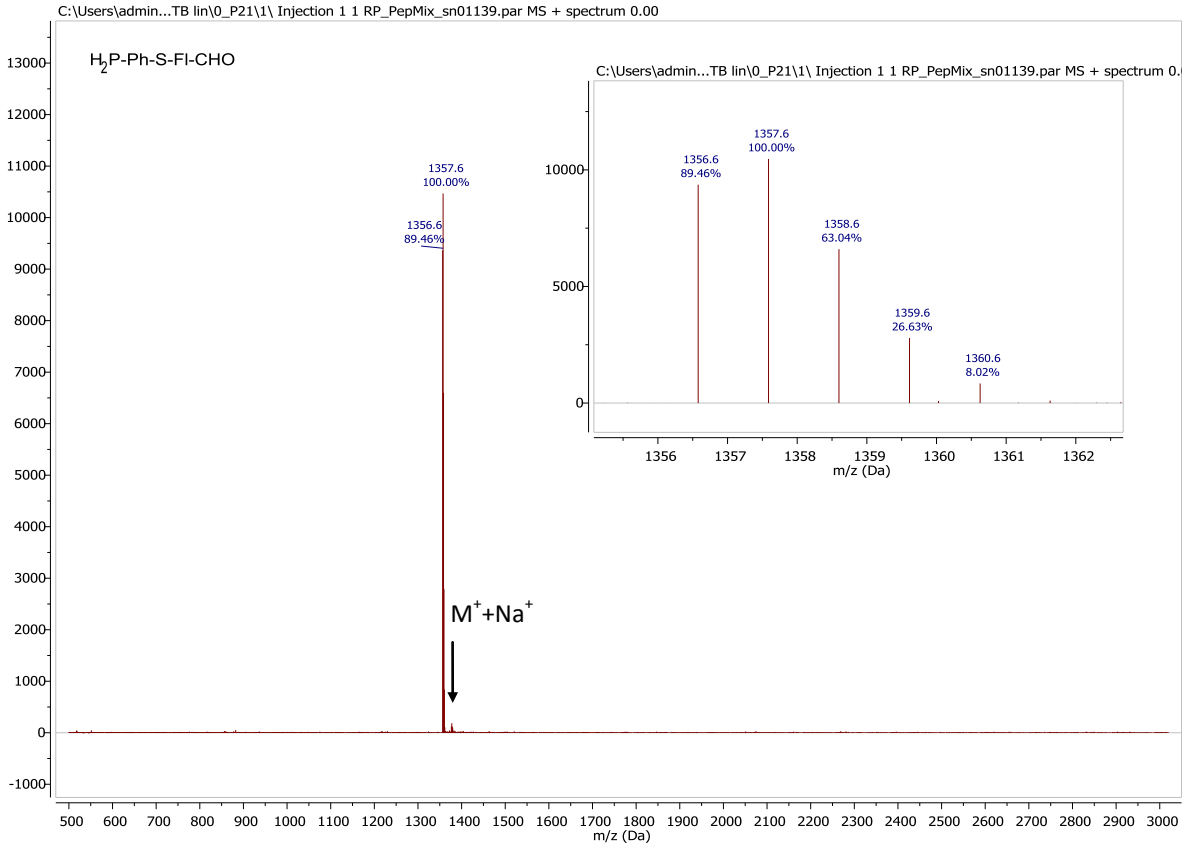

H_2P-Ph-Fl-S-Fl-CHO (14): ^{1}H (400 MHz, $CDCl_3$)

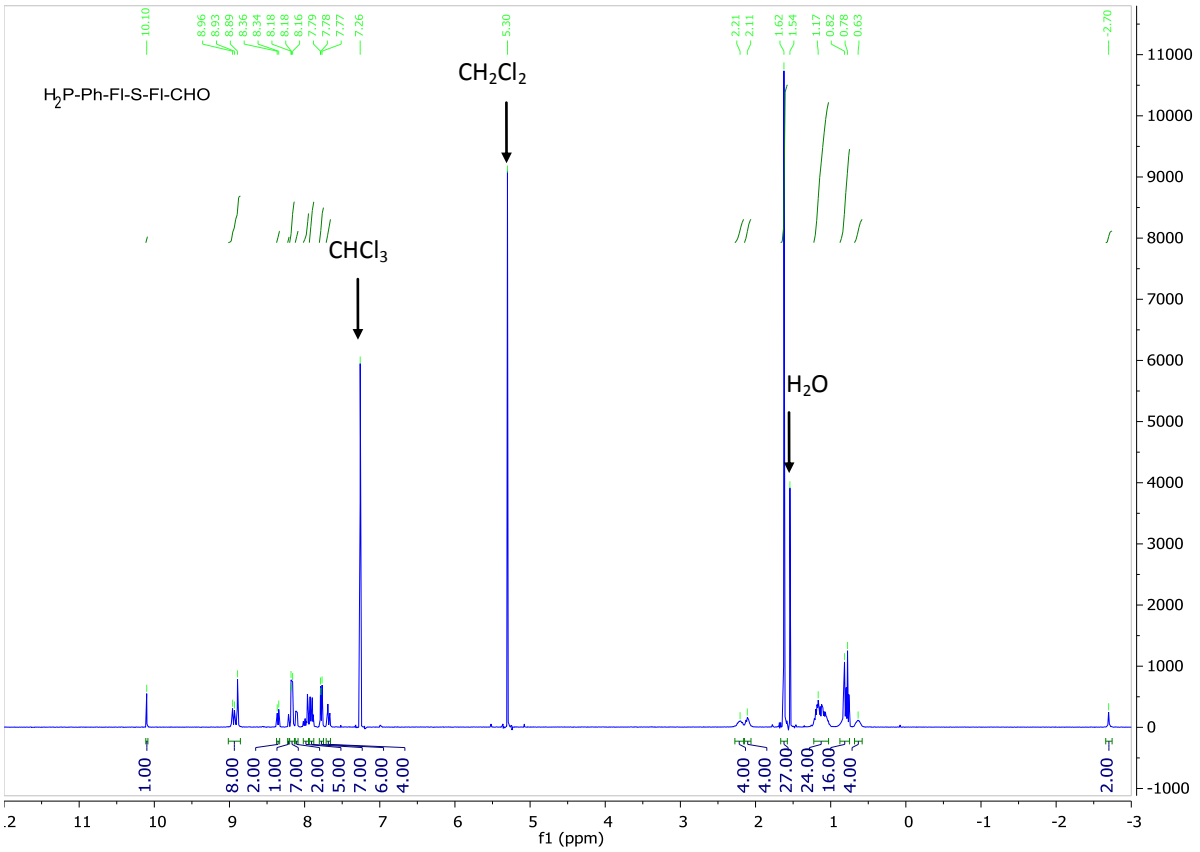

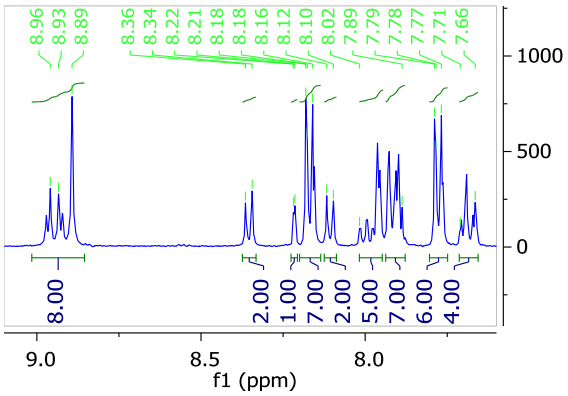

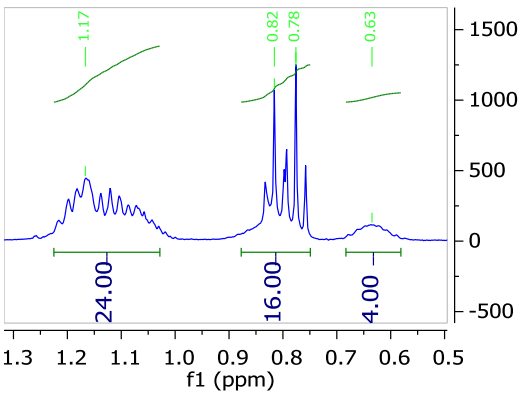

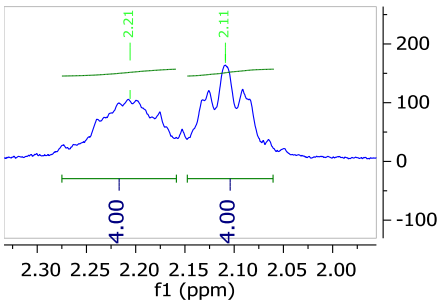

H_2P-Ph-Fl-S-Fl-CHO (14): ^{13}C (176 MHz, $CDCl_3$)

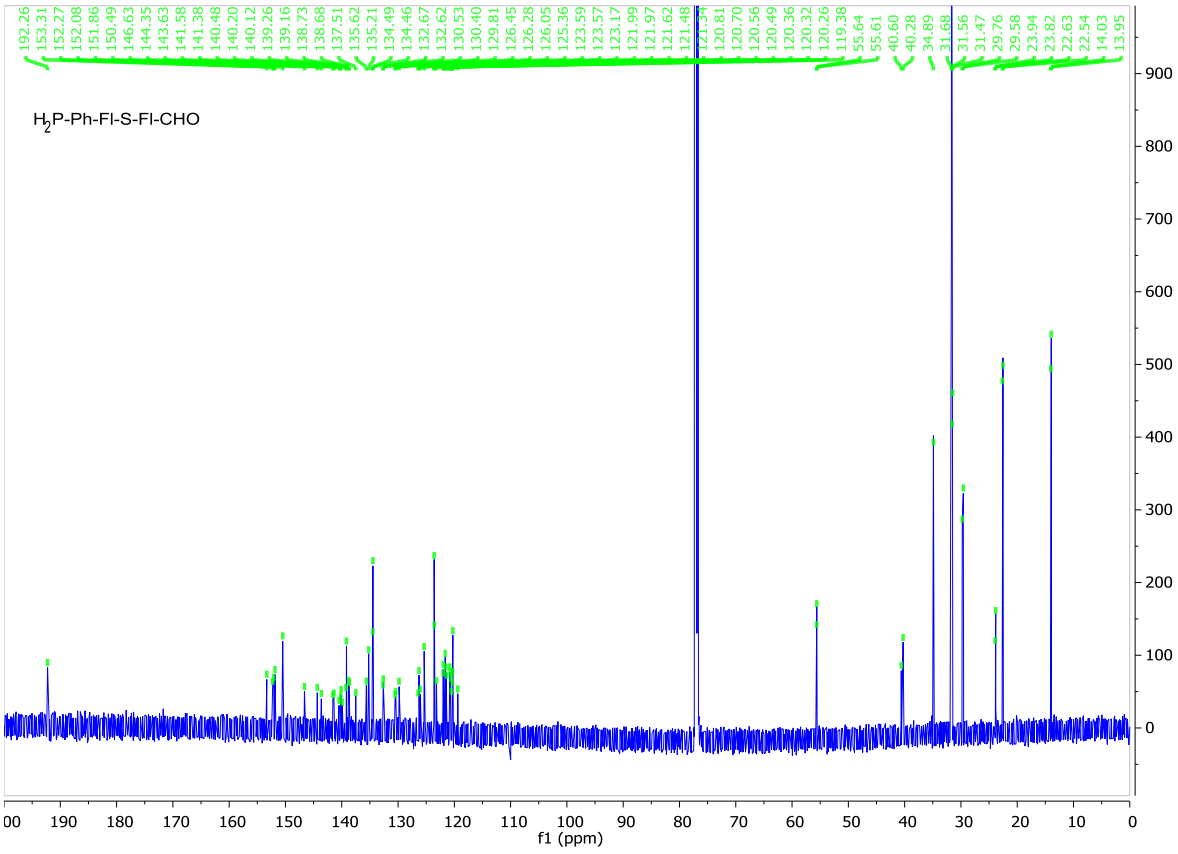

H_2P-Ph-Fl-S-Fl-CHO (14): MALDI-TOF MS

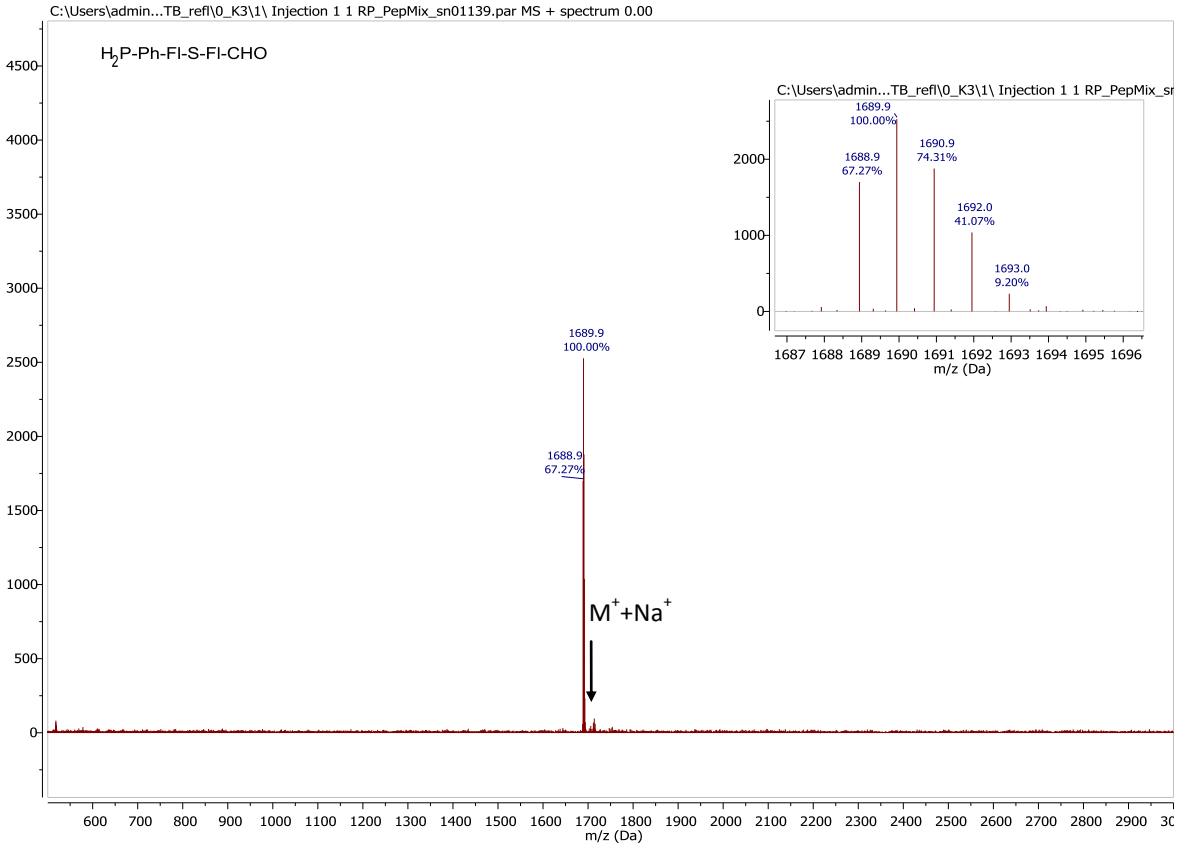

ZnP-Ph-Fl-S-CHO (15): ^{1}H (400 MHz, $CDCl_3$)

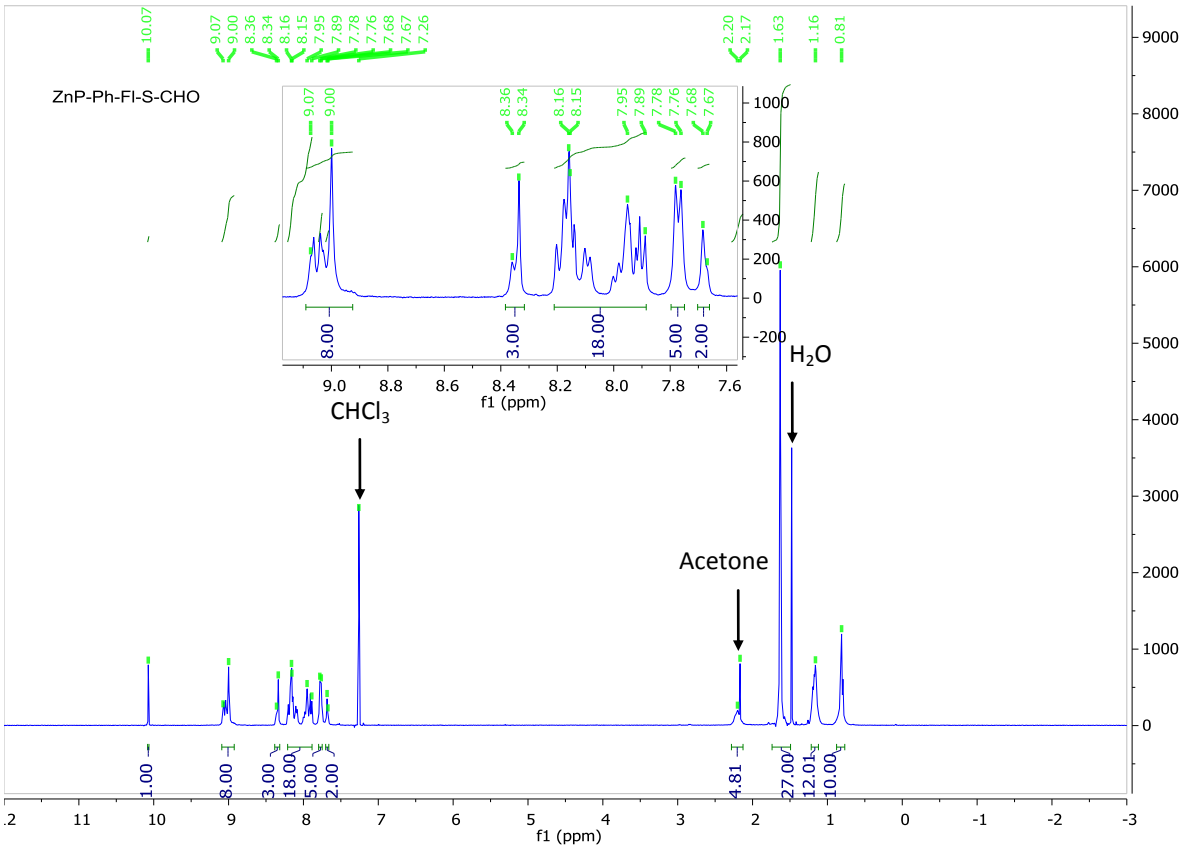

ZnP-Ph-Fl-S-CHO (15): MALDI-TOF MS

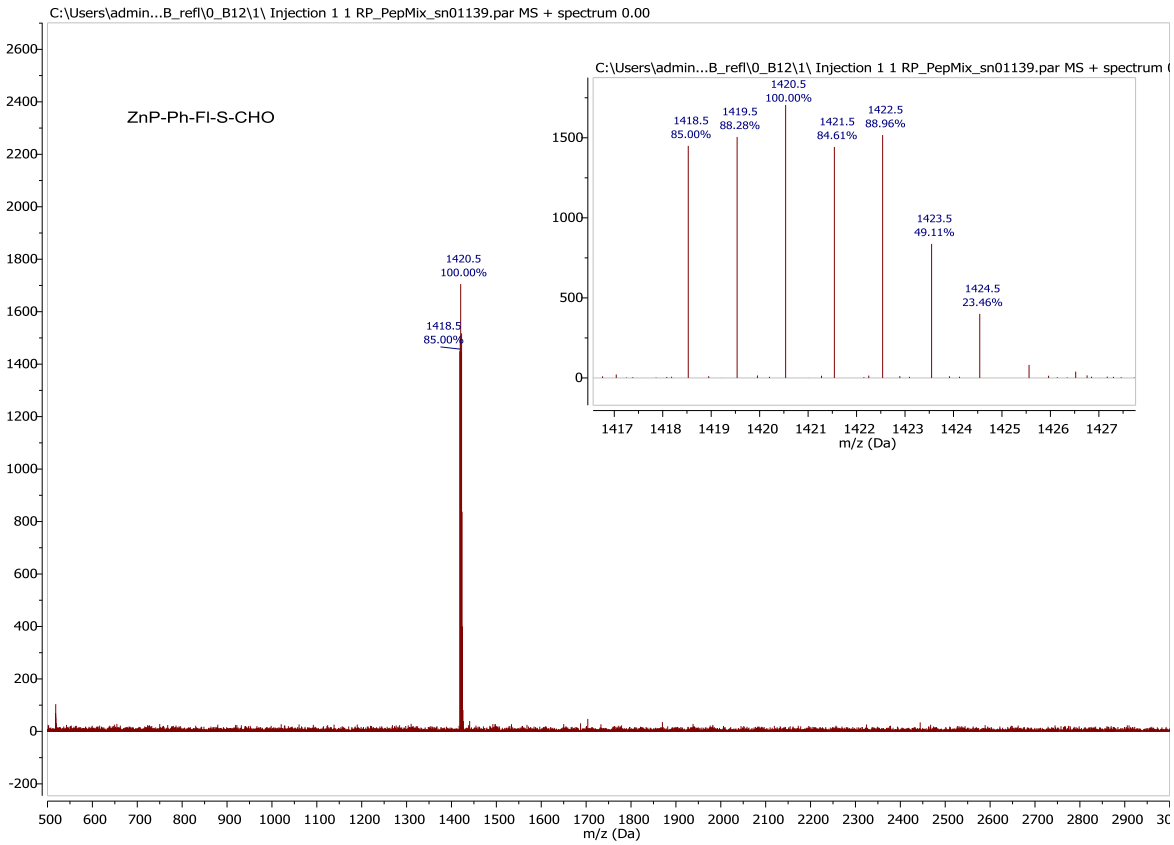

ZnP-Ph-S-Fl-CHO (16): ^{1}H (400 MHz, $CDCl_3$)

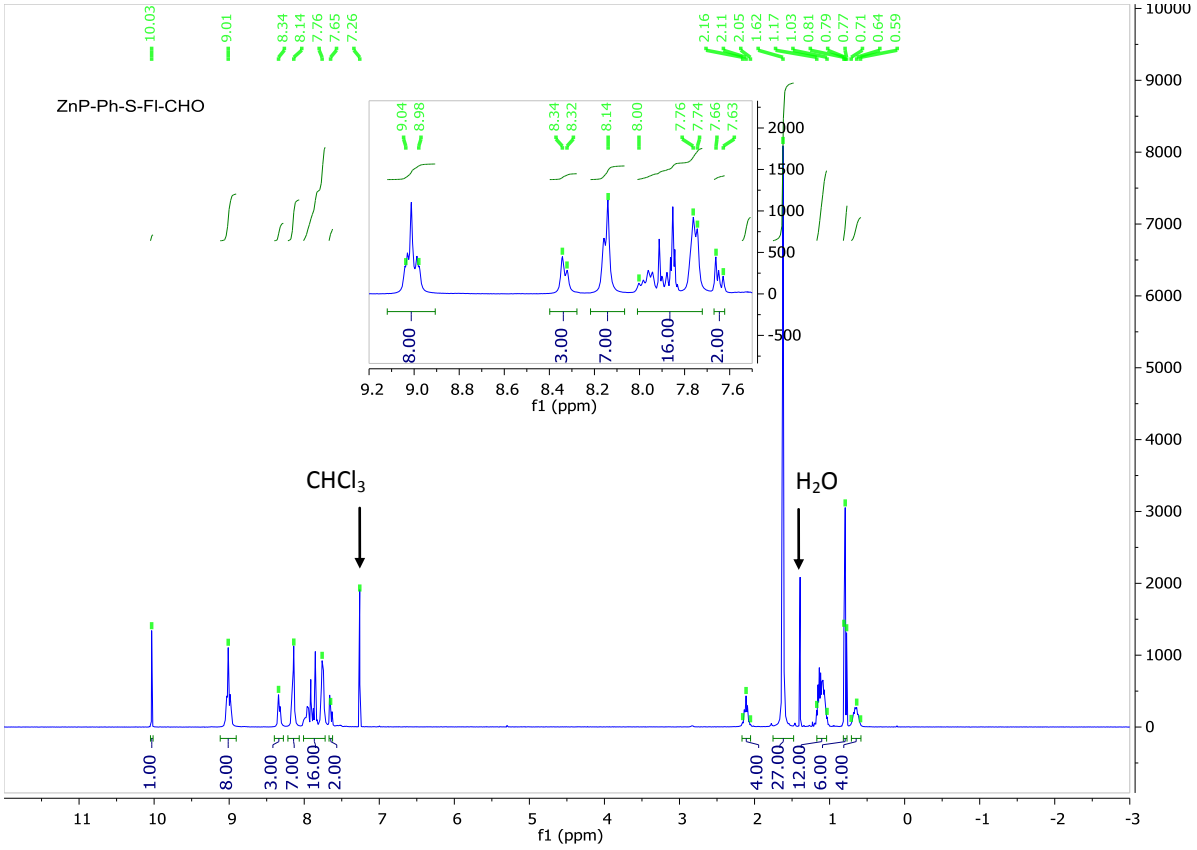

ZnP-Ph-S-Fl-CHO (16): MALDI-TOF MS

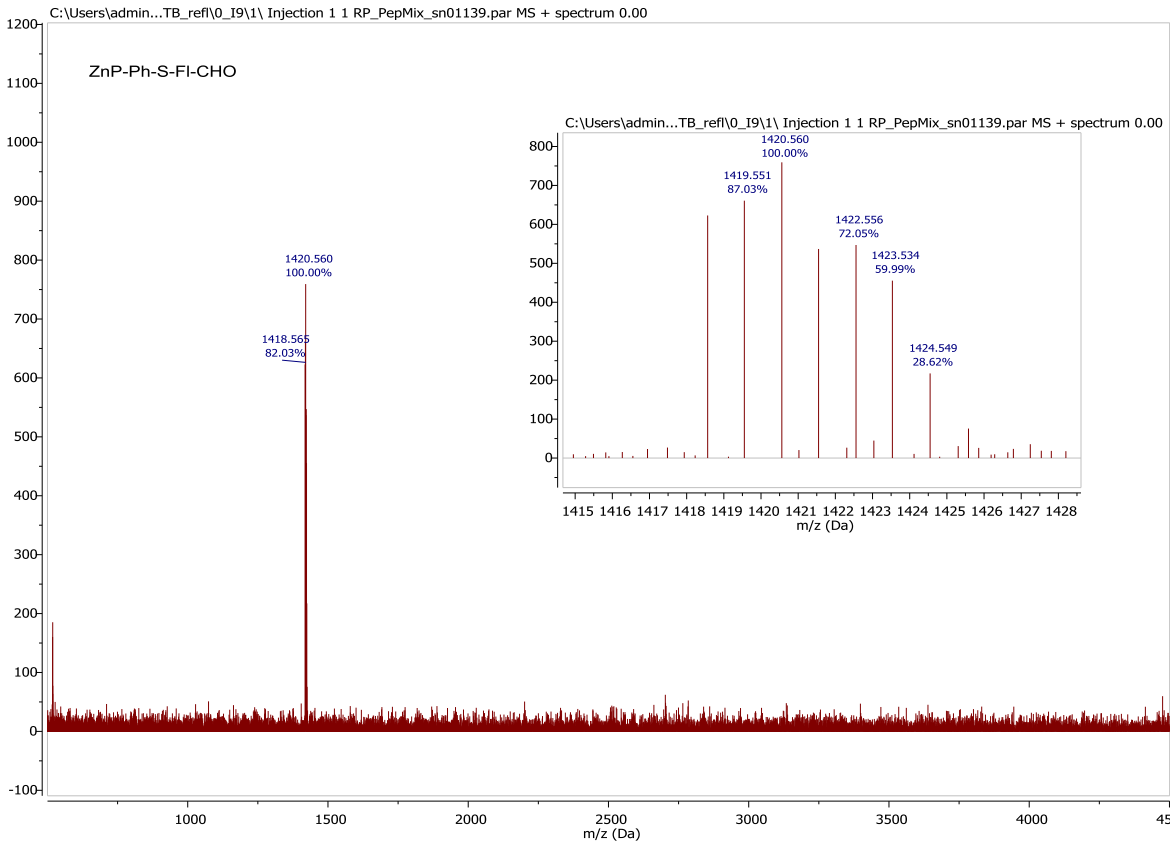

ZnP-Ph-Fl-S-Fl-CHO (17): ^{1}H (700 MHz, $CDCl_3$)

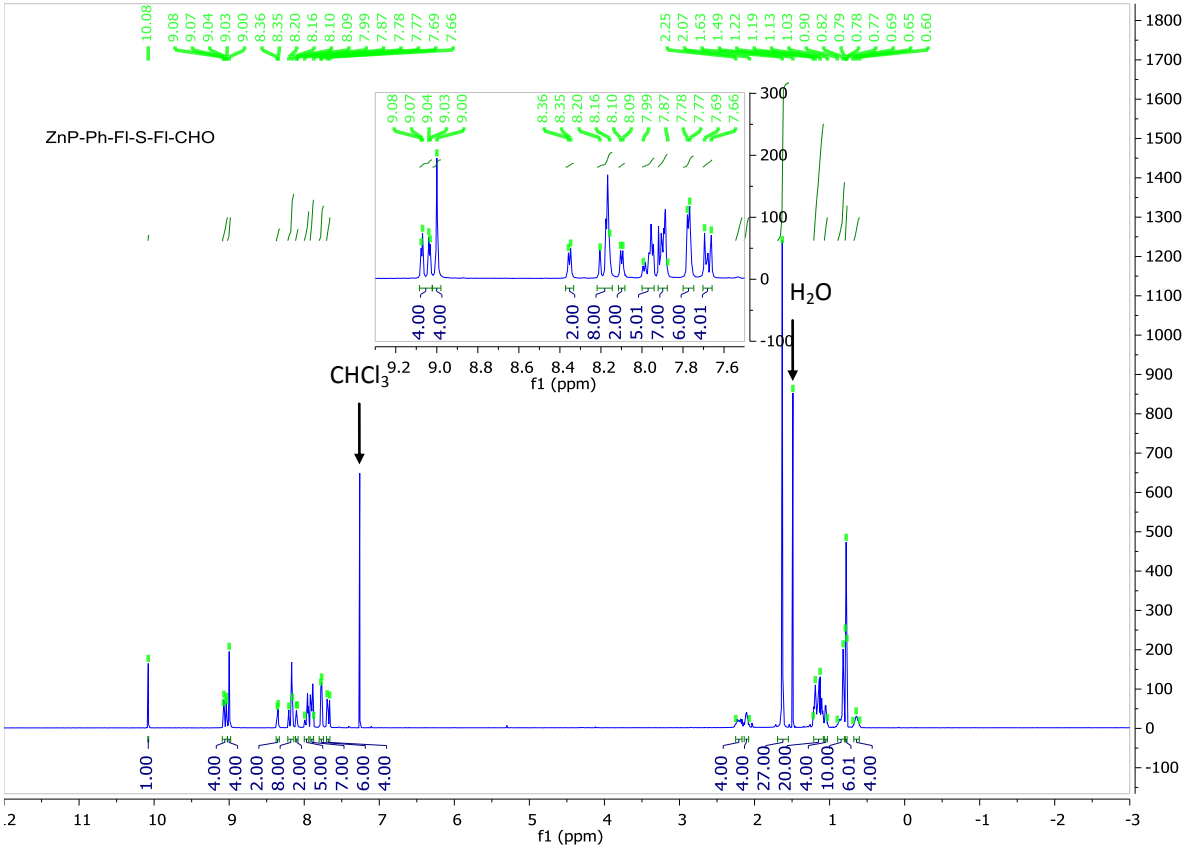

ZnP-Ph-Fl-S-Fl-CHO (17): MALDI-TOF MS

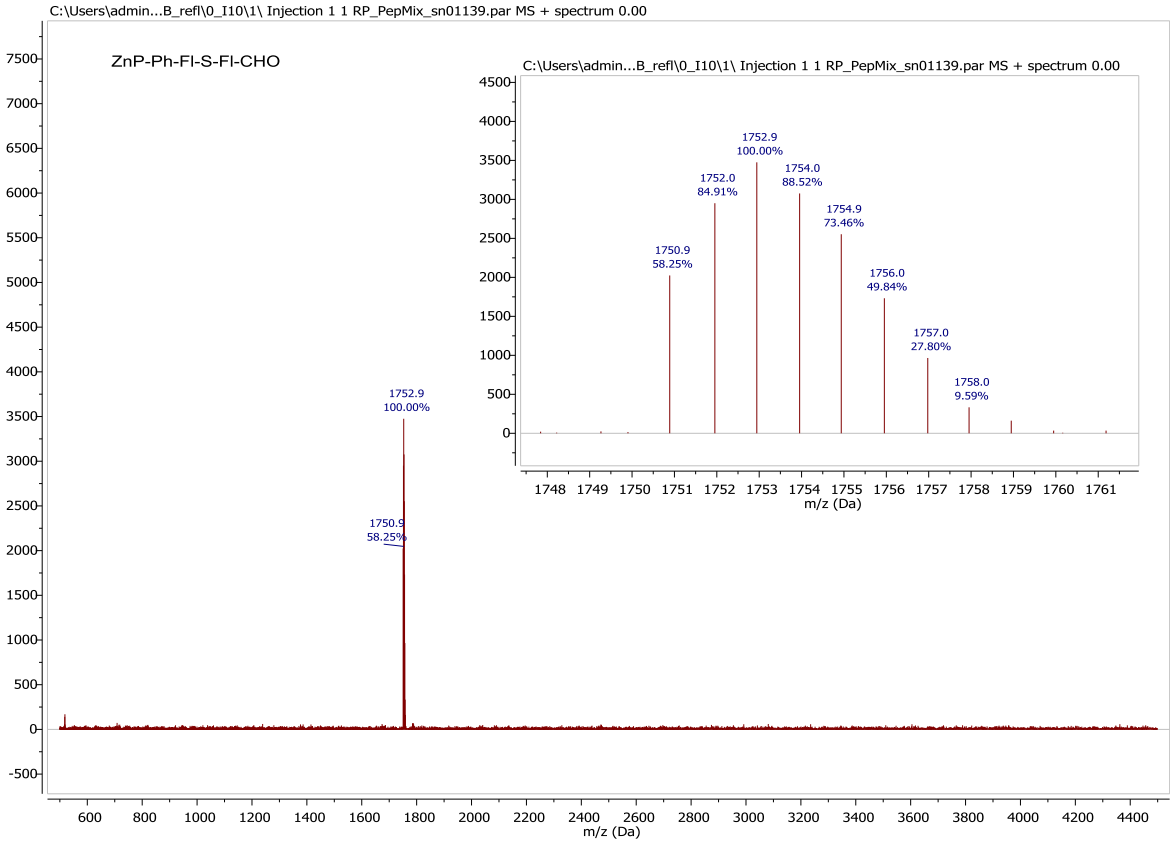

ZnP-Ph-Fl-S-C60 (18): ^{1}H (400 MHz, $CDCl_3$)

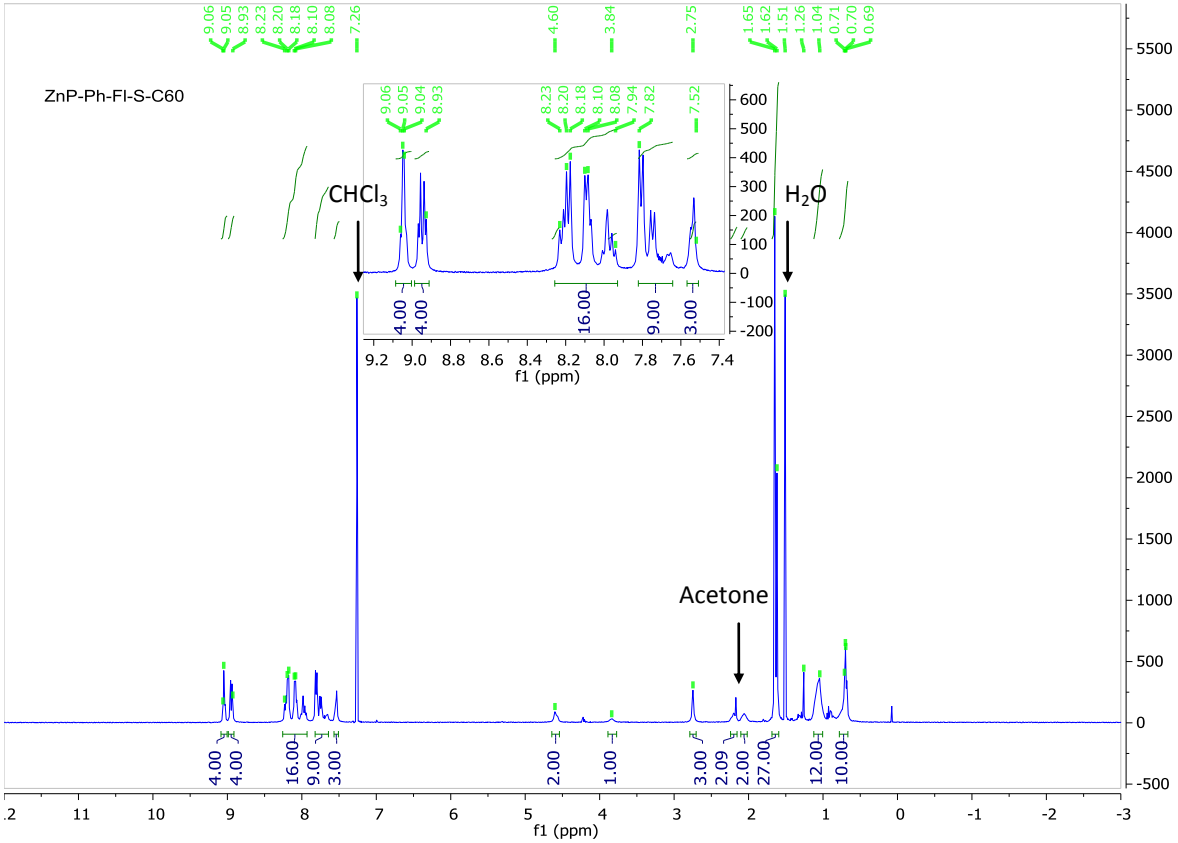

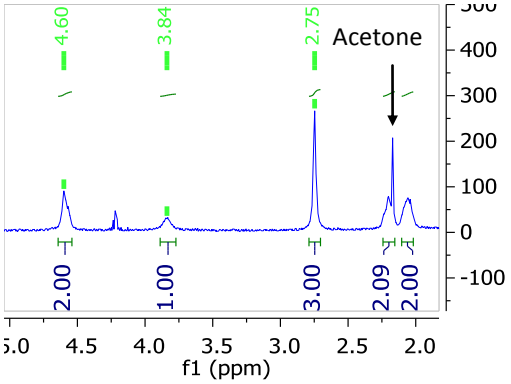

ZnP-Ph-Fl-S-C60 (18): MALDI-TOF MS

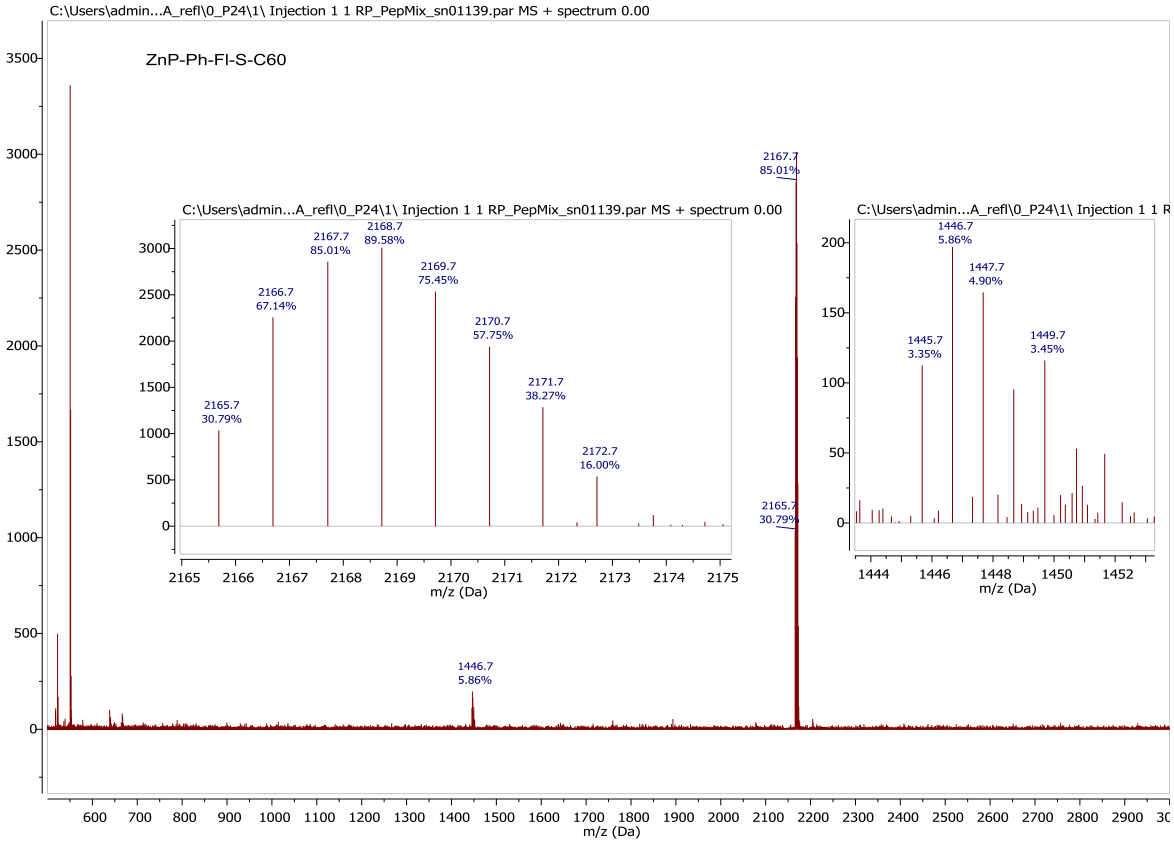

ZnP-Ph-S-Fl-C60 (19): ^{1}H (400 MHz, $CDCl_3$)

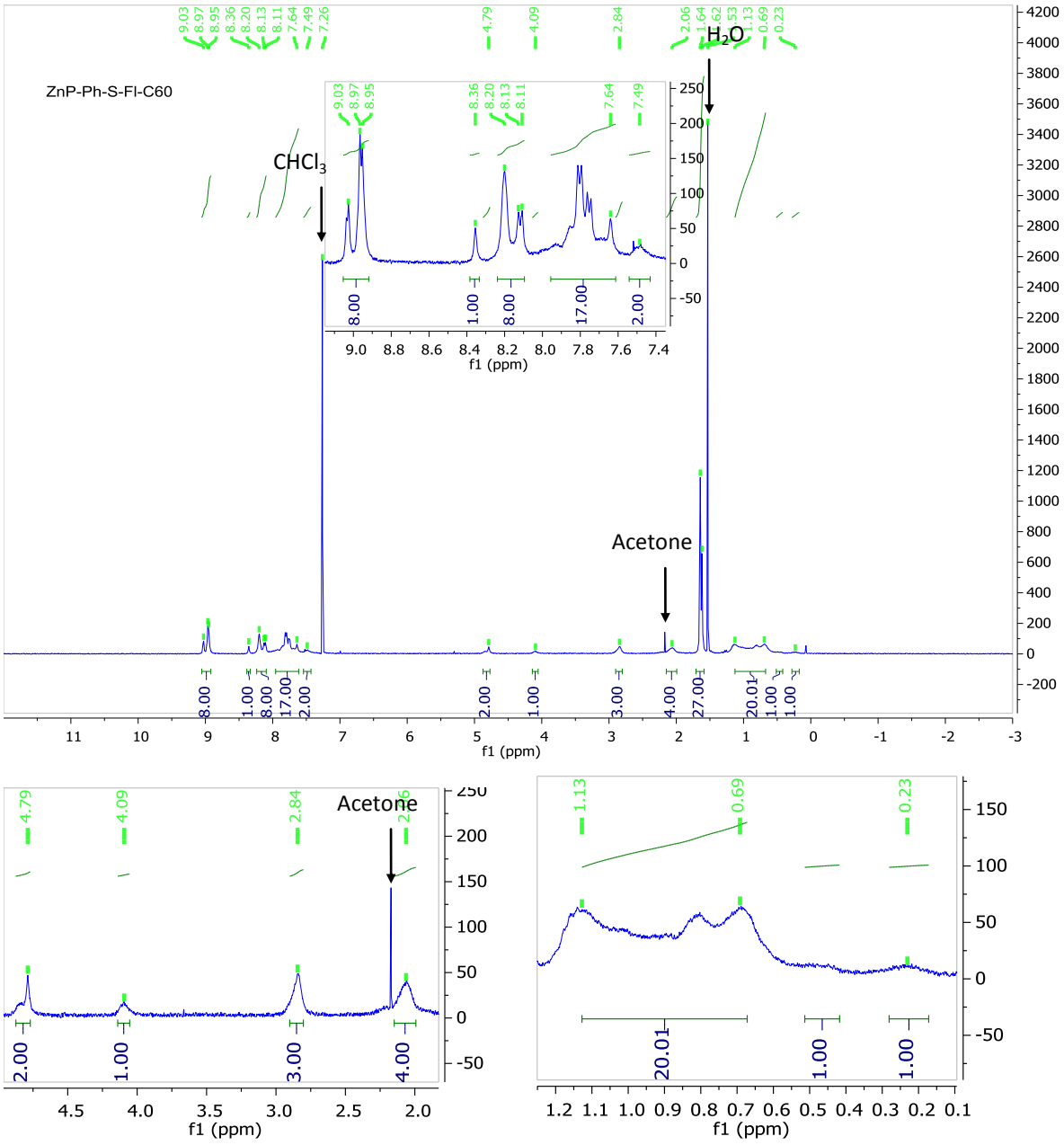

ZnP-Ph-S-Fl-C60 (19): MALDI-TOF MS

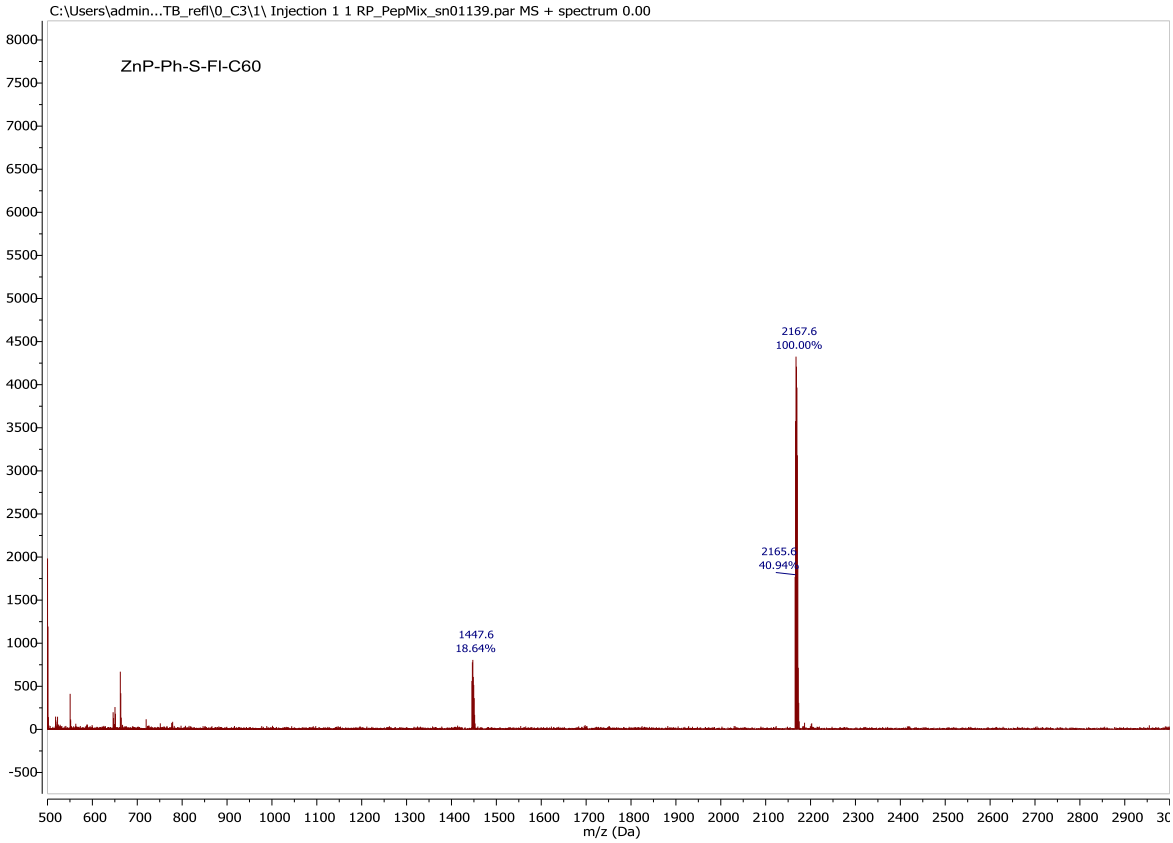

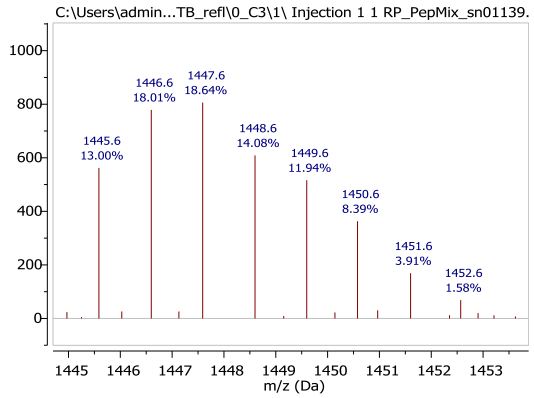

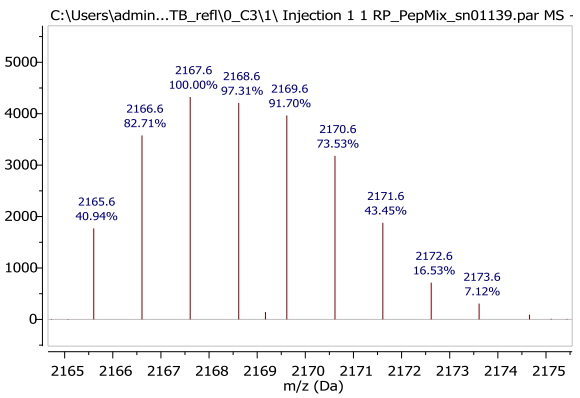

ZnP-Ph-Fl-S-Fl-C60 (20): ^{1}H (400 MHz, $CDCl_3$)

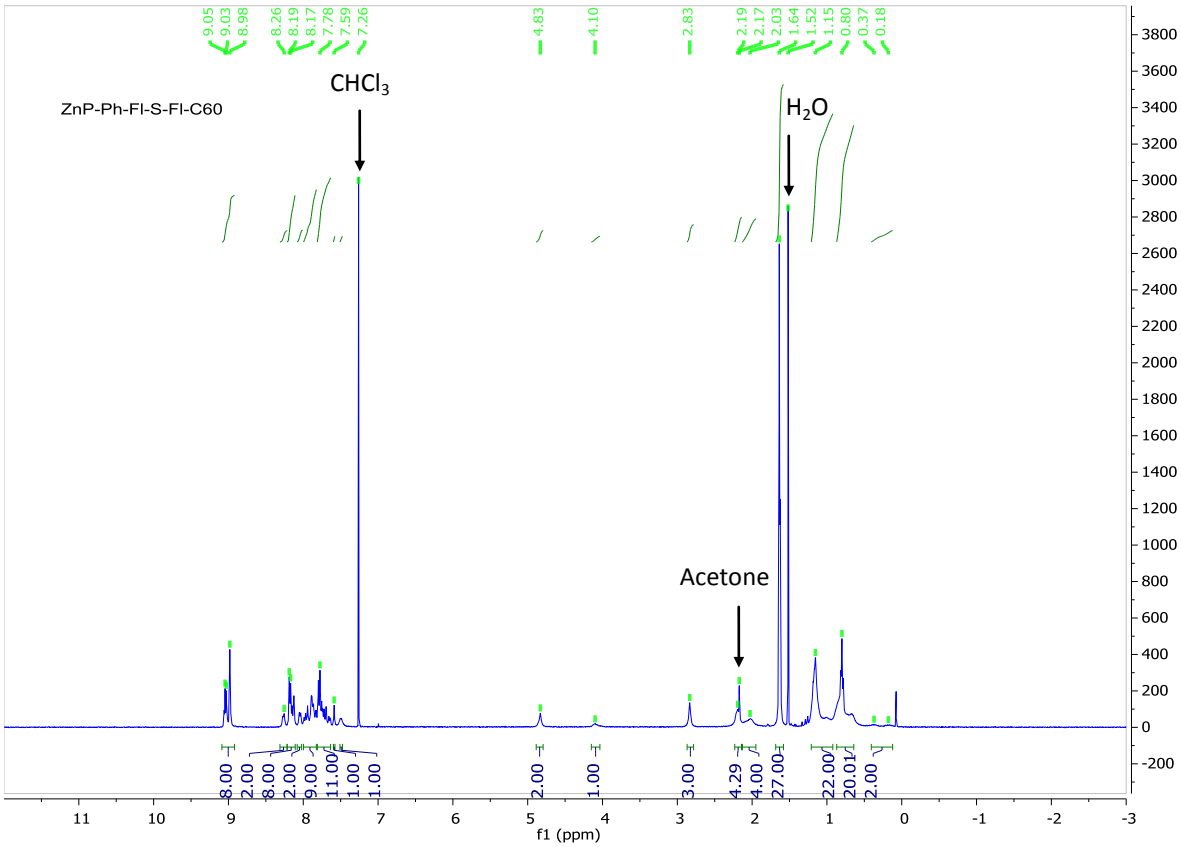

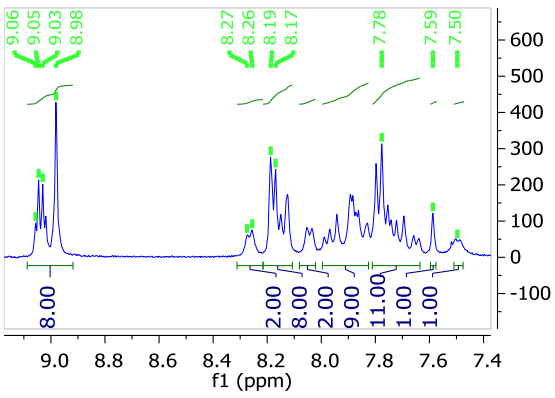

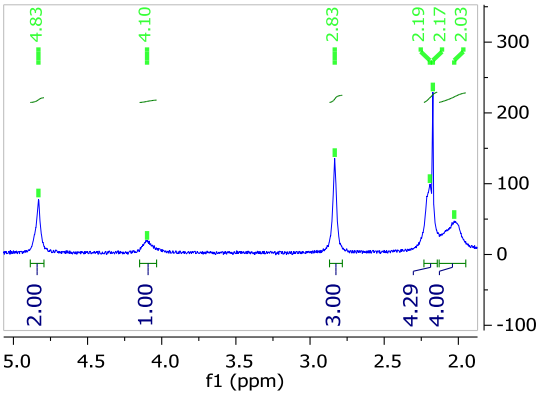

ZnP-Ph-Fl-S-Fl-C60 (20): MALDI-TOF MS

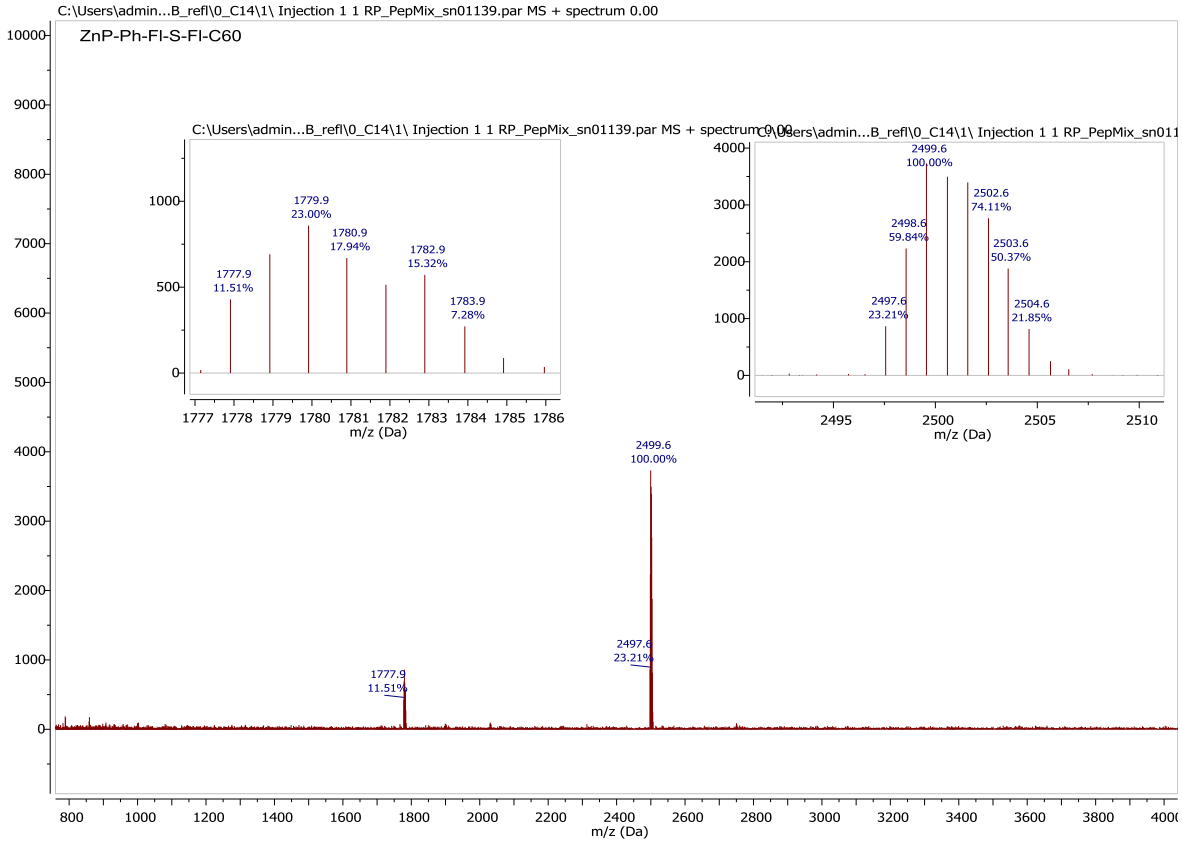

Fl-S-CHO (23): ^{1}H (700 MHz, $CDCl_3$)

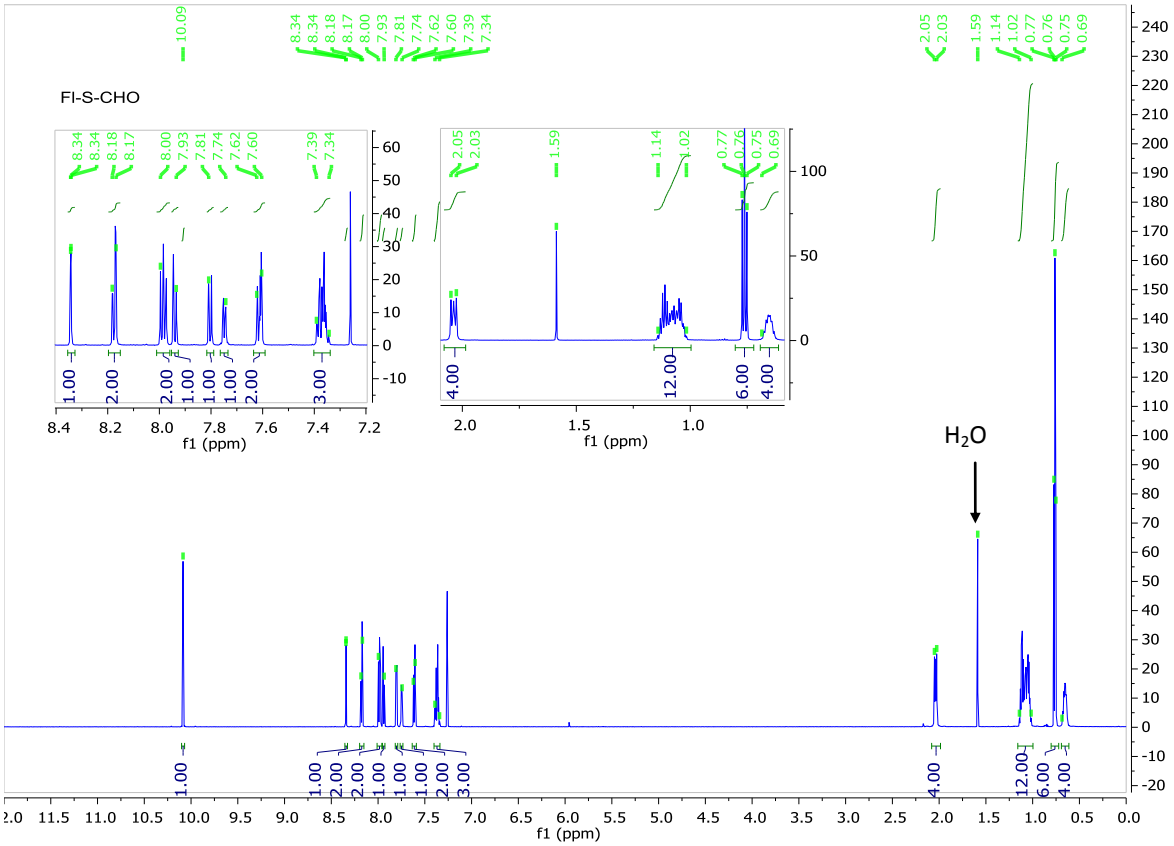

FI-S-CHO (23): ^{13}H (176 MHz, $CDCl_3$)

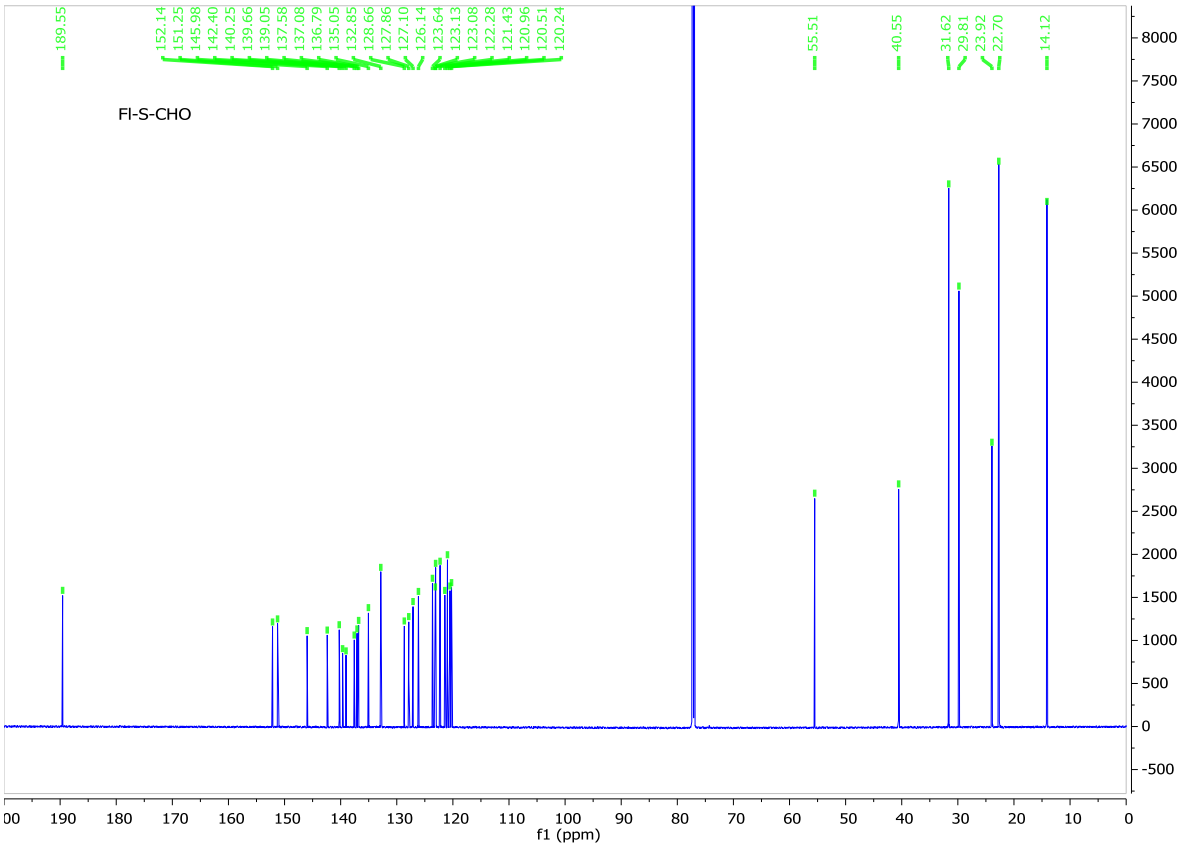

FI-S-CHO (23): Mass Spec

Single Mass Analysis
Tolerance = 5.0 PPM / DBE: min = -1.5, max = 50.0
Element prediction: Off
Number of isotope peaks used for i-FIT = 3

Monoisotopic Mass, Odd and Even Electron Ions
320 formula(e) evaluated with 4 results within limits (up to 50 best isotopic matches for each mass)
Elements Used:
C: 0-45 H: 0-50 N: 0-4 O: 0-4 S: 0-2

LCT Premier 350 °C GY_GY111_532 68 (0.546) Cm (62:68-1:38)
1: TOF MS AP+
4.13e+002

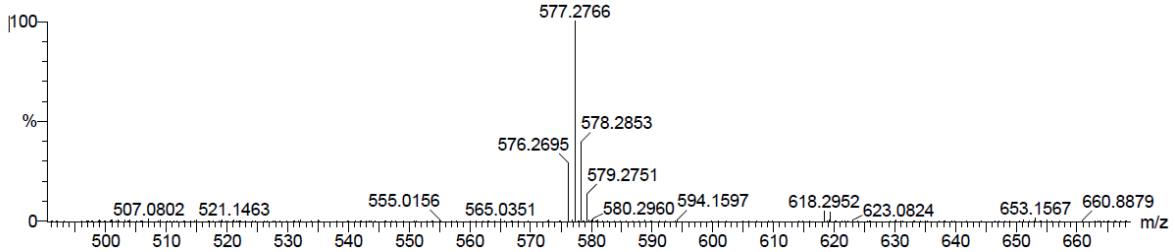

C_{60}-Fl-S-Fl-C_{60} (24): ^{1}H (400 MHz, $CDCl_3$)

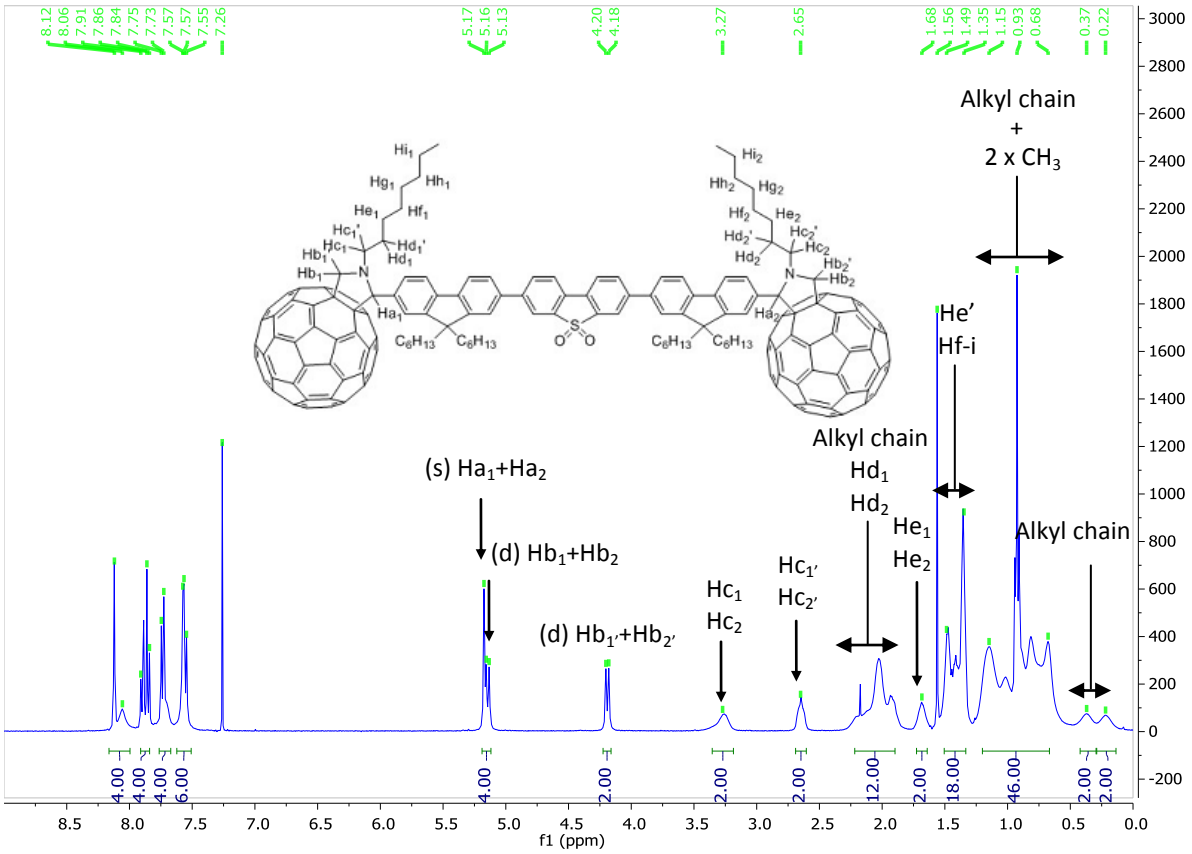

IV. Electrochemistry.

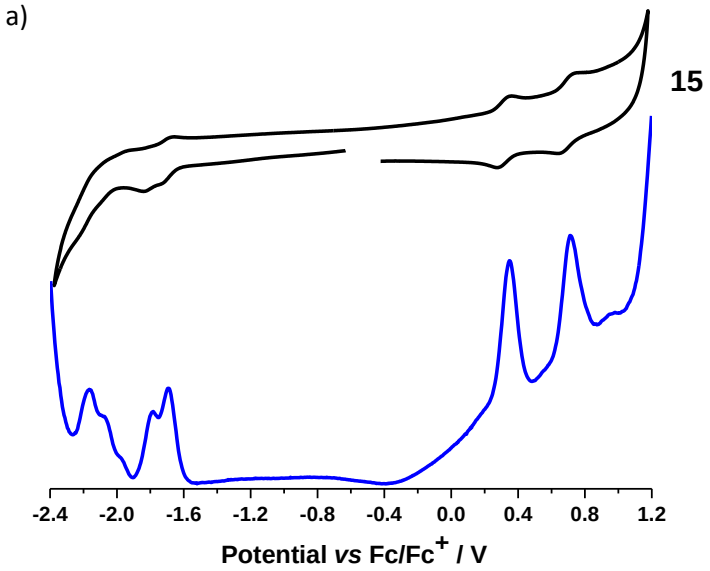

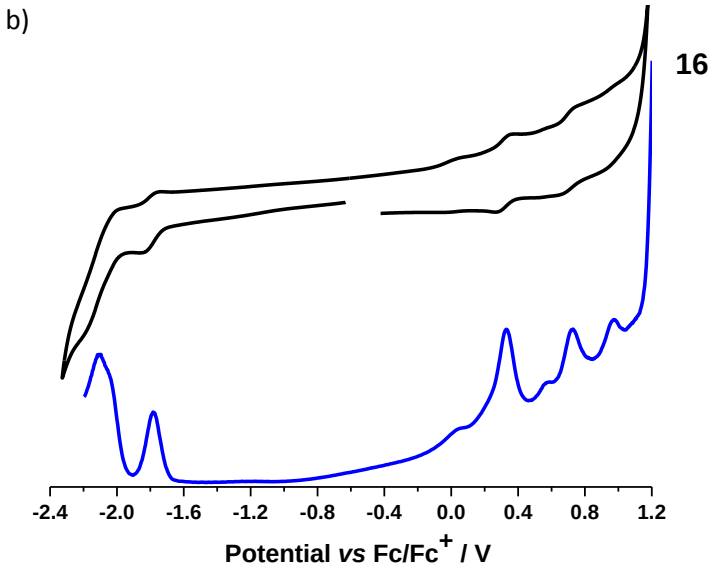

c)

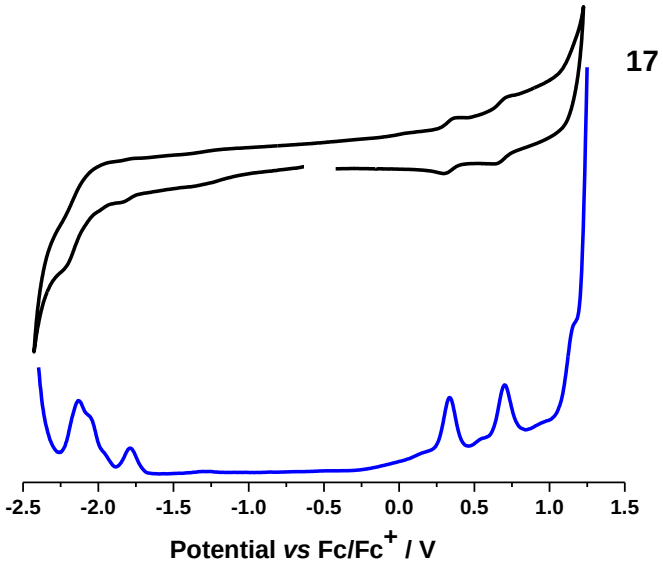
17
-2.5
-2.0
-1.5
-1.0
-0.5
0.0
0.5
1.0
1.5
Potential vs Fc/Fc+ / V

d)

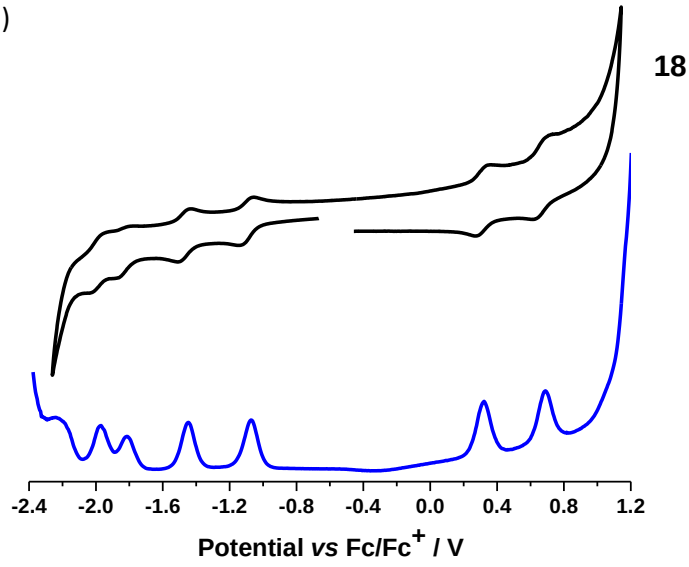
18
-2.4
-2.0
-1.6
-1.2
-0.8
-0.4
0.0
0.4
0.8
1.2
Potential vs Fc/Fc+ / V

e)

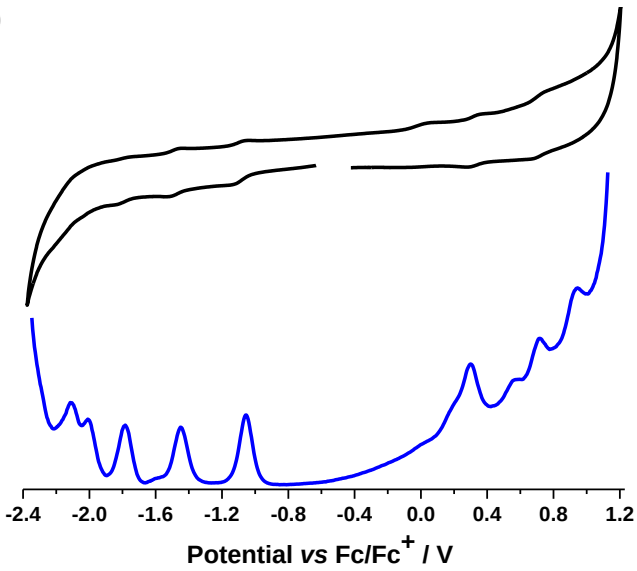
19
-2.4
-2.0
-1.6
-1.2
-0.8
-0.4
0.0
0.4
0.8
1.2
Potential vs Fc/Fc+ / V

f)

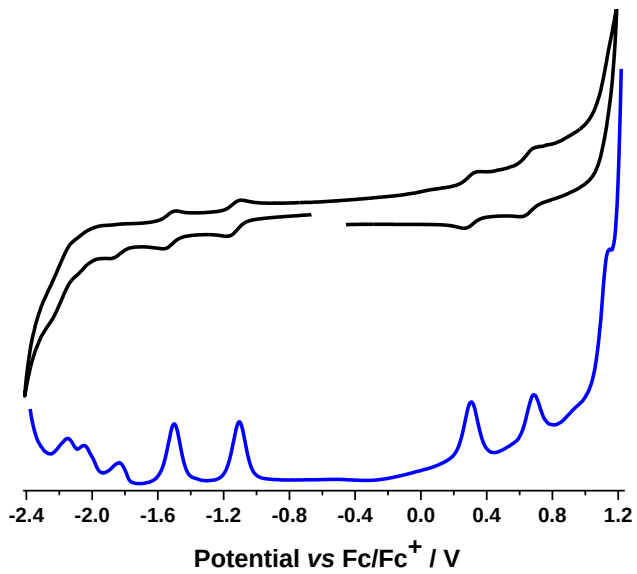
20
-2.4
-2.0
-1.6
-1.2
-0.8
-0.4
0.0
0.4
0.8
1.2
Potential vs Fc/Fc+ / V

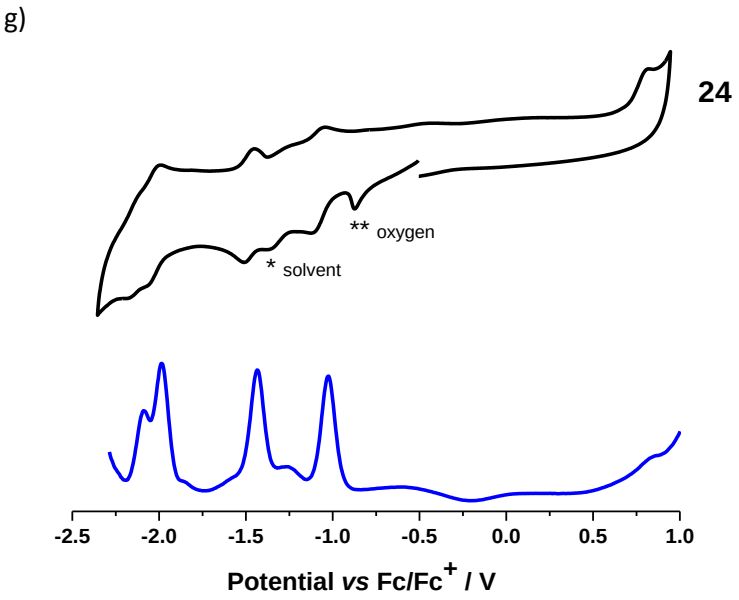

Figure S1. Cyclic (black) and differential pulse (blue) voltammograms of **15**-**20** and **24** measured in dichloromethane with 0.1 M $TBAPF_6$ as supporting electrolyte, glassy carbon as the working electrode, Pt wire as a counter electrode, and Ag-wire as a quasi-reference electrode. The values are corrected for ferrocene as an internal standard.

V. Photophysics.

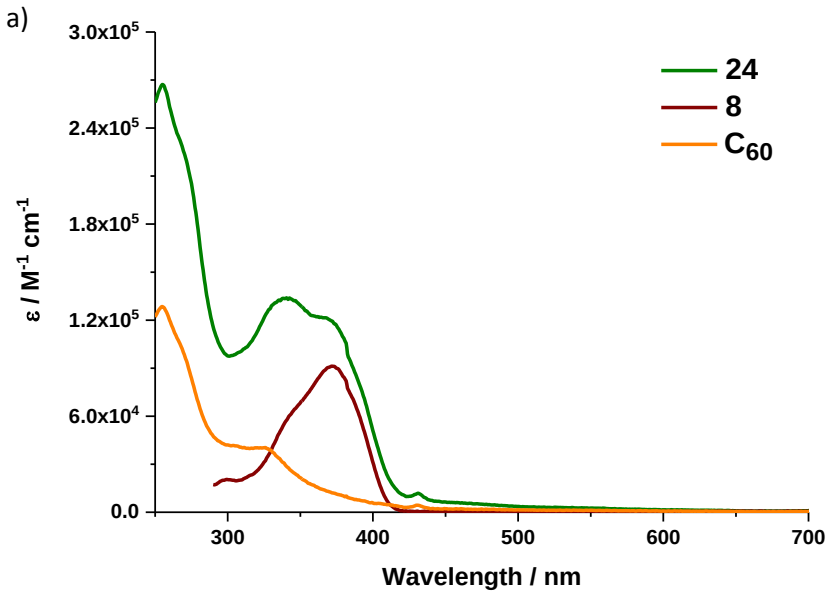

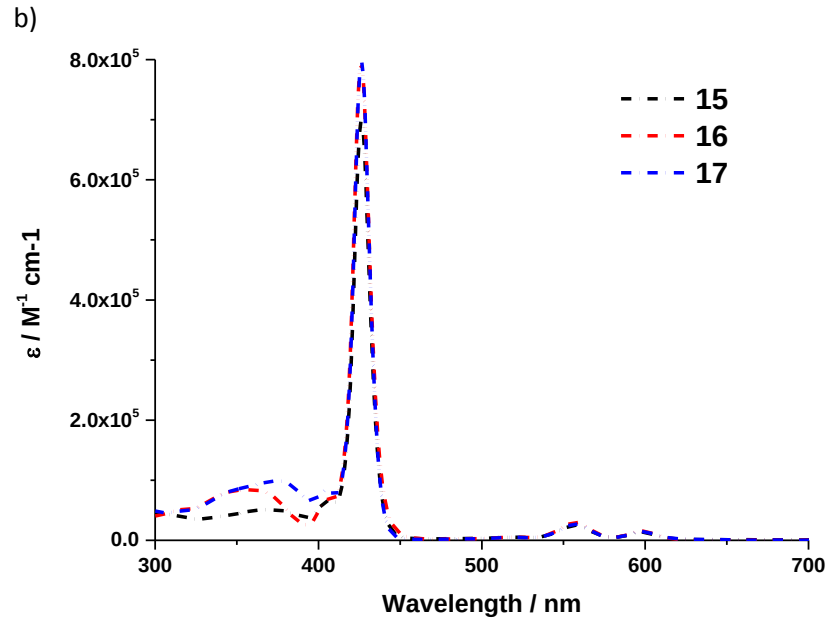

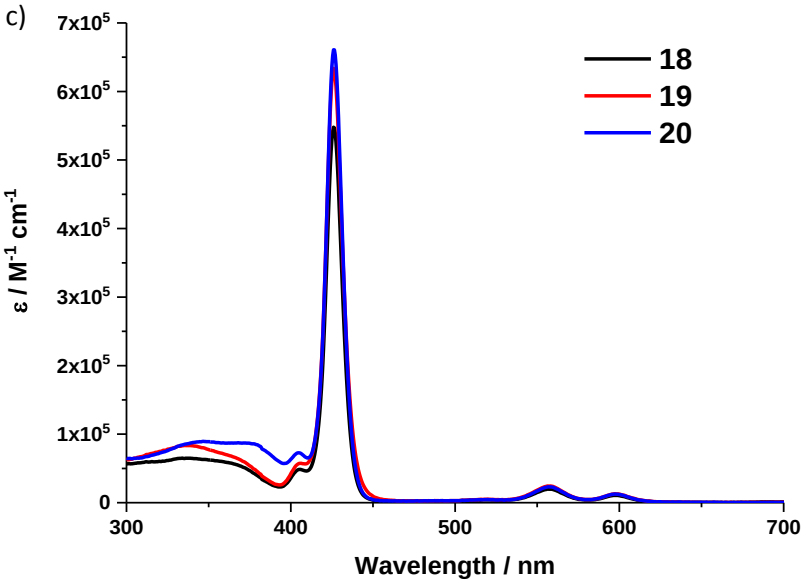

Figure S2. Room temperature absorption spectra of a) **24**, **8**, and C_{60}, b) references **15**-**17** and c) conjugates **18**-**20** in THF.

Table S1. Quantum yields of C_{60} emission in **24** upon 380 nm excitation.

Solvent	Toluene	THF	PhCN
QY	5.9×10^{-4}	5.3×10^{-4}	5.7×10^{-4}

Reference: C_{60} (QY = 6×10^{-4} in toluene)[7]

Table S2. Quantum yields of the conjugates **18**-**20** and their references **15**-**17**.

Solvent	Toluene		THF		PhCN	
λ_{exc} =	350 nm	420 nm	350 nm	420 nm	350 nm	420 nm
15	0.088	0.055	0.090	0.045	0.089	0.054
16	0.11	0.065	0.087	0.055	0.11	0.08
17	0.082	0.056	0.076	0.053	0.077	0.061
18	0.024	0.034	0.014	0.016	0.012	0.020
19	0.034	0.039	0.022	0.024	0.016	0.018
20	0.045	0.058	0.043	0.046	0.048	0.052

References: 350 nm excitation - 4-(dicyanomethylene)-2-methyl-6-(p-dimethylaminostyryl)-4*H*-pyran (QY = 0.43 in methanol),[8] 420 nm excitation - ZnP (QY = 0.04 in toluene).[9]

Table S3. Charge separation (k_{CS}) and charge recombination (k_{CR}) rates upon 430 nm excitation.

	k_{CS} / s^{-1}		k_{CR} / s^{-1}	
	THF	PhCN	THF	PhCN
18	2.2×10^{9}	4.4×10^{9}	2.2×10^{8}	5.4×10^{8}
19	2.6×10^{9}	2.2×10^{9}	1.3×10^{8}	3.5×10^{8}
20	-	-	-	-

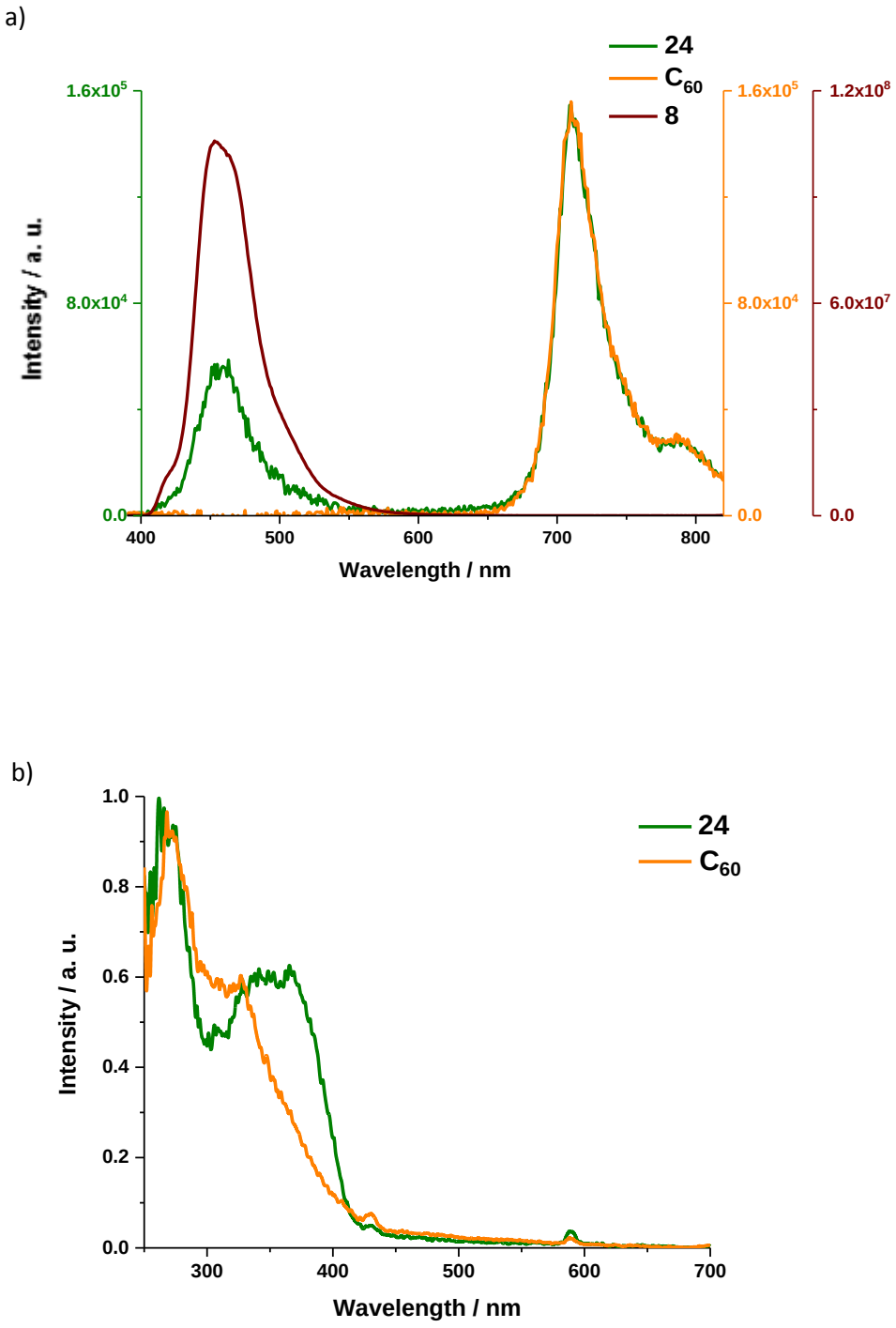

Figure S3. Room temperature a) fluorescence spectrum of **24**, **8,** and C_{60} upon 380 nm excitation with matching optical density of 0.2 (recorded with 450 nm optical filter), and b) comparison of the excitation spectra of **24** and C_{60} with the detection at 713 nm in THF.

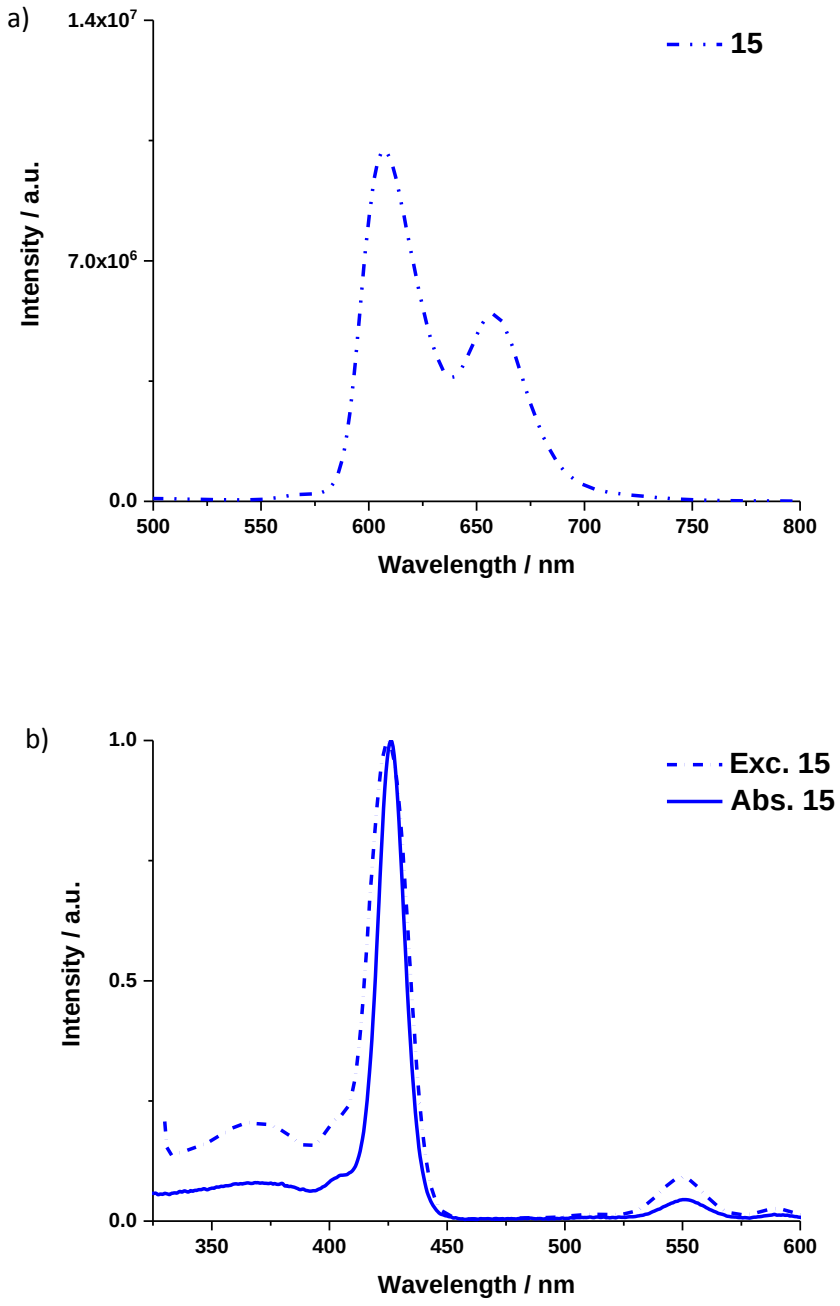

Figure S4. Room temperature a) fluorescence spectrum of **15** upon 350 nm excitation, and b) comparison of the absorption and excitation spectra of **15** with the detection at 650 nm in toluene.

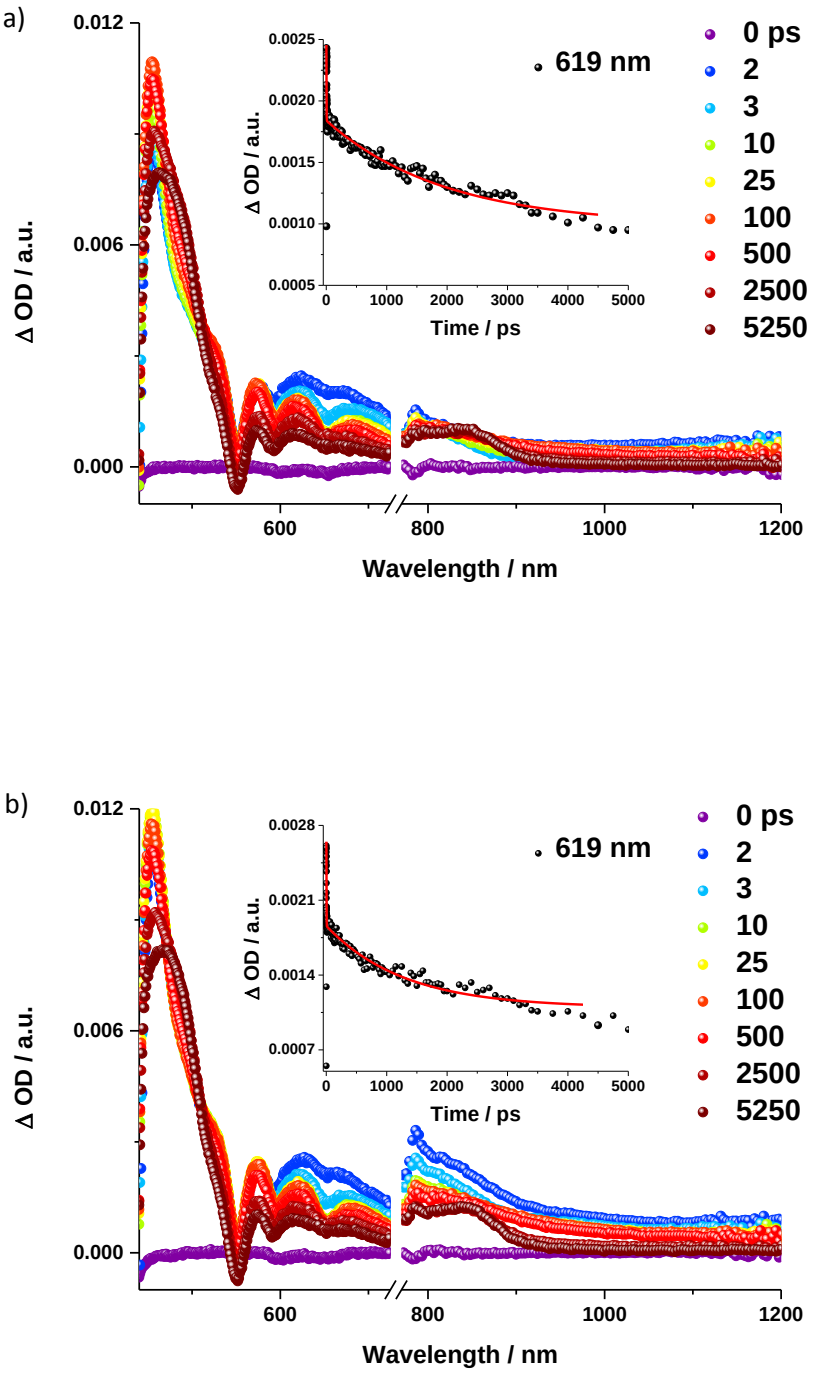

Figure S5. Differential absorption spectra (visible and near-infrared) obtained upon femtosecond flash photolysis (387 nm) of a) **15** and b) **17** in argon-saturated toluene with several time delays between 0 and 5250 ps at room temperature. Insets show corresponding bi-exponential decay profiles probed at indicated wavelengths.

a)

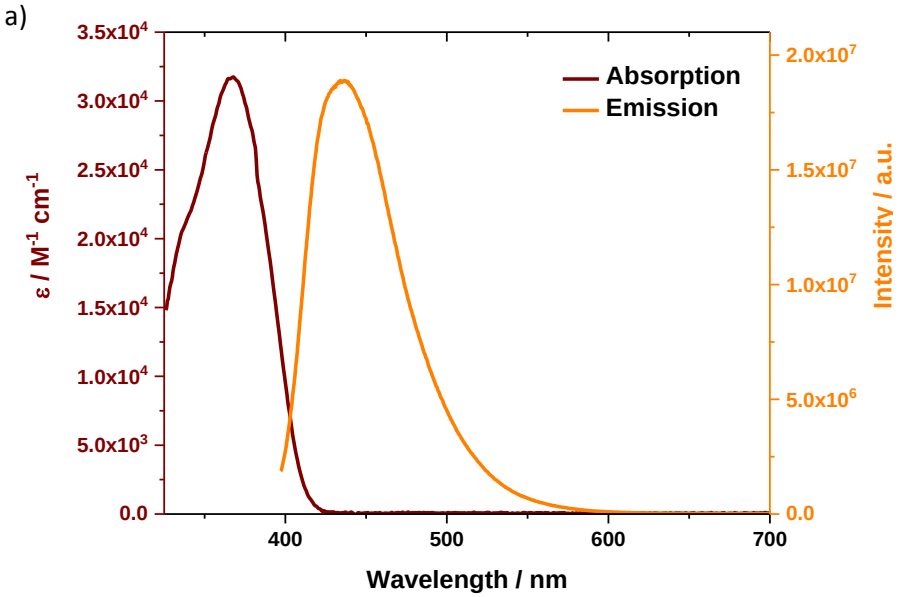
Absorption
Emission
ε / M-1 cm-1
Intensity / a.u.
Wavelength / nm
3.5x10^4
3.0x10^4
2.5x10^4
2.0x10^4
1.5x10^4
1.0x10^4
5.0x10^3
0.0
2.0x10^7
1.5x10^7
1.0x10^7
5.0x10^6
0.0
400
500
600
700

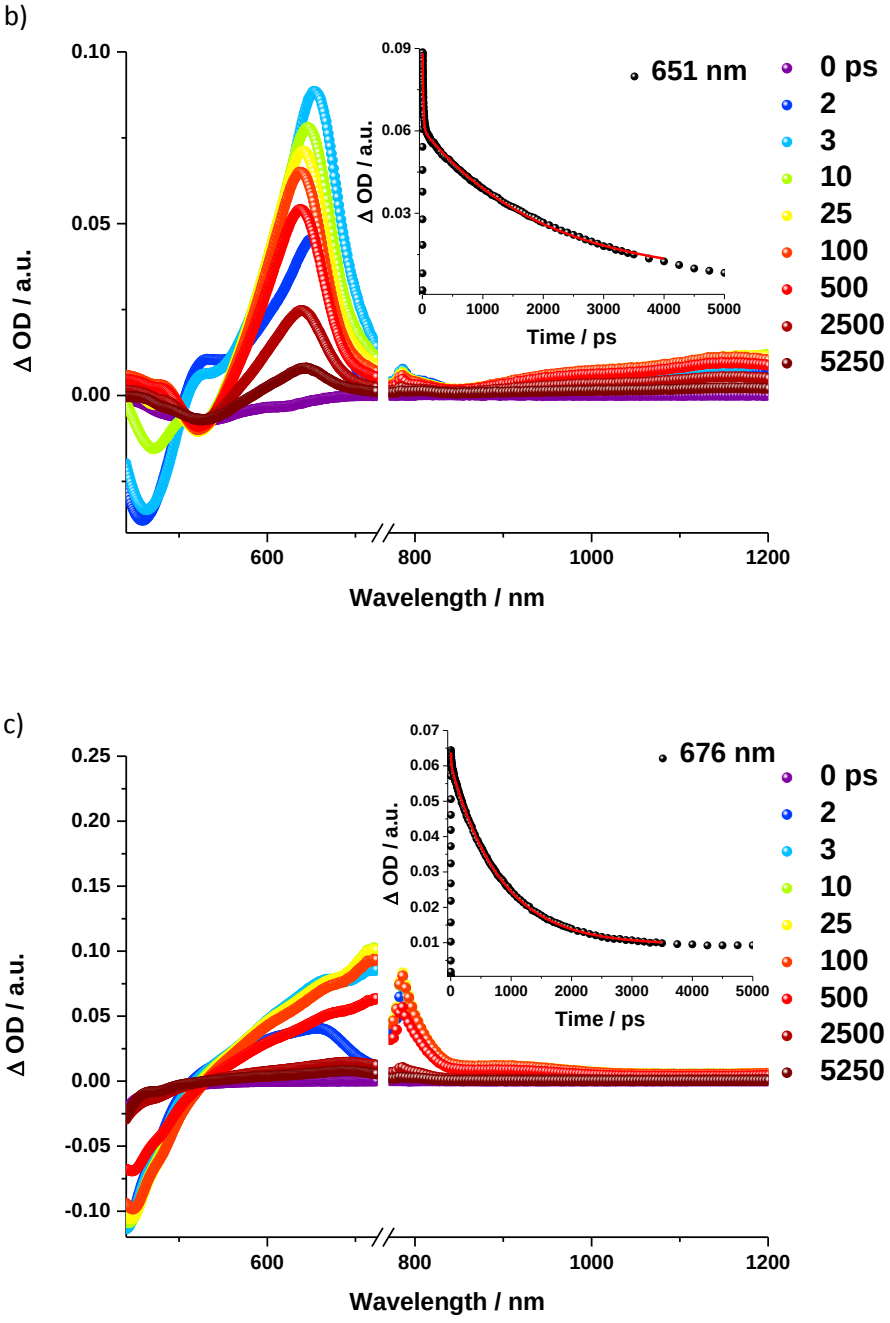

Figure S6. a) Room temperature absorption and emission (upon 387 nm excitation) spectra of **23** in toluene, and differential absorption spectra (visible and near-infrared) obtained upon femtosecond flash photolysis (387 nm) of b) **23** and c) **8** in argon-saturated PhCN with several time delays between 0 and 5250 ps at room temperature. Insets show corresponding decay profiles probed at indicated wavelengths.

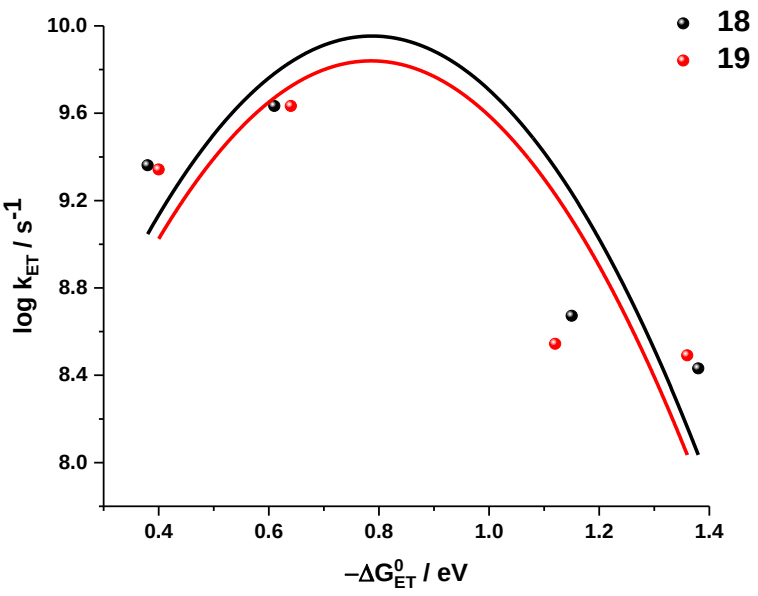

	λ / eV	V / cm^{-1}
18	0.78 ± 0.06	5.54 ± 1.87
19	0.78 ± 0.07	4.68 ± 1.88

Figure S7. Driving force ($-\Delta G^0_{ET}$) dependence on the rate constants for charge separation and charge recombination upon 387 nm excitation in **18** and **19** according to the classical Marcus theory. The driving forces were estimated in THF and PhCN using Weller's model.

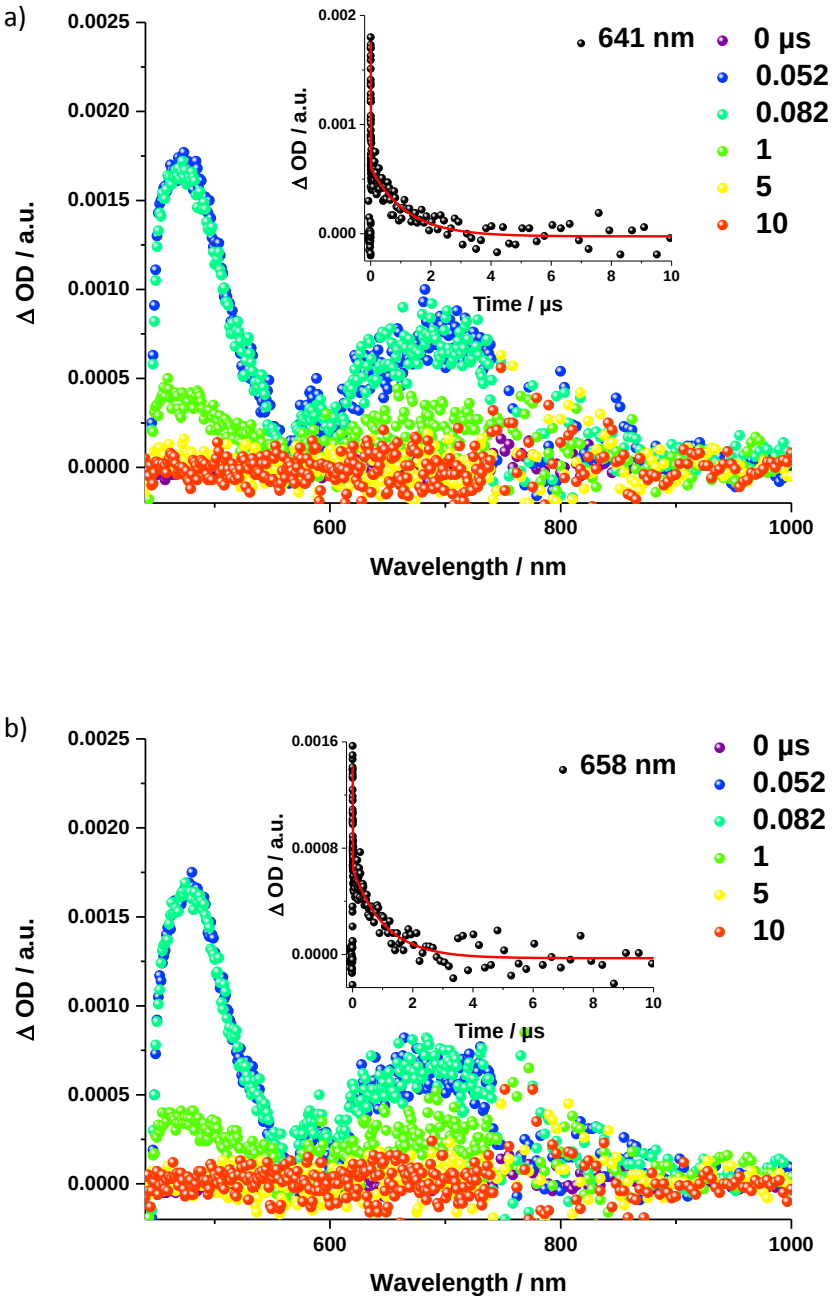

Figure S8. Differential absorption spectra (visible and near-infrared) obtained upon femtosecond flash photolysis (387 nm) of a) **18** and b) **19** in argon-saturated PhCN with several time delays between 0 and 10 µs at room temperature. Insets show corresponding decay profiles probed at indicated wavelengths.

a)

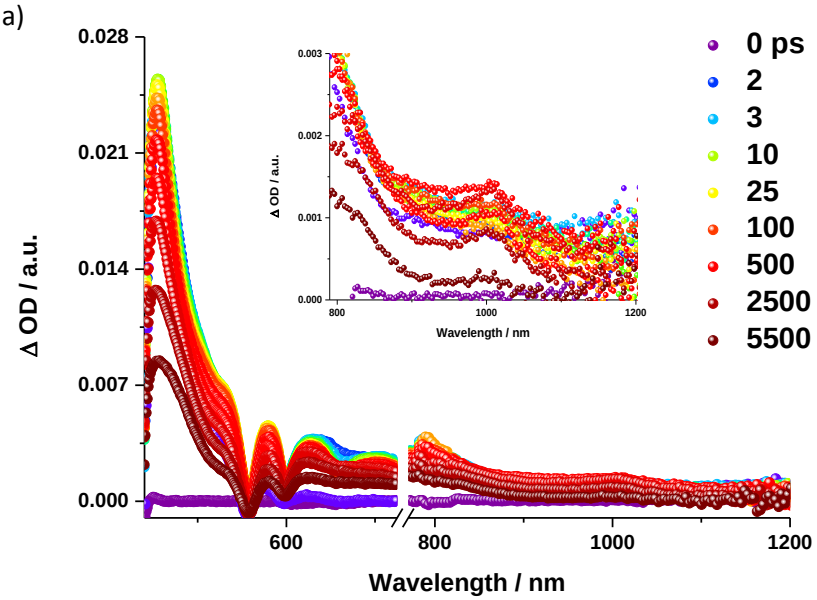
0.028
0.021
0.014
0.007
0.000
Δ OD / a.u.
600
800
1000
1200
Wavelength / nm
0.003
0.002
0.001
0.000
Δ OD / a.u.
800
1000
1200
Wavelength / nm
0 ps
2
3
10
25
100
500
2500
5500

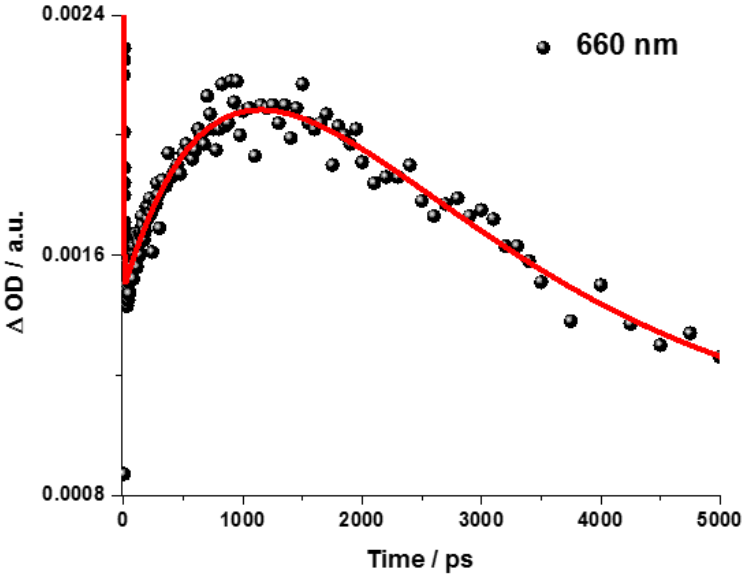
0.0024
0.0016
0.0008
Δ OD / a.u.
0
1000
2000
3000
4000
5000
Time / ps
660 nm

b)

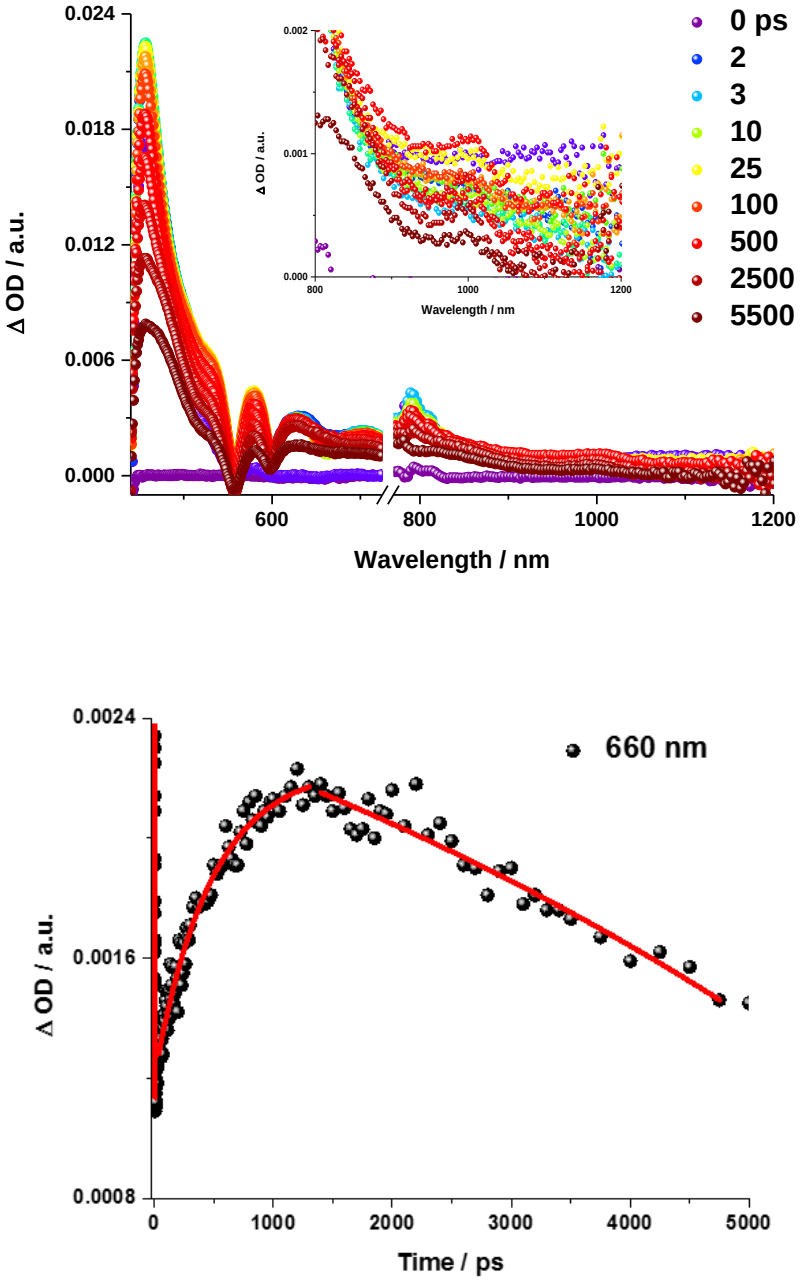

Figure S9. Differential absorption spectra (visible and near-infrared) obtained upon femtosecond flash photolysis (430 nm) of a) **18** and b) **19** in argon-saturated THF with several time delays between 0 and 5500 ps at room temperature. Insets show the 800-1200 nm range for a better visualization of the C_{60} radical anion. The graphs below transient absieption spectra represent corresponding decay profiles probed at indicated wavelengths.

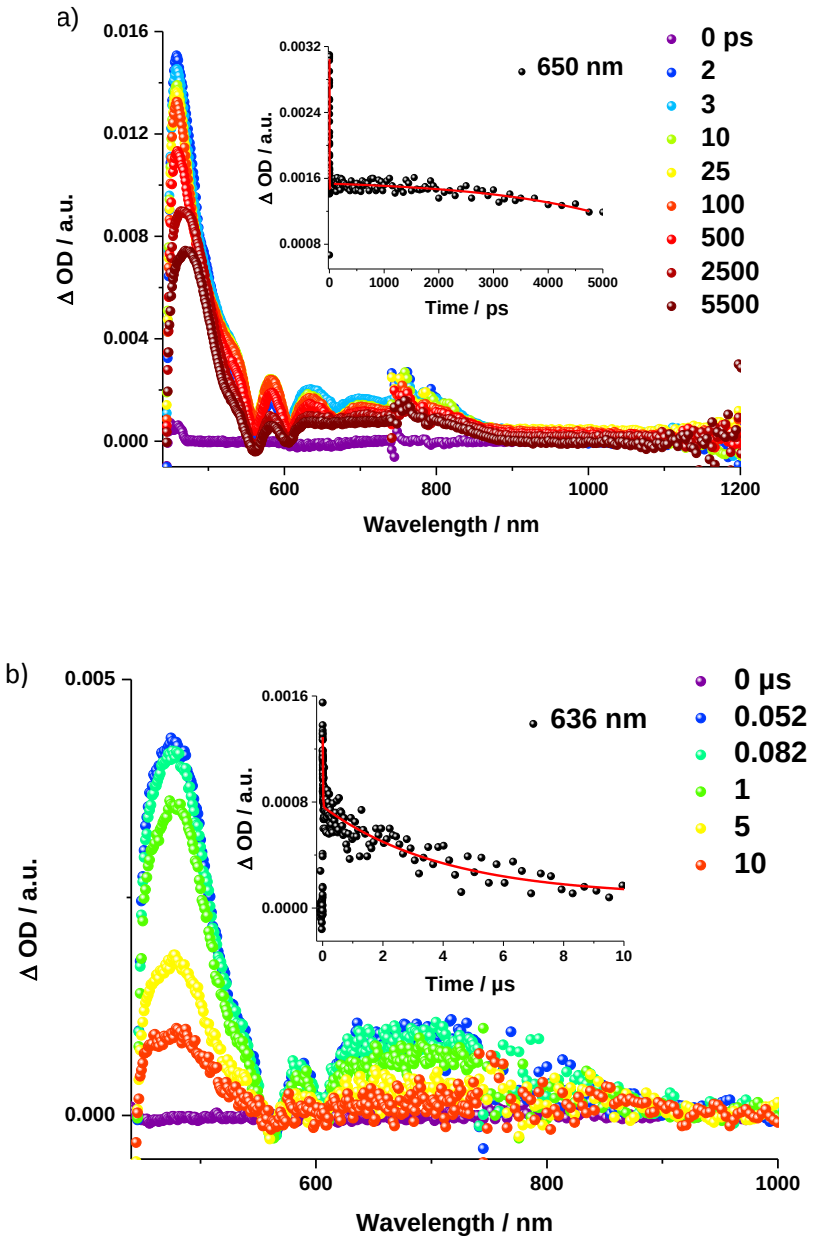

Figure S10. Differential absorption spectra (visible and near-infrared) obtained upon femtosecond flash photolysis of **20** upon a) 430 nm (ps), b) 387 nm (µs) excitation in argon-saturated PhCN with several time delays at room temperature. Insets show corresponding decay profiles probed at indicated wavelengths.

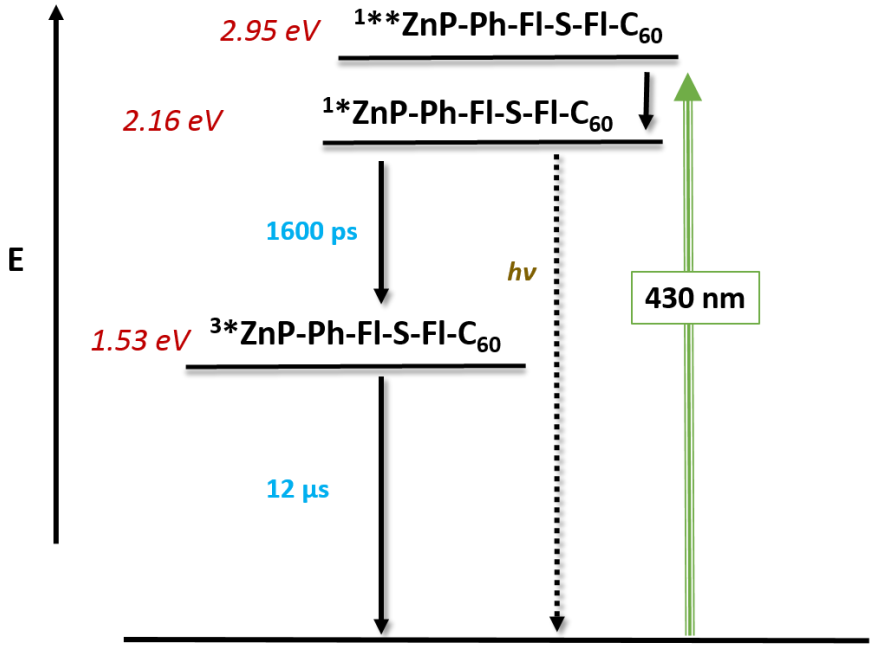

Figure S11. Energy level diagram of **20** reflecting the energetic pathways in PhCN after excitation upon 430 nm. The dashed arrow refers to fluorescence, whereas black lines refer to nonradiative processes.

VI. Theoretical Details.

To understand and explain the experimentally observed electron- and hole-transfer behavior of the three different bridged ZnP-C_{60}-dyads, theoretical calculations were carried out. To ensure finding minimal geometries the structures were treated with 20 annealing cycles using the Dreiding force field method as implemented in the Forcite package of Materials Studio,[10] followed by DFT optimization and vibrational analysis of the minima structures at the B3LYP/cc-pVDZ level of theory using Gaussian09[11] in the gas phase. Furthermore, structures were reoptimized in solvent environments of benzene and benzonitrile using the PCM solvation model. Based on these structures, TD-B3LYP/cc-pVDZ calculations including 100 excited states were conducted to examine vertical excitation energies.

In addition, the semi-empirical AM1* method was used to elucidate ground- and excited-state properties. Gas-phase calculations were conducted with EMPIRE using configuration interaction singles (CIS) including an active space of 125 occupied and 125 virtual orbitals. Solvation effects could not be treated with EMPIRE, therefore AM1*/CIS calculations were also conducted with VAMP and an active space of 80 orbitals. After obtaining the vertical excitation energies the excited states of interest were taken as root to obtain excited state energies in the relaxed solvent continuum. Please note that these energies still are based on the ground state geometry, so no excited state optimization was performed.

Visualization of the DFT results was performed with Vesta,[12] Vamp and Empire[13,14] results were visualized with Materials Studio 2016 and Gabedit.[15]

Table S4. Natural population analysis B3LYP/cc-pVDZ calculations compared to the reference ZnP and *N*-methylpyrrolidinofullerene, as well as the calculated charge difference Δ = charge-charge$_{ref}$.

	18			19			20			ZnP			Δ	Δ	Δ
	Atom	No	Charge	Atom	No	Charge	Atom	No	Charge	Atom	No	Charge	18	19	20
porphyrin moiety	C	1	-0,06	C	1	-0,06	C	1	-0,06	C	1	-0,06	-2E-04	-3E-04	-6E-04
	C	2	-0,25	C	2	-0,25	C	2	-0,25	C	2	-0,25	-2E-04	-6E-04	-3E-04
	C	3	-0,25	C	3	-0,24	C	3	-0,25	C	3	-0,25	4E-04	1E-03	7E-04
	C	4	0,20	C	4	0,20	C	4	0,20	C	4	0,20	1E-04	3E-04	1E-05
	N	5	-0,66	N	5	-0,66	N	5	-0,66	N	5	-0,66	-4E-04	-1E-04	-9E-05
	C	6	0,20	C	6	0,20	C	6	0,20	C	6	0,20	3E-04	7E-04	7E-04
	C	7	-0,06	C	7	-0,05	C	7	-0,05	C	7	-0,06	1E-04	5E-04	6E-04
	C	8	0,20	C	8	0,20	C	8	0,20	C	8	0,20	9E-05	4E-04	-8E-05
	C	9	-0,25	C	9	-0,25	C	9	-0,25	C	9	-0,25	4E-05	2E-04	3E-04
	C	10	-0,25	C	10	-0,25	C	10	-0,25	C	10	-0,25	1E-04	3E-04	2E-05
	C	11	0,20	C	11	0,20	C	11	0,20	C	11	0,20	3E-05	1E-04	5E-05
	N	12	-0,66	N	12	-0,66	N	12	-0,66	N	12	-0,66	2E-04	2E-04	3E-04
	C	13	-0,05	C	13	-0,05	C	13	-0,05	C	13	-0,06	2E-04	9E-04	4E-04
	C	14	0,20	C	14	0,20	C	14	0,20	C	14	0,20	3E-05	3E-05	3E-05
	C	15	-0,25	C	15	-0,25	C	15	-0,25	C	15	-0,25	2E-04	3E-04	8E-05
	C	16	-0,25	C	16	-0,25	C	16	-0,25	C	16	-0,25	1E-04	2E-04	4E-04
	C	17	0,20	C	17	0,20	C	17	0,20	C	17	0,20	5E-05	2E-04	-6E-05
	N	18	-0,66	N	18	-0,66	N	18	-0,66	N	18	-0,66	-2E-04	3E-04	2E-04
	C	19	-0,05	C	19	-0,05	C	19	-0,05	C	19	-0,06	2E-04	7E-04	6E-04
	C	20	0,20	C	20	0,20	C	20	0,20	C	20	0,20	-7E-05	4E-05	-4E-05
	C	21	-0,25	C	21	-0,25	C	21	-0,25	C	21	-0,25	2E-04	1E-03	8E-04
	C	22	-0,25	C	22	-0,25	C	22	-0,25	C	22	-0,25	-2E-04	-8E-04	-3E-04
	C	23	0,20	C	23	0,20	C	23	0,20	C	23	0,20	3E-04	8E-04	7E-04
	N	24	-0,66	N	24	-0,66	N	24	-0,66	N	24	-0,66	1E-05	5E-05	-1E-04
	C	25	-0,06	C	25	-0,06	C	25	-0,06	C	25	-0,06	-1E-03	-4E-03	-1E-03
	H	26	0,25	H	26	0,25	H	26	0,25	H	26	0,25	-1E-04	-2E-04	-8E-05
	H	27	0,25	H	27	0,25	H	27	0,25	H	27	0,25	1E-04	3E-04	6E-05
	C	28	-0,06	C	28	-0,06	C	28	-0,06	C	28	-0,06	-8E-05	-3E-04	-4E-04
	H	29	0,25	H	29	0,25	H	29	0,25	H	29	0,25	4E-05	2E-04	-2E-05
	H	30	0,25	H	30	0,25	H	30	0,25	H	30	0,25	8E-05	2E-04	1E-04
	C	31	-0,06	C	31	-0,06	C	31	-0,06	C	31	-0,06	-2E-04	-1E-04	-1E-05
	H	32	0,25	H	32	0,25	H	32	0,25	H	32	0,25	4E-05	1E-04	5E-05
	H	33	0,25	H	33	0,25	H	33	0,25	H	33	0,25	5E-05	1E-04	-1E-05
	H	34	0,25	H	34	0,25	H	34	0,25	H	34	0,25	7E-05	3E-04	0E+00
	H	35	0,25	H	35	0,25	H	35	0,25	H	35	0,25	-3E-05	-2E-04	-1E-04
	C	36	-0,06	C	36	-0,05	C	36	-0,06	C	36	-0,06	1E-03	8E-03	2E-03

	Zn	200	1,21	Zn	200	1,21	Zn	233	1,21	Zn	76	1,21	2E-04	1E-03	5E-04
∑			-0,29			-0,28			-0,29			-0,29	2E-03	1E-02	5E-03

	18			19			20			*N*-methyl-fullerenopyrrolidine			Δ	Δ	Δ
	Atom	No	Charge	Atom	No	Charge	Atom	No	Charge	Atom	No	Charge	18	19	20
fullerene moiety	C	130	-0,0019	C	130	-0,0022	C	163	-0,0023	C	1	-0,0024	5E-04	2E-04	1E-04
	C	131	-0,0007	C	131	-0,0011	C	164	-0,0011	C	2	-0,0013	7E-04	3E-04	2E-04
	C	132	-0,0010	C	132	-0,0012	C	165	-0,0012	C	3	-0,0013	4E-04	1E-04	2E-04
	C	133	-0,0019	C	133	-0,0023	C	166	-0,0024	C	4	-0,0024	5E-04	6E-05	-3E-05
	C	134	-0,0012	C	134	-0,0014	C	167	-0,0013	C	5	-0,0015	4E-04	1E-04	2E-04
	C	135	-0,0010	C	135	-0,0013	C	168	-0,0013	C	6	-0,0015	6E-04	3E-04	2E-04
	C	136	-0,0002	C	136	-0,0005	C	169	-0,0006	C	7	-0,0007	5E-04	2E-04	1E-04
	C	137	-0,0002	C	137	-0,0005	C	170	-0,0005	C	8	-0,0007	5E-04	2E-04	2E-04
	C	138	-0,0021	C	138	-0,0024	C	171	-0,0024	C	9	-0,0026	5E-04	3E-04	3E-04
	C	139	-0,0009	C	139	-0,0013	C	172	-0,0013	C	10	-0,0014	5E-04	1E-04	1E-04
	C	140	-0,0020	C	140	-0,0024	C	173	-0,0025	C	11	-0,0026	6E-04	2E-04	2E-04
	C	141	-0,0001	C	141	-0,0005	C	174	-0,0003	C	12	-0,0007	7E-04	3E-04	4E-04
	C	142	-0,0026	C	142	-0,0027	C	175	-0,0028	C	13	-0,0031	5E-04	3E-04	2E-04
	C	143	-0,0002	C	143	-0,0002	C	176	-0,0001	C	14	-0,0002	-5E-05	-8E-05	5E-05
	C	144	-0,0036	C	144	-0,0045	C	177	-0,0045	C	15	-0,0049	1E-03	4E-04	4E-04
	C	145	-0,0018	C	145	-0,0023	C	178	-0,0022	C	16	-0,0023	5E-04	4E-05	1E-04
	C	146	-0,0043	C	146	-0,0047	C	179	-0,0046	C	17	-0,0049	6E-04	2E-04	3E-04
	C	147	0,0004	C	147	-0,0001	C	180	0,0000	C	18	-0,0002	5E-04	9E-05	1E-04
	C	148	-0,0027	C	148	-0,0030	C	181	-0,0029	C	19	-0,0031	4E-04	6E-05	1E-04
	C	149	-0,0026	C	149	-0,0028	C	182	-0,0029	C	20	-0,0031	5E-04	3E-04	2E-04
	C	150	-0,0005	C	150	-0,0009	C	183	-0,0009	C	21	-0,0012	7E-04	3E-04	3E-04
	C	151	-0,0010	C	151	-0,0015	C	184	-0,0015	C	22	-0,0016	5E-04	1E-04	8E-05
	C	152	-0,0059	C	152	-0,0068	C	185	-0,0067	C	23	-0,0076	2E-03	7E-04	9E-04
	C	153	-0,0097	C	153	-0,0104	C	186	-0,0103	C	24	-0,0106	8E-04	2E-04	3E-04
	C	154	-0,0020	C	154	-0,0028	C	187	-0,0027	C	25	-0,0033	1E-03	5E-04	6E-04
	C	155	0,0074	C	155	0,0070	C	188	0,0071	C	26	0,0065	9E-04	5E-04	6E-04
	C	156	-0,0030	C	156	-0,0031	C	189	-0,0031	C	27	-0,0033	3E-04	2E-04	2E-04
	C	157	-0,0079	C	157	-0,0090	C	190	-0,0090	C	28	-0,0106	3E-03	2E-03	2E-03
	C	158	-0,0002	C	158	-0,0006	C	191	-0,0008	C	29	-0,0007	5E-04	8E-05	-7E-05
	C	159	-0,0035	C	159	-0,0035	C	192	-0,0035	C	30	-0,0011	-2E-03	-2E-03	-2E-03
	C	160	-0,0061	C	160	-0,0066	C	193	-0,0066	C	31	-0,0081	2E-03	1E-03	2E-03
	C	161	-0,0097	C	161	-0,0106	C	194	-0,0106	C	32	-0,0105	9E-04	-5E-05	-1E-04
	C	162	-0,0021	C	162	-0,0022	C	195	-0,0022	C	33	-0,0030	1E-03	8E-04	8E-04
	C	163	-0,0193	C	163	-0,0211	C	196	-0,0212	C	34	-0,0213	2E-03	3E-04	2E-04

	C	164	-0,0662	C	164	-0,0674	C	197	-0,0674	C	35	-0,0861	2E-02	2E-02	2E-02
	C	165	0,0296	C	165	0,0374	C	198	0,0375	C	36	0,0421	-1E-02	-5E-03	-5E-03
	C	166	-0,0026	C	166	-0,0007	C	199	-0,0002	C	37	-0,0014	-1E-03	6E-04	1E-03
	C	167	-0,0072	C	167	-0,0075	C	200	-0,0076	C	38	-0,0076	4E-04	4E-05	0E+00
	C	168	-0,0004	C	168	-0,0007	C	201	-0,0006	C	39	-0,0016	1E-03	9E-04	1E-03
	C	169	-0,0012	C	169	-0,0016	C	202	-0,0017	C	40	-0,0012	2E-05	-4E-04	-5E-04
	C	170	0,0000	C	170	-0,0001	C	203	-0,0001	C	41	-0,0002	2E-04	2E-04	2E-04
	C	171	-0,0042	C	171	-0,0049	C	204	-0,0049	C	42	-0,0051	9E-04	2E-04	2E-04
	C	172	-0,0018	C	172	-0,0021	C	205	-0,0021	C	43	-0,0024	6E-04	3E-04	3E-04
	C	173	0,0071	C	173	0,0068	C	206	0,0067	C	44	0,0068	4E-04	3E-05	-5E-05
	C	174	-0,0027	C	174	-0,0030	C	207	-0,0032	C	45	-0,0030	3E-04	-2E-05	-2E-04
	C	175	-0,0200	C	175	-0,0202	C	208	-0,0201	C	46	-0,0213	1E-03	1E-03	1E-03
	C	176	0,0408	C	176	0,0409	C	209	0,0409	C	47	0,0414	-6E-04	-5E-04	-5E-04
	C	177	-0,0830	C	177	-0,0835	C	210	-0,0836	C	48	-0,0861	3E-03	3E-03	3E-03
	C	178	-0,0089	C	178	-0,0126	C	211	-0,0128	C	49	-0,0180	9E-03	5E-03	5E-03
	C	179	-0,0169	C	179	-0,0176	C	212	-0,0176	C	50	-0,0180	1E-03	5E-04	5E-04
	C	180	0,0431	C	180	0,0428	C	213	0,0427	C	51	0,0421	1E-03	7E-04	7E-04
	C	181	-0,0014	C	181	-0,0018	C	214	-0,0020	C	52	-0,0014	-5E-05	-5E-04	-7E-04
	C	182	-0,0003	C	182	-0,0007	C	215	-0,0006	C	53	-0,0011	8E-04	5E-04	5E-04
	C	183	-0,0072	C	183	-0,0078	C	216	-0,0080	C	54	-0,0081	9E-04	2E-04	1E-04
	C	184	-0,0094	C	184	-0,0100	C	217	-0,0099	C	55	-0,0105	1E-03	6E-04	6E-04
	C	185	0,0003	C	185	0,0000	C	218	-0,0001	C	56	-0,0002	5E-04	2E-04	2E-04
	C	186	-0,0045	C	186	-0,0048	C	219	-0,0049	C	57	-0,0051	7E-04	3E-04	3E-04
	C	187	-0,0026	C	187	-0,0028	C	220	-0,0027	C	58	-0,0031	5E-04	3E-04	4E-04
	C	188	-0,0011	C	188	-0,0014	C	221	-0,0014	C	59	-0,0014	3E-04	2E-05	0E+00
	C	189	0,0392	C	189	0,0414	C	222	0,0412	C	60	0,0414	-2E-03	-4E-05	-2E-04
∑			-0,18			-0,19			-0,19			-0,23	5E-02	4E-02	4E-02

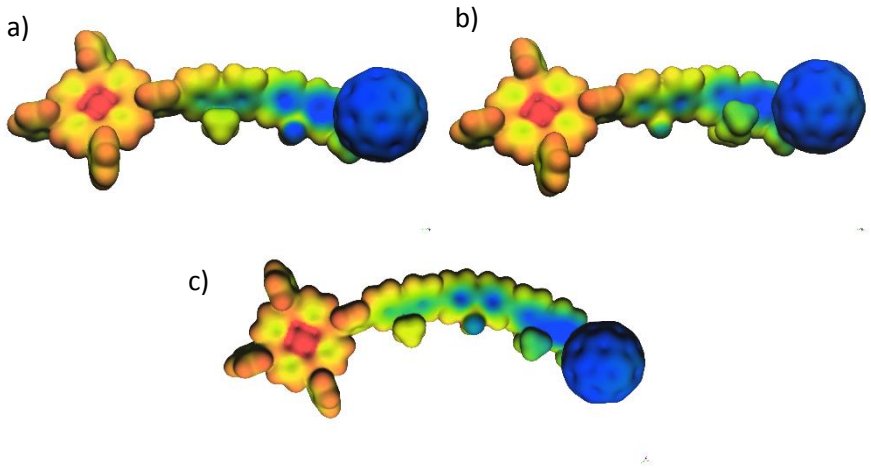

Figure S12. Electrostatic potential from -0.2 (blue) until 0.2 (red) mapped on the electron density (iso = 0.05 $e^-/Å^3$) for the fully charge separated state of a) **18**, b) **19**, and c) **20**.

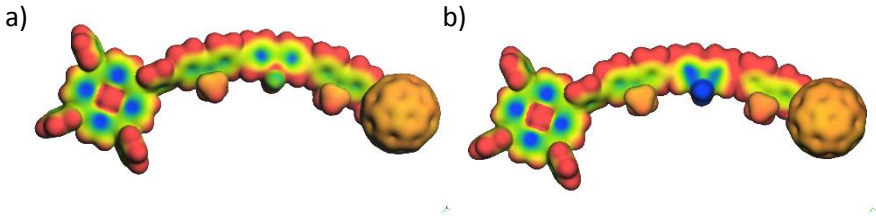

Figure S13. Calculated electrostatic potential for a) the ground state and for b) the bridge centred charge transfer state for compound **20** mapped from -0.2 to 0.02.

Table S5: Ground state (GS) heat of formation (kcal/mol) and excited state energies as calculated with AM1* (left) and TD-B3LYP (right) compared to experimental accessible values. Excited state energies in eV with respect to the ground state. Deviations (dark grey) are given relative to experimental values in %.

	Configuration intreraction																				exp	TD-B3LYP			
	18								**20**								**19**								**18**	**20**	**19**	ZnP
	GP		Benzene		ACN		H_2O		GP		Benzene		ACN		H_2O		GP		Benzene		ACN		H_2O			PhCN		
CI	250		80		80		80		250		80		80		80		250		80		80		80					
GS	1370		1383		1366		1363		1418		1431		1414		1430		1370		1384		1370		1363					
ZnP S1	2.16	-0.1	2.20	1.6	2.26	4.5	2.30	6.3	2.16	0.1	2.44	13.1	2.42	12.2	2.43	12.5	2.17	0.6	2.29	5.8	2.25	3.9	2.17	0.6	2.16	2.29	2.18	2.18	2.28
ZnP S2	3.01	3.6	3.23	10.9	3.17	9.0	3.10	6.5	2.97	2.1	3.11	6.7	3.23	10.9	3.12	7.3	3.11	6.7	2.97	2.0	2.92	0.4	2.88	-1.2	2.91	2.94	2.92	3.05	3.08
C_{60}	1.86	9.6	1.70	-0.1	1.74	2.1	1.70	-0.1	1.88	10.3	1.69	-0.5	1.70	-0.2	1.69	-0.6	1.88	10.8	1.70	-0.1	1.73	1.7	1.70	-0.1	1.70	1.87	1.86	1.86	
bridge	3.19	-4.7	3.68	9.8	3.53	5.4	3.67	9.5	3.22	-3.9	3.65	8.9	3.67	9.5	3.59	7.3	3.34	-0.3	3.60	7.3	3.53	5.3	3.54	5.8	3.35	3.14	3.05	3.17	
CSS	4.04		3.03		3.05		3.06		4.08		3.06		2.77		2.23		4.01		3.06		2.78		2.81		*		3.05		
bridge CT	-		-		-		-		3.994		3.00		2.78		2.62		-		-		-		-						
ZnP^+-B^-	-		3.50		3.47		3.30		-		-		-		-		-		3.61		3.34		3.19						
$\bar{\Delta}_{rel}$		2.8		3.7		2.9		3.3		2.8		4.3		4.7		4.1		3.2		2.4		1.7		1.5		3.3	3.3	3.0	4.1
	3.1																									3.4			

*reference 23

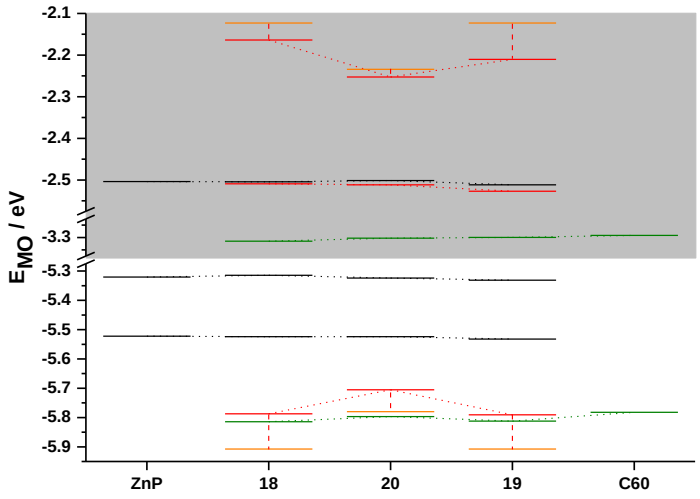

Figure S14. Molecular orbital energies of **18**-**20**, ZnP (black), and C_{60} (green) including solvation in benzonitrile (PhCN) using PCM solvation model and B3LYP/cc-pVDZ. MOs with bridge contributions are in red, while MOs of unfunctionalized bridge reference are in orange.

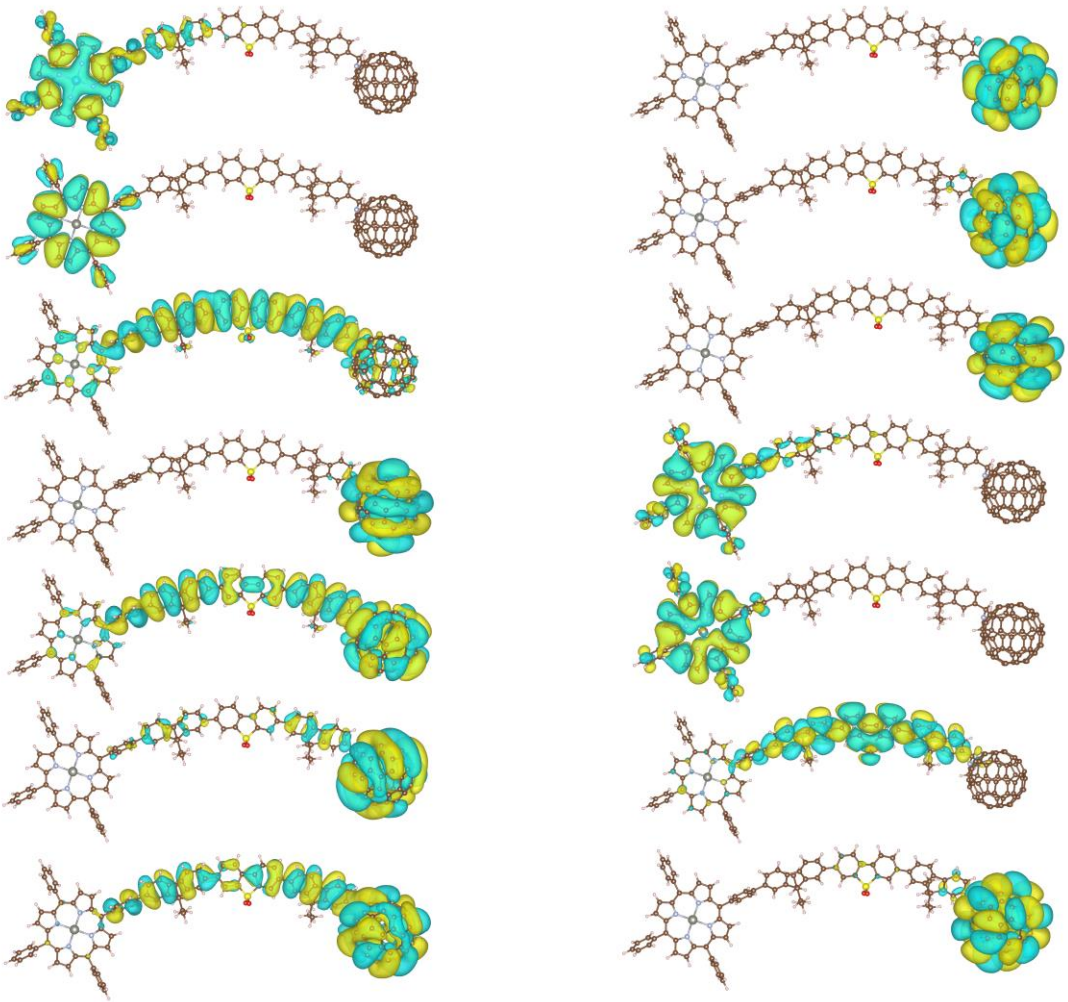

Figure S15. Molecular orbitals of **20**, left side: HOMO (top) to HOMO -6 (down), right side: LUMO (top) to LUMO +6 (down), calculated including solvation in benzonitrile (PhCN) using PCM solvation model and B3LYP/cc-pVDZ.

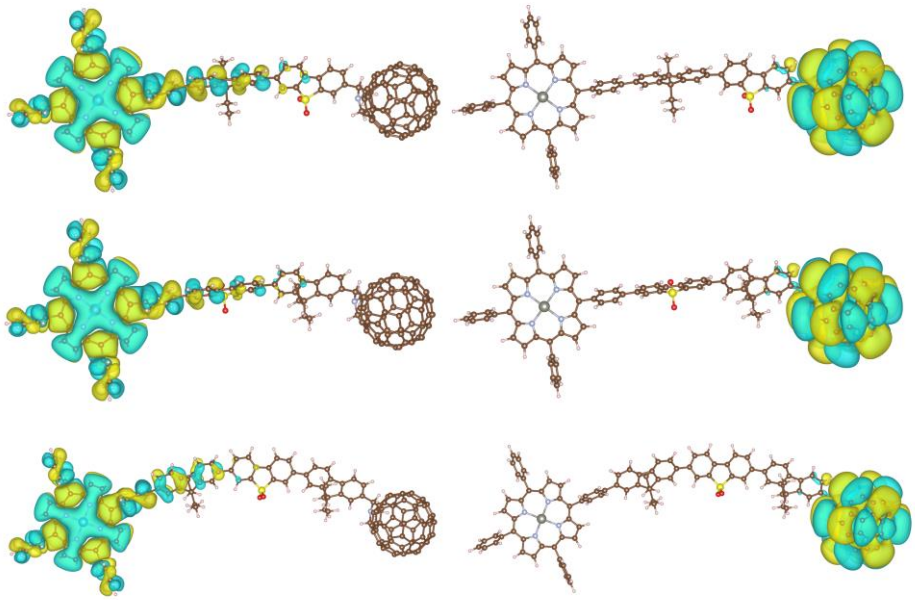

Figure S16. Highest occupied molecular orbital (HOMO, left) and lowest unoccupied molecular orbital (LUMO, right) of **18** (top) **19** (middle) and **20** (down), calculated including solvation in benzonitrile (PhCN) using PCM solvation model and B3LYP/cc-pVDZ.

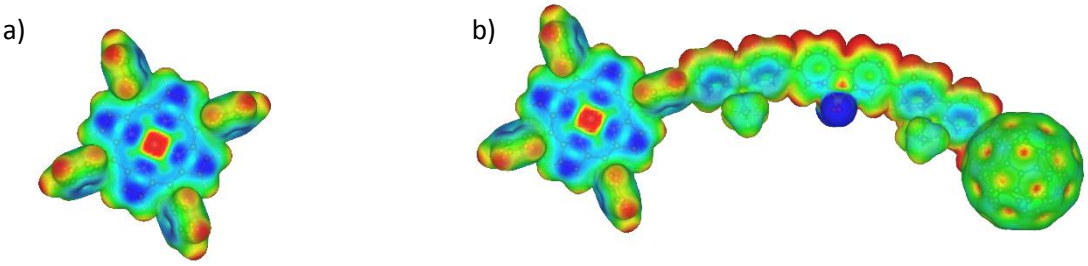

Figure S17. Ground state electrostatic potential of a) ZnP and b) **20** mapped on the electron density isosurface (iso = 0.05 $e^-/Å^3$).

(1) van der Pol, C.; Bryce, M. R.; Wielopolski, M.; Atienza-Castellanos, C.; Guldi, D. M.; Filippone, S.; Martín, N. Energy Transfer in Oligofluorene-C60 and C60-Oligofluorene-C60 Donor-Acceptor Conjugates. *J. Org. Chem*. **2007**, *72*, 6662-6671.

(2) Moss, K. C.; Bourdakos, K. N.; Bhalla, V.; Kamtekar, K. T.; Bryce, M. R.; Fox, M. A.; Vaughan, H. L.; Dias, F. B.; Monkman, A. P. Tuning the Intramolecular Charge Transfer Emission from Deep Blue to Green in Ambipolar Systems Based on Dibenzothiophene-S,S-Dioxide by Manipulation of Conjugation and Strength of the Electron Donor Units. *J. Org. Chem.* **2010**, *75*, 6771-6781.

(3) Wielopolski, M.; de Miguel Rojas, G.; van der Pol, C.; Brinkhaus, L.; Katsukis, G.; Bryce, M. R.; Clark, T.; Guldi, D. M. Control over Charge Transfer through Molecular Wires by Temperature and Chemical Structure Modifications. *ACS Nano* **2010**, *4,* 6449-6462.

(4) Anémian, R.; Mulatier, J.-C.; Andraud, C.; Stéphan, O.; Vial, J.-C. Monodisperse Fluorene Oligomers Exhibiting Strong Dipolar Coupling Interactions. *Chem. Commun.* **2002**, 1608-1609.

(5) Li, J.; Grennberg, H. Microwave-Assisted Covalent Sidewall Functionalization of Multiwalled Carbon Nanotubes. *Chem. Eur. J.* **2006**, *12*, 3869-3875.

(6) Cavigli, P.; Da Ros, T.; Kahnt, A.; Gamberoni, M.; Indelli, M. T.; Iengo, E. Zinc Porphyrin-Re(I) Bipyridyl-Fullerene Triad: Synthesis, Characterization, and Kinetics of the Stepwise Electron-Transfer Processes Initiated by Visible Excitation. *Inorg. Chem.* **2015**, *54*, 280-292.

(7) Williams, R. M.; Zwier, J. M.; Verhoeven, J. W. Photoinduced Intramolecular Electron Transfer in a Bridged C_{60} (Acceptor)-Aniline (Donor) System; Photophysical Properties of the First "Active" Fullerene Diad. *J. Am. Chem. Soc.* **1995**, *117*, 4093-4099.

(8) Drake, J. M.; Lesiecki, M. L.; Camaioni, D. M., Photophysics and Cis-Trans Isomerisation of DCM. *Chem. Phys. Lett.* **1985**, *113*, 530-534.

(9) Harriman, A.; Porter, G.; Searle, N. Reversible Photo-Oxidation of Zinc Tetraphenylporphine by Benzo-1,4-Quinone. *J. Chem. Soc., Faraday Trans. 2* **1979**, *75*, 1515-1521.

(10) Dassault Systèmes BIOVIA, Materials Studio 2016, version 16.1.2.21, San Diego: Dassault Systèmes, 2016.

(11) Gaussian 09, Revision A.02, M. J. Frisch, G. W. Trucks, H. B. Schlegel, G. E. Scuseria, M. A. Robb, J. R. Cheeseman, G. Scalmani, V. Barone, G. A. Petersson, H. Nakatsuji, X. Li, M. Caricato, A. Marenich, J. Bloino, B. G. Janesko, R. Gomperts, B. Mennucci, H. P. Hratchian, J. V. Ortiz, A. F. Izmaylov, J. L. Sonnenberg, D. Williams-Young, F. Ding, F. Lipparini, F. Egidi, J. Goings, B. Peng, A. Petrone, T. Henderson, D. Ranasinghe, V. G. Zakrzewski, J. Gao, N. Rega, G. Zheng, W. Liang, M. Hada, M. Ehara, K. Toyota, R. Fukuda, J. Hasegawa, M. Ishida, T. Nakajima, Y. Honda, O. Kitao, H. Nakai, T. Vreven, K. Throssell, J. A. Montgomery, Jr., J. E. Peralta, F. Ogliaro, M. Bearpark, J. J. Heyd,

E. Brothers, K. N. Kudin, V. N. Staroverov, T. Keith, R. Kobayashi, J. Normand, K. Raghavachari, A. Rendell, J. C. Burant, S. S. Iyengar, J. Tomasi, M. Cossi, J. M. Millam, M. Klene, C. Adamo, R. Cammi, J. W. Ochterski, R. L. Martin, K. Morokuma, O. Farkas, J. B. Foresman, and D. J. Fox, Gaussian, Inc., Wallingford CT, 2016.

(12) Momma, K.; Izumi, F. VESTA 3 for three-dimensional visualization of crystal, volumetric and morphology data. *J. Appl. Crystallogr*. **2011**, *44*, 1272-1276.

(13) Hennemann, M.; Timothy Clark, T. "EMPIRE: a highly parallel semiempirical molecular orbital program: 1: self-consistent field calculations. *J. Mol. Model.* **2014**, *20*, 2331-2341.

(14) Margraf, J. T.; Hennemann, M.; Meyer, B.; Clark, T. EMPIRE: a highly parallel semiempirical molecular orbital program: 2: periodic boundary conditions. *J. Mol. Model.* **2015**, *21*, 144-150.

(15) Allouche, A.-R. Gabedit—A graphical user interface for computational chemistry softwares. *J. Comput. Chem*. **2011**, *32,* 174–182.